INTEGRATING PRETREATMENT TECHNIQUES IN A "BENIGN-BY-DESIGN STRATEGY" IN THE CONTEXT OF BIOMASS VALORIZATION

Richard Ahorsu

UNIVERSITAT
ROVIRA i VIRGILI

Integrating pretreatment techniques in a "benign-by-design strategy" in the context of biomass valorization

---

Richard Ahorsu

DOCTORAL THESIS

2021

UNIVERSITAT ROVIRA I VIRGILI
INTEGRATING PRETREATMENT TECHNIQUES IN A "BENIGN-BY-DESIGN STRATEGY"
IN THE CONTEXT OF BIOMASS VALORIZATION
Richard Ahorsu

Richard Ahorsu

Integrating pretreatment techniques in a "benign-by-design strategy" in the context of biomass valorization

Doctoral Thesis

Supervised by:

Dr. Francesc Medina Cabello

Dr. Magdalena Constanti Garriga

Departament d'Enginyeria Quimica

UNIVERSITAT
ROVIRA i VIRGILI

Tarragona (Spain)

UNIVERSITAT ROVIRA i VIRGILI

I STATE that the present study, entitled "**Integrating pretreatment techniques in a "benign-by-design strategy" in the context of biomass valorization**", presented by Richard Ahorsu for the award of the degree of Doctor, has been carried out under our supervision at the Department of Chemical Engineering (DEQ) of University Rovira i Virgili.

Tarragona 8th November. 2021

Doctoral Thesis Supervisors:

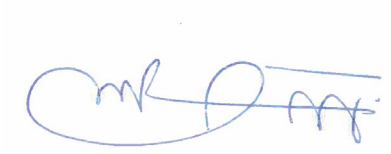

Dr. Francesc Medina Cabello

Dr. Madga Constanti

UNIVERSITAT ROVIRA I VIRGILI
INTEGRATING PRETREATMENT TECHNIQUES IN A "BENIGN-BY-DESIGN STRATEGY"
IN THE CONTEXT OF BIOMASS VALORIZATION
Richard Ahorsu

Acknowledgements

I embarked on this incredible PhD journey with both excitement and trepidation. I never imagined such a journey would come to an end so quickly. At this point, I would want to express my appreciation to my supervisors, Dr. Francesc Medina Cabello and Dr. Magdalena Constanti, for allowing me to work on my thesis in their group. I am grateful.

Dr. Pablo Dominguez de Maria and Dr. Daniel Montane were extremely generous and considerate to me. I appreciate you both for your guidance and assistance. All the other senior members, particularly Dr. Sandra Contreras, Anton, and Abel, who assisted me with my PhD thesis, need to be recognized as well. In finishing my thesis, Susana, who helped me with all of the logistical and administrative responsibilities, was an enormous help. I would also like to thank Dr. Joan Rosell Llompart, from whom I learned a lot when I first arrived at Rovira I Virgili University.

I would want to express my gratitude to Dr. Roberto Rinaldi Sobrinho for accepting me into his group “Tomorrow Chemical Technologies” at Imperial College London. It was an excellent opportunity to learn about new pretreatment procedures. I also had the opportunity to tour all of London's scientific museums. Here, I developed a new perspective on how "science" may be used to alter a civilization as a whole.

All funding sources are gratefully acknowledged: Marti Franques grant 2017PMF-PIPF-43, Spanish Ministry of Science, Innovation and Universities, project RTI2018-098310-B-I00, Diputació de Tarragona, and Erasmus Mobility Grant.

Sandra Yurani, Hande Demir, and Raiana Tomazini deserve special gratitude. When I first joined the group, these beautiful ladies provided me with all the support I required. I hope we can keep up such a solid connection and cross paths again eventually. I would want to thank Jacob Sole Beltran for his encouragement during the most trying times of my PhD journey. Antonio, Nikolas, Ievgenii, Dominic, Vaibhav and Saleem have also provided me with warm company.

In addition, the affection of my family, particularly my dear mother, cannot be measured.

Finally, I would want to extend my gratitude to all the members of the CATHETER and INTERFIBIO groups. I'm grateful, to say the least.

UNIVERSITAT ROVIRA I VIRGILI
INTEGRATING PRETREATMENT TECHNIQUES IN A "BENIGN-BY-DESIGN STRATEGY"
IN THE CONTEXT OF BIOMASS VALORIZATION
Richard Ahorsu

Dedication

…to my dearest mother and late father…

Table of Contents

List of Tables

List of Figures

Figure 2.1. Schematic diagram of circular bioeconomy with vegetal biomass as the feedstock 67
Figure 2.2. The twelve principles of green chemistry , adapted and modified from reference [1]....68

UNIVERSITAT ROVIRA I VIRGILI
INTEGRATING PRETREATMENT TECHNIQUES IN A "BENIGN-BY-DESIGN STRATEGY"
IN THE CONTEXT OF BIOMASS VALORIZATION
Richard Ahorsu

List of Acronyms

Summary

Circular bioeconomy concept was used as an anchor in the valorization of walnut shell. Even though, upstream processes such as microwave, mechanocatalysis and deep eutectic solvents have shown potential in biorefinery processes, they exhibit some limitations when they are used in isolation. Here, we demonstrate the application of these upstream processes in a combination in an integrated approach. In this thesis, a cheap and easily available resource (walnut shell) was selected as feedstock for input of the biorefinery set up. Microwave process was used to deconstruct walnut shell to obtain xylose as the major intermediate compound. The optimum condition to give high yield of xylose achieved without the assistance of homogeneous and heterogenous catalyst. The thermal and chemical effect of microwave process on walnut shell were monitored to reveal the viability of the residue left after the reaction. Autohydrolysis assisted by microwave processes was used to depolymerize hemicellulose and amorphous cellulose in walnut shell to yield 63.5% w/w of xylose in a liquid fraction (hydrolysate) with a minimum yield of glucose. The optimum reaction conditions to obtain a high xylose yield with a low byproduct titer were 190 °C for 25 min. The xylose and glucose obtained from walnut shell was transformed into L-lactic acid for the first time with a productivity of 0.2g/L/h through homolactic fermentation by *Bacillus coagulans DSM 2314*. Prior to the fermentation of the sugars, various media were tested for the best productivity and growth *for Bacillus coagulans DSM 2314*. It was found a simple yeast extract, peptone and sugar substrate were rich enough to promote the growth of the bacteria. Microwave pretreatment and the adoption of thermophilic bacteria prevented the vigorous sterilization required for most fermentation processes.

Subsequently, the residue obtained after microwave processes was characterized and used in other experiment as a substrate to immobilize *Bacillus coagulans DSM 2314*. This experiment was carried out to investigate the potential maximation of the productivity of lactic acid and re-usability of the immobilized bacteria.

Secondly, poplar wood which is readily available in Europe was used as a feedstock for production of bioethanol. At first stage of biorefinery processes, mechanocatalysis technique was employed to depolymerized poplar to produce high quality glucose for the production of bioethanol. Common yeast *Saccharomyces cerevisiae* was used in the fermentation process. For the first time, sugars streams from mechanocatalytic processes of poplar wood were investigated for their fermentability. Mechanocatalytic process gave a high glucose yield of

ca. 80 % with accompanying inhibitory compounds. The most significant inhibitory compounds found in the crude hydrolysate after mechanocatalysis and hydrolysis of water-soluble products were furfural, HMF and dissolved phenolics. A novel and easy approach of polybenzene as an adsorbent was adopted to purify the crude hydrolysate. It removed 99.9% of furfural, HMF, and a significant amount dissolved phenolics. The purified hydrolysate was used in the fermentation process.

Cellulosic content could easily be accessible, after deconstruction of walnut shell through DESs by cleavage of ether bonds linking carbohydrate and lignin, hence freeing lignin into solution. The lignin dissolved in solution is subsequently precipitated and recovered. The combination of ball milling (BM), microwave irradiation (MI) and Deep Eutectic Solvents (DES) results synergistic for an efficient, selective, and very rapid (10 minutes) delignification of materials with high lignin content (ca. 50 wt%) such as walnut shells (WS). Lignin is dissolved in the DES media, whereas the polysaccharide fractions remain suspended with reduced degradation, due to the rapid pretreatment. After ball milling procedure (3 h), biomass loadings in the range of 100-200 g L^{-1} are selectively delignified in 10 minutes at 150 ºC by using choline chloride – formic acid DES (1:2 molar ratio), rendering lignin yields of 60-80 % (ca. ~60 g lignin L^{-1}). Combined ball milling, microwave irradiation and DES result much more efficient in comparison to BM, conventional heating, and DES. This recovered lignin can also serve as feedstock to produce bio-renewable platform chemicals and biofuels.

The inhibitory compounds (furans) which were recovered after purification of hydrolysate could be converted into bio-jet fuel precursors such as 2,5-bis(2-furylmethylidene) cyclopentanone (F2Cp or C15) and 2-(2-furylmethylidene) cyclopentanone (FCp or C10). Here, we evaluated the feasibility of this proposal, commercial furan derivatives such as furfural and cyclopentanone in a cross- aldol condensation reaction in the presence of mixed oxide catalyst. Two major problems associated with the production of biojet fuel precursors during aldol condensation are (i) solidification of products and (ii) longer reaction time. We solve this problem by using microwave as source of heat supply and performing the reaction in binary mixture (ethanol:water) with monophasic configuration.

Resumen

El concepto de bioeconomía circular se utilizó como ancla en la valorización de la cáscara de nuez. A pesar de que los procesos ascendentes como las microondas, la mecanocatálisis y los disolventes eutécticos profundos han mostrado potencial en los procesos de biorrefinería, presentan algunas limitaciones cuando se utilizan de forma aislada. Aquí, demostramos la aplicación de estos procesos ascendentes en una combinación en un enfoque integrado. En esta tesis, se seleccionó un recurso barato y fácilmente disponible (cáscara de nuez) como materia prima para la entrada de la biorrefinería establecida. Se utilizó el proceso de microondas para deconstruir la cáscara de nuez y obtener xilosa como el principal compuesto intermedio. La condición óptima para dar un alto rendimiento de xilosa se logra sin la ayuda de un catalizador homogéneo ni heterogéneo. Se controló el efecto térmico y químico del proceso de microondas en la cáscara de nuez para revelar la viabilidad del residuo que queda después de la reacción. Se utilizó autohidrólisis asistida por procesos de microondas para despolimerizar hemicelulosa y celulosa amorfa en cáscara de nuez para producir 63,5% p / p de xilosa en una fracción líquida (hidrolizado) con un rendimiento mínimo de glucosa. Las condiciones óptimas de reacción para obtener un alto rendimiento de xilosa con un título de subproducto bajo fueron 190 ° C durante 25 min. La xilosa y la glucosa obtenidas de la cáscara de nuez se transformaron en ácido L-láctico por primera vez con una productividad de 0.2g / L / h mediante fermentación homoláctica por *Bacillus coagulans DSM 2314.* Previo a la fermentación de los azúcares, se probaron varios medios para la mejor productividad y crecimiento de *Bacillus coagulans DSM 2314.* Se encontró que un sustrato simple de extracto de levadura, peptona y azúcar era lo suficientemente rico como para promover el crecimiento de las bacterias. El pretratamiento con microondas y la adopción de bacterias termófilas impidieron la esterilización vigorosa requerida para la mayoría de los procesos de fermentación.

Posteriormente, se caracterizó el residuo obtenido tras los procesos de microondas y se utilizó en otro experimento como sustrato para *Bacillus coagulans DSM 2314* inmovilizado. Este experimento se llevó a cabo para investigar la potencial maximización de la productividad del ácido láctico y la reutilización de las bacterias inmovilizadas.

En segundo lugar, la madera de álamo, que está fácilmente disponible en Europa, se utilizó como materia prima para la producción de bioetanol. En la primera etapa de los procesos de biorrefinería, se empleó la técnica de mecanocatálisis para despolimerizar el álamo para

producir glucosa de alta calidad para la producción de bioetanol. En el proceso de fermentación se utilizó la levadura común *Saccharomyces cerevisiae*. Por primera vez, se investigaron las corrientes de azúcares de los procesos mecanocatalíticos de la madera de álamo para determinar su fermentabilidad. El proceso mecanocatalítico dio un alto rendimiento de glucosa de aprox. 80% con compuestos inhibidores acompañantes. Los compuestos inhibidores más significativos encontrados en el hidrolizado crudo después de la mecanocatálisis e hidrólisis de productos solubles en agua fueron furfural, HMF y fenólicos disueltos. Se adoptó un enfoque novedoso y sencillo del polibenceno como adsorbente para purificar el hidrolizado crudo. Se eliminó el 99,9% de furfural, HMF y una cantidad significativa de fenoles disueltos. El hidrolizado purificado se utilizó en el proceso de fermentación.

El contenido celulósico podría ser fácilmente accesible, después de la deconstrucción de la cáscara de nuez a través de DES mediante la escisión de enlaces éter que unen carbohidratos y lignina, liberando así la lignina en solución. A continuación, la lignina disuelta en solución se precipita y se recupera. La combinación de molienda de bolas (BM), irradiación de microondas (MI) y solventes eutécticos profundos (DES) resulta sinérgica para una deslignificación eficiente, selectiva y muy rápida (10 minutos) de materiales con alto contenido de lignina (aproximadamente 50% en peso). como cáscaras de nuez (WS). La lignina se disuelve en el medio DES, mientras que las fracciones de polisacárido permanecen suspendidas con degradación reducida, debido al rápido pretratamiento. Después del procedimiento de molienda de bolas (3 h), las cargas de biomasa en el rango de 100-200 g L-1 se deslignifican selectivamente en 10 minutos a 150 ºC utilizando cloruro de colina - ácido fórmico DES (relación molar 1: 2), obteniendo rendimientos de lignina de 60-80% (aproximadamente ~ 60 g de lignina L-1). El molino de bolas, la irradiación de microondas y el DES resultan mucho más eficientes en comparación con el BM, el calentamiento convencional y el DES. Esta lignina recuperada también puede servir como materia prima para producir productos químicos de plataforma bio-renovables y biocombustibles.

Los compuestos inhibidores (furanos) que se recuperaron después de la purificación del hidrolizado podrían convertirse en precursores de bio-jet fuel tales como 2,5-bis (2-furilmetiliden) ciclopentanona (F2Cp) y 2- (2-furilmetiliden) ciclopentanona (FCp) . Aquí, evaluamos la viabilidad de esta propuesta, derivados de furano comerciales como furfural y ciclopentanona en una reacción de condensación cruzada aldólica en presencia de un catalizador de óxido mixto. Dos problemas principales asociados con la producción de

precursores de combustible biojet durante la condensación aldólica son (i) solidificación de productos y (ii) mayor tiempo de reacción. Resolvemos este problema utilizando microondas como fuente de suministro de calor y realizando la reacción en mezcla binaria (etanol: agua) con configuración monofásica.

Resum

El concepte de bioeconomia circular es va utilitzar com a àncora en la valorització de la closca de la nou. Tot i que els processos ascendents com el microones, la mecanocatàlisi i els dissolvents eutèctics profunds han demostrat potencial en els processos de biorefineria, presenten algunes limitacions quan s'utilitzen de manera aïllada. Aquí, demostrem l'aplicació d'aquests processos ascendents en una combinació en un enfocament integrat. En aquesta tesi, es va seleccionar un recurs barat i de fàcil accés (la closca de nou) com a matèria primera per a l'entrada de la biorefineria instal·lada. El procés de microones es va utilitzar per deconstruir la closca de la nou per obtenir xilosa com a compost intermedi principal. La condició òptima per donar un alt rendiment de xilosa s'aconsegueix sense l'ajuda d'un catalitzador homogeni o heterogeni. Es va controlar l'efecte tèrmic i químic del procés de microones sobre la closca de la nou per revelar la viabilitat del residu deixat després de la reacció. L'autohidròlisi assistida per processos de microones es va utilitzar per despolimeritzar l'hemicel·lulosa i la cel·lulosa amorfa a la closca de la noguera per obtenir un 63,5% p/p de xilosa en una fracció líquida (hidrolitzat) amb un rendiment mínim de glucosa. Les condicions de reacció òptimes per obtenir un alt rendiment de xilosa amb un títol de subproducte baix eren de 190 ° C durant 25 min. La xilosa i la glucosa obtingudes de la closca de la nou es van transformar per primera vegada en àcid L-làctic amb una productivitat de 0,2 g/L/h mitjançant fermentació homolàctica per *Bacillus coagulans DSM 2314*. Abans de la fermentació dels sucres, es van assajar diversos medis. per a la millor productivitat i creixement per al *Bacillus coagulans DSM 2314*. Es va trobar que un substrat senzill d'extracte de llevat, peptona i sucre eren prou rics per promoure el creixement dels bacteris. El pretractament amb microones i l'adopció de bacteris termòfils van impedir la vigorosa esterilització necessària per a la majoria dels processos de fermentació.

Posteriorment, el residu obtingut després dels processos de microones es va caracteritzar i es va utilitzar en altres experiments com a substrat del *Bacillus coagulans DSM 2314* immobilitzat. Aquest experiment es va dur a terme per investigar el màxim potencial de la productivitat de l'àcid làctic i la reutilització dels bacteris immobilitzats.

En segon lloc, la fusta d'àlber que està fàcilment disponible a Europa es va utilitzar com a matèria primera per a la producció de bioetanol. En la primera etapa dels processos de biorefineria, es va utilitzar la tècnica de mecanocatàlisi per a l'àlber despolimeritzat per produir glucosa d'alta qualitat per a la producció de bioetanol. En el procés de fermentació

es va utilitzar el llevat comú *Saccharomyces cerevisiae*. Per primera vegada, es van investigar els corrents de sucres dels processos mecanocatalítics de la fusta d'àlber per a la seva fermentabilitat. El procés mecanocatalític va donar un alt rendiment de glucosa de ca. 80% amb compostos inhibidors acompanyats. Els compostos inhibidors més significatius trobats a l'hidrolitzat brut després de la mecanocatàlisi i la hidròlisi de productes solubles en aigua van ser furfural, HMF i fenòlics dissolts. Es va adoptar un enfocament nou i fàcil del polibenzè com a adsorbent per purificar l'hidrolitzat cru. Va eliminar el 99,9% de furfural, HMF i una quantitat significativa de fenòlics dissolts. L'hidrolitzat purificat es va utilitzar en el procés de fermentació.

El contingut cel·lulòsic podria ser fàcilment accessible, després de la deconstrucció de la closca de nou a través dels DES mitjançant l'escissio dels enllaços èter que uneixen els hidrats de carboni i la lignina, alliberant així la lignina en solució. La lignina dissolta en solució es precipita posteriorment i es recupera. La combinació de mòlta de boles (BM), irradiació de microones (MI) i dissolvents eutèctics profunds (DES) resulta sinèrgica per a una deslignificació eficient, selectiva i molt ràpida (10 minuts) de materials amb alt contingut de lignina (aproximadament 50% en pes). com ara closques de nous (WS). La lignina es dissol al medi DES, mentre que les fraccions de polisacàrids romanen suspeses amb una degradació reduïda, a causa del pretractament ràpid. Després del procediment de mòlta de boles (3 h), les càrregues de biomassa en el rang de 100-200 g L-1 es deslignifiquen selectivament en 10 minuts a 150 ºC mitjançant l'ús de clorur de colina: àcid fòrmic com a DES (proporció molar 1:2), donant rendiments de lignina. del 60-80 % (aprox. ~60 g de lignina L-1). La combinacio del fresat de boles, la irradiació de microones i el DES resulten molt més eficients en comparació amb el BM, la calefacció convencional i el DES. Aquesta lignina recuperada també pot servir com a matèria primera per produir productes químics i biocombustibles de plataforma biorenovables.

Els compostos inhibidors (furans) que es van recuperar després de la purificació de l'hidrolitzat es podrien convertir en precursors de biocarburants com ara 2,5-bis (2-furilmetilideno) ciclopentanona (F2Cp) i 2-(2-furilmetilideno) ciclopentanona (FCp) . Aquí, es va avaluar la viabilitat d'aquesta proposta, derivats comercials del furan com el furfural i la ciclopentanona en una reacció de condensació d'aldol creuat en presència d'un catalitzador d'òxid mixt. Dos problemes principals associats a la producció de precursors de combustible de biojet durant la condensació aldòlica són (i) la solidificació dels productes i (ii) el temps de

reacció més llarg. Solucionem aquest problema utilitzant microones com a font de subministrament de calor i realitzant la reacció en una barreja binària (etanol:aigua) amb configuració monofàsica.

Chapter 1.
Introduction

1.1. Introduction

This introduction presents an overview of relevant information on circular bioeconomy, climate change, plastic pollution, biomass, hydrolysate, fermentation (Bacillus coagulans DSM 2314), lactic acid and polylactic acid, biofuels, heterogeneous catalyst (mixed oxides), microwave processes, and autohydrolysis, mechanocatalysis, and finally Deep Eutectic Solvents.

1.2. Circular bioeconomy

The dominant and current way of industry to the market transaction has been linear. Linear economy deals with the conversion of raw materials to end-product and single usage of the product. The effect of this linear tradition of" take-make-dispose" is deemed unsustainable and heavily damaging to the environment. To remediate this unsustainable practice, a new concept Circular Bio-Economy CBE or Green Economy GE was introduced. CBE is either viewed as an intersection of Circular Economy (CE) and Bioeconomy (BE) [1] or explained as BE being an integral part of CE [2]. The principle of CE was an idea of a closed system to highlight the finite natural resources available to the human race by Boulding in 1966 [3]. However, the term CE has first been identified as a work that investigated the inter-linkages between the environment and economic activities [4]. Various organizations and authors have defined this concept concerning what sector it applies to. European Union (EU) asserts CE as where the value of products, materials, and resources is maintained in the economy for as long as possible, and the generation of waste is minimized [5]. This supports EU directive EU Waste Framework Directive (2008/98/EC), which gives policies and legislations to a waste management system of Reuse, Recycling, other Recovery 3Rs (i.e., energy recovery) with a focus on prevention and reuse of waste [6]. McCormick and Kautto defined BE as an economy where the basic constituents for the manufacturing of materials, chemicals, and energy are derived from renewable biological resources [7]. However, with the optimism of benefits associated with the use of biorenewable resources in BE concept, other authors expressed concerns about the pressure and competition on the usage of arable land, water bodies, thus causing potential harm to the environment [8]. Hetemäki et al. foresaw a potential risk of linear business with the adoption of BE alone with the integration of "*circularity"* [9]. This has led to the emergence of the two concepts of CE and BE to formulate CBE to resolve the potential risk posed by the latter. The EU asserts that the CBE adopts the CE framework, utilizing biomass as an integral constituent to produce various, biochemicals, bio-products, and bioenergy in a biorefinery [10]. The circular bioeconomy concentrates on valorization of

biomass in integrated biorefineries and reusing and optimizing residue by *cascading*. Such optimization could be streamlining toward economic, environmental, or social aspects, and ideally considers all 12 pillars of green chemistry. The *cascading* steps aim at retaining resource quality by adhering to the bio-based value pyramid and the waste hierarchy where possible and adequate (Figure 1.1).

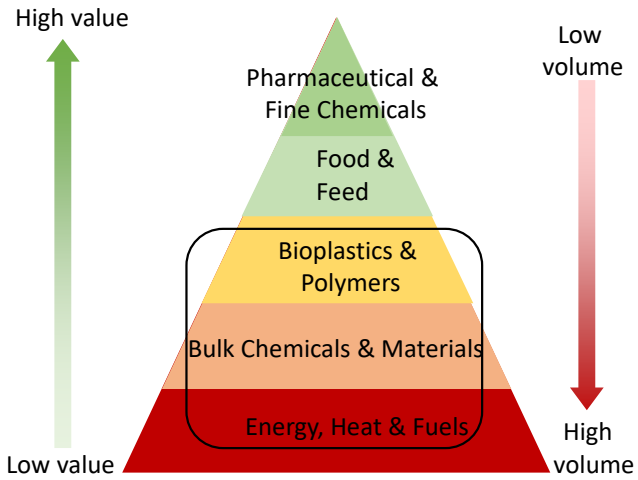

Figure 1.1. Bio-based value adapted and modified [11,12]

With the CBE concept, biorefinery feedstock could solidly tailor to the exigency of the problem at hand. High value application products are produced from high-quality biomass, while lower quality biomass is directed toward energetic purposes. It is desirable to stay at the upper part of the bio-based value pyramid. However, impending environmental catastrophe suggests that plastics and greenhouse gases (GHG) threatening the human civilization need mitigation. Using biomass to replace fossil-fuel electricity, heat, and transport at a large scale could offer absolute GHG mitigation [13]. In this thesis, agricultural feedstock as walnut shell and, poplar wood was incorporated into an integrated biorefinery state to produce L- lactic acid (fundamental chemical for bioplastics), bio-jet fuel, and bioethanol. This occupies the base and the middle level of the bio-value pyramid (Figure 1.1).

1.3. Environmental pollution

The two major environmental issues confronting our planet are plastic pollution and climate change.

1.4. Plastic pollution

In 1907, Leo Baekeland invented synthetic plastic, which has become indispensable in lives of human beings. He mixed phenol and formaldehyde under heat and pressure to form bakelite. He coined the term plastics from the Greek word *plastikos*; meaning moldable [14]. The common types of plastic found are polypropylene (PP), polyethylene (PE), and high-density polyethylene (HDPE).

Every year, about 380 million tons of plastics are produced, [15] and many of these plastics are disposed of after single use into landfills and environment. Plastics disposed into the environment remain undecomposed for hundreds and thousands of years [16]. If current production condition remains unchanged, about 12,000 Mt of plastic waste will be in landfills or in the natural environment by 2050 [15]. Another recent report from the World Economic Forum stipulates that " an overwhelming 72% of plastic packaging is not recovered at all: 40% is landfilled, and 32% leaks out of the collection system – either it is not collected, or it is collected, but then, illegally dumped or mismanaged." [17] If this trend continues, about 12 billion metric tons of plastic trash would be accumulated in landfills or natural environment by 2050 either littered onshore and finding their way into the oceans [15]. When the sun rays strike these plastics in the ocean and couple- with constant wave blasting, plastics break down into micro-then to nanoplastics [18,19]. These microplastics then travel along the food chain when ingested by humans. A recent study has revealed that, out of 24 samples of German beer analyzed, one sample showed about 109 plastic fragments per liter [20]. Sea salt tested in China also revealed that a kilogram of sea salt contained 681 fragments of microplastics [21]. It has also been discovered that out of 89 fish species analyzed for microplastic contamination and 49 being favored on dinner plates, including Atlantic herring, albacore, bluefin tuna, and anchovies have ingested some form of microplastic in their gut. Microplastics have been detected in mussels, clams, oysters, and scallops [22].

From a scientific perspective, synthesizing a new generation of degradable plastic will play a huge role in remediating the earth burden of plastic waste pollution. Bioplastics are a green and sustainable alternative to plastics that can assist in salvaging the plastic problem because they are degradable.

Bio-based and biodegradable plastics adopted into circular bioeconomy can help reduce the dependency on fossil fuels, GHG and plastic pollution. Among the biobased and biodegradable polymers, the precursor of polylactic acid (PLA), which is lactic acid, has been discussed and investigated in this thesis, (See chapter 3).

1.5. Climate change

Forces within and outside the earth's confinement have contributed to the changing climate since the inception of life. However, human activities over the past decades have worsened the climate change considerably over a short time [30]. The term "global warming" which is associated with climate change, is simply defined as the measured rise of the earth's temperature. This rise in temperature is caused by GHG that builds up in the atmosphere because of continual combustion of fossil fuel [31]. The most notable effects of global warming on earth are rise in sea level, drought, extreme weather conditions, changes in precipitation, and more [32]. The largest contributor to the predicted human-induced climate change arises from the burning of fossil fuels that produce carbon dioxide (CO_2), GHG [33]. Increases in CO_2 concentration influence the acidity of the oceans [34]. Fossil resource is the major supply line for transportation with road transport accounting for 81% of overall energy usage among the transport sector [35]. CO_2 emissions from average car were estimated to be 76% due to the combustion of fuel, further 9% and 15% from manufacturing of vehicles and emission losses in the fuel supply system respectively [36].

To keep global warming temperatures below 2°C, "Fuel-switching" from the dominant fossil fuels used in transportation (gasoline and diesel) to lower-carbon replacements, namely, electricity, hydrogen, and biofuels (each from low-carbon sources) route is plausible [40]. In this thesis, biofuels such as ethanol and bio-jet fuel precursor were considered in a circular bioeconomy (See Chapter 6 and 7).

1.6. Lactic acid

Lactic acid (LA) is an alpha-hydroxy acid with bi-functional groups, making it chiral and easily chemically manipulated for the production of various products [41]. Due to LA's wide range of applications, such as those in pharmaceutical, cosmetics, and food industry, and global demands, LA market size is expected to reach $ 8.77 billion by 2025. It has been predicted that the growing awareness of consumer desire to use biodegradable packaging and bags will further drive the demand for LA and PLA [42].

1.7. Biofuels

In this study, bioethanol and bio jet fuel precursors were considered for downstream process investigations. Bioethanol is a chemical compound that belongs to the alcohol family. Its molecular formula is C_2H_5OH, and it is frequently referred to as "alcohol." Ethanol has excellent fuel properties having an octane rating of approximately 103 and a high heat of vaporization, both of which are advantageous to power cars. Ethanol use has increased to the point where it now accounts for about 10% of total liquid fuel used in internal combustion engines in the United States and approximately 50% of that fuel class in Brazil. Despite this remarkable increase in ethanol use, starch and sugar crops are not available in sufficient quantity to meet the enormous demand in the fuel market, and their use for ethanol production raises concerns for possible food shortage and negative effects on the environment [53–55]. The ethical implications of using food as a raw material for combustion have prompted researchers to focus on the possibility of inedible feedstock alternatives [56]. Lignocellulosic biomass materials provide a crucial renewable substrate for bioethanol synthesis as they are not used in food and animal feed production. In addition, these cellulosic materials aid in ensuring environmental sustainability [57,58]. Moreover, lignocellulosic biomass can be produced in vast quantities from a variety of low-cost raw sources, including municipal and industrial waste, wood, and agricultural residues [59,60]. Ethanol is a key component of alcoholic beverages and is frequently used in mouthwash, medications, tonics, colognes, and solvents, among other things. However, what makes it suitable for use as a transportation fuel is its propensity to burn rapidly with oxygen (Wyman et al., 1990). Due to ethanol's high octane number and high heat of vaporization, engines run on ethanol can operate at higher compression ratios, resulting in more efficient use of ethanol than that of gasoline in lower compression ratio engines [62]. As ethanol requires less oxygen to burn than gasoline, only dedicated ethanol vehicles or flexible fuel vehicles equipped with instrumentation that adjusts the air/fuel ratio can accommodate ethanol. Ethanol mixed with gasoline, for example, as E85—a mixture of 85% ethanol and 15% of gasoline by volume is used as an alternative fuel [58].

1.8. Biomass

Biomass constituents are polymers of cellulose, hemicellulose, lignin, and pectin. They offer many advantages such as (i) The high quantities available worldwide (ii) agricultural and forestry waste generate vast amounts of lignocellulosic biomass (3) It is renewable in nature and sustainable (4) It’s a carbon source that is non-edible feedstock. The composition of

biomass varies in cellulose (40–80%), hemicellulose (10–40%), and lignin (5–25%) content depending on the type of biomass and the geographical location [70]. Cellulose is the most abundant organic material in nature. **Cellulose** is made up of glucose monomers linked together by β-(1-4) glycosidic bonds to form a linear polysaccharide. These long chains are bonded through inter-and intra-molecular hydrogen bonds and van der Waals forces and making cellulose a highly crystalline polymer. **Hemicellulose** is a branched polysaccharide that consists of pentoses with xylose and arabinose being the major constituents, and with some hexoses such as glucose, galactose, and mannose units present. Cellulose and hemicellulose are embedded in a lignin matrix (Figure 1.2). **Lignin** is a polymer of phenolic units and acts as a binder of the biomass constituents, giving the plant structural support. The proportion of C6 units in hemicellulose of softwoods is higher compared to that of hardwood hemicellulose. Hardwood hemicellulose contains C5 units, usually xylose. Agricultural wastes such as rice straw, corn stover, wheat straw, walnut shell, almond shell, and hazelnut shell are reported to contain large proportions of both glucose and xylose units and some mannose and galactose. Lignin finds application in down streams biorefineries.

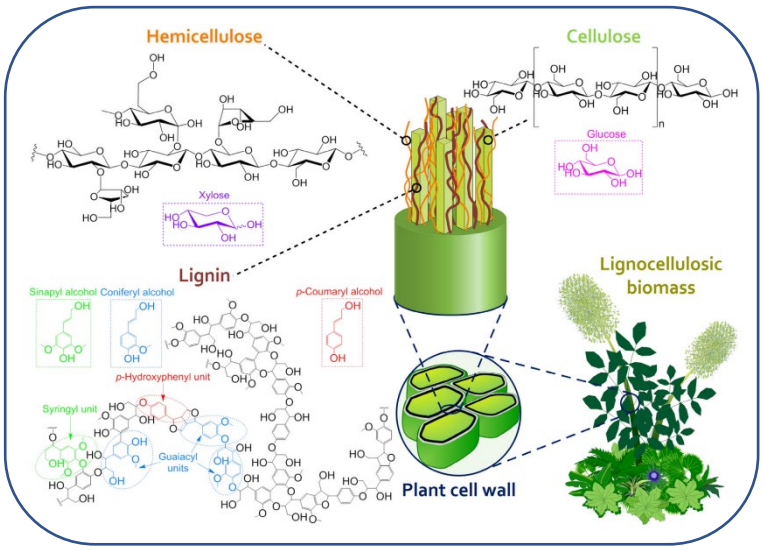

Figure 1.2. Structure of biomass, adopted ref [71]

1.9. Interactions in lignocellulose biomass

It is important to reveal the interaction between the polymers in lignocellulosic biomass because these interactions also contribute to its recalcitrance. Hence, making pretreatment is a challenging task. Through hydrogen bonds, cellulose and hemicelluloses are inextricably linked[86]. Lignin and hemicelluloses are covalently linked to form a lignin-carbohydrate complex (LCC) [87]. Five different types of lignin-carbohydrate linkages given in the literature are as follows: benzyl ethers (BE), phenyl glycosides (PG), ferulate/coumarate esters (FE/CE), γ-esters esters (GE), and hemiacetal/acetal linkages that are bonded to lignin at 4-OH and 4-O positions [88] (Figure 1.3). In this study, lignocellulosic biomass was deconstructed by selectively breaking either glycosidic bonds within glucose units or benzyl ether bonds to free glucose units and/or lignins into small molecular weights for further downstream process through pretreatment processes (upstream process). The glucose or xylose units were obtained in form of hydrolysate while lower molecular lignins were precipitated. Walnut shell as agricultural feedstock was used as a case study in this research.

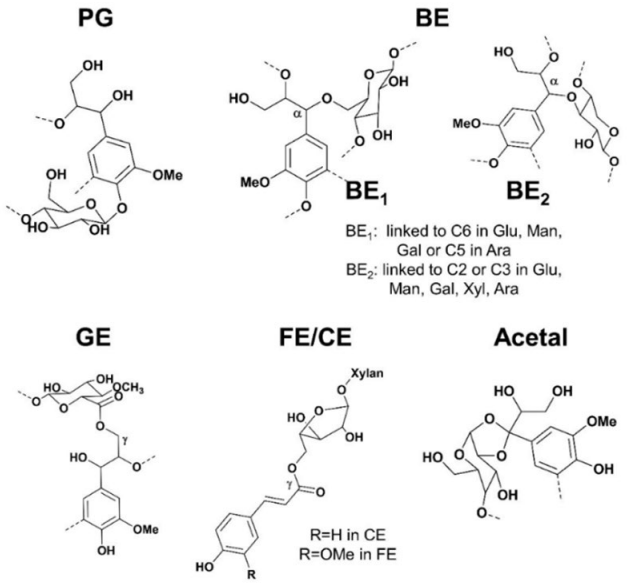

Figure 1.3. Suggested structures of Lignin-Carbohydrate bonds (LC) in wood and grass. In the figure, PG=phenyl glycosides, BE=benzyl ethers; GE= γ -esters; FE=ferulate esters; CE=coumarate esters [88].

1.10. Pre-treatment

Lignocelluloses are complex structures made of cellulose, hemicelluloses, and lignin that are resistant to degradation. Enzymatic saccharification is one of the finest ways of converting such biomass to sugars due to its low energy need and low pollutant output; nonetheless, the key issue is the inaccessibility of cellulose due to its stiff linkage with lignin [89]. This creates difficulties throughout the conversion process; thus, one of the primary goals of pretreatment is to break down the lignin seal to make cellulose more accessible to enzymatic hydrolysis for conversion. Pretreatment, in other words, is a critical and costly unit procedure in the conversion of lignocellulosic resources to fuels [90]. Typically, the pretreatment technique involves (i) disrupting hydrogen bonds in crystalline cellulose, (ii) deconstructing the cross-linked matrix of hemicelluloses and lignin, and (3) increasing the porosity and surface area of cellulose in preparation enzymatic hydrolysis [91,92]. Many pretreatment techniques investigated included pretreatments such as grinding and milling, microwave, extrusion, alkali, acid, organosolv, ozonolysis, and ionic liquid, deep eutectic solvents (DES), steam explosion, liquid hot water, ammonia fiber explosion, wet oxidation, CO_2 explosion, mechanocatalysis, and biological pretreatment. However, irrespective of the pretreatment method utilized, certain inhibitory chemicals are formed during the process, which has a damaging effect on microbial activity during the hydrolysis step. There are three major classes of inhibitors: (1) weak acids such as levulinic, acetic, and formic acids, (2) furan derivatives such as HMF (5-hydroxy-2-methylfurfural) and furfural, and (3) phenolic chemicals [93]. To avoid the impact of inhibitors in product yield during fermentation processes, a combination of environmentally benign pretreatment techniques was applied to walnut shells to produce sugar streams for downstream process.

1.11. The significance of upstream technologies

The selected pretreatment technology should

(i) have high recovery of sugar monomers

(ii) produce hydrolysate with a minimum number of inhibitory products (for fermentation processes)

(iv) produce a high concentration of sugars in the hydrolysate

(v) require low energy to operate

for the realization of higher yields for downstream processes.

In this research, microwave process, mechanocatalysis, and deep eutectic solvents were investigated for upstream processes while biocatalysis and heterogeneous catalysis were employed for downstream processes.

1.12. Microwave processes

Microwaves are electromagnetic waves with frequencies ranging from 0.3 to 300 GHz and wavelengths ranging from 1 m to 1 mm [94]. When microwaves are transmitted, they are transformed into precise frequencies, where the wave energy is absorbed by the material to be heated [95]. As a result of the continually shifting electric fields, dipoles in polar liquids undergo continuous alignment and realignment [96]. Together with the migration of ions (as a result of the electromagnetic field), these continually shifting dipoles create friction within the material, and this internal energy, which is diffused as heat, causes the bulk of the material to heat [94,96]. Microwave-heated materials are defined by their ability to absorb and store energy (also known as their ”dielectric constant”) and their capacity to disperse this internal energy as heat (also known as their “dielectric loss”) [97]. These materials are frequently referred to as “dielectrics” or “lossy dielectrics,” and their thermal conductivity is proportional to their ratio of “dielectric loss” to 'dielectric constant' [97].

1.13. Comparison of microwave and conventional heating

Unlike traditional heating, microwaves penetrate the heating container's walls and directly heat the material [98,99]. With conventional heating, the container's wall is heated first, followed by the substance, resulting in loss of energy and heat [100,101]. As a result, any material exposed to MW irradiation will have a higher temperature at the center than at the outside surface, but with conventional heating, the reverse is true [102], as demonstrated in Figure 1.4. Despite such benefits, microwave heating of heterogeneous materials may result in non-uniform heating, resulting in "thermal runaways" or instabilities and "hotspots" in the material being pre-treated [94,103]. This disadvantage, however, can be mitigated by continuously mixing the heated material [94]. Dielectric heating is the term used to describe the process by which a high- frequency alternating electric field heats the dielectric material. A material that can be polarized as a result of an applied electric field is considered dielectric.

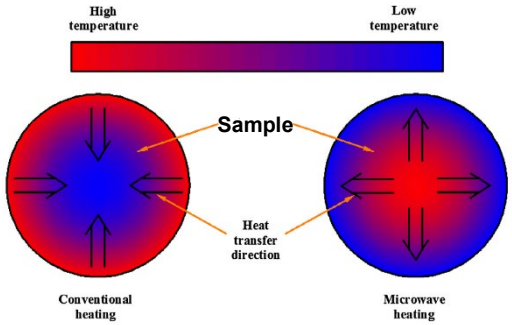

Figure 1.4 Comparative temperature dispersion during conventional and microwave heating. From ref [102,104]

In this context, dielectrics are substances that absorb and convert microwaves (electro-magnetic energy) to heat (thermal energy), with microwave heating being a sub-category of dielectric heating. Microwave heating is accomplished by transmitting electromagnetic waves created by an emitter (magnetron) through space to the sample under heating.

Two critical parameters govern a material's dielectric properties: (i) the dielectric constant (ε′) and the dielectric loss factor (ε″) [109]. The dielectric constant (ε′) is a property of materials that determines how much electromagnetic energy is reflected and how much is absorbed when an electric field is applied.

Nevertheless, the dielectric loss factor (ε″) represents the efficiency with which electromagnetic energy is transferred to heat. The dielectric loss tangent (tan δ) or dissipation factor of a material is defined as the quotient of the dielectric loss factor (ε ″) and the dielectric constant (ε ′): tan δ =ε″/ε′. The dielectric loss tangent tan is a critical property that determines a material's ability to absorb and convert electromagnetic energy to thermal energy at a particular temperature and frequency.

Thus, it shows the heating rate and the maximum temperature that can be reached. Substances with a high tan δ value are considered to be excellent microwave receivers due to their high capacity to transfer electromagnetic energy to thermal energy. A high value of tan δ is essential for efficient microwave absorption and subsequent quick heating with a high ultimate temperature [108].

1.14. Effects of microwave irradiation on lignocellulosic biomass (lignin, hemicellulose, and cellulose content)

The impacts of MW pretreatment either in a single or combinatory route have focused on lignocellulosic material deconstruction, surface area and particle size, lignin, hemicellulose, and cellulose content. Fractionation and disintegration of the crystalline structure of cellulose molecules have also been observed [104,105], as has the solubilization of organics such as proteins, polysaccharides, and lipids [106,107]. Following that, other research examining the other effects reported the elimination of hemicellulose following pretreatment of cornstalk [110] and wheat straw [111]. Studies by other authors on the effect of MW pretreatment residence times and temperatures on lignin removal from switchgrass showed that increasing both pretreatment residence times and temperatures resulted in increased delignification [111,112]. Keshwani et al. also observed that [119] increasing the MW-irradiation period of reactions increased the effectiveness of coastal Bermuda grass and switchgrass delignification [113]. Table 5 summarizes further studies on the impacts of MW pretreatment on lignocellulosic content. As shown in Table 1.2, most research showed the elimination of lignin and hemicellulose while increasing the cellulose content, following pretreatment. By comparing MW-irradiation alone to MW-assisted pretreatments, it was possible to determine that MW-assisted pretreatments resulted in more lignin and hemicellulose elimination. When MW-assisted acid and alkali pretreatments were compared, it was evident that MW-assisted acid pretreatments had a more profound effect on hemicellulose removal; but MW-assisted alkali pretreatments had affected lignin removal more. However, in some situations (mostly solitary MW-irradiation), the lignin concentration of pretreated biomass increased, which was attributed to a drop in hemicellulose content, being more susceptible to thermal impacts from MW-irradiation [114,115]. As seen in Table 1.2, most research focused on the reduction of biomass recalcitrance before enzymatic digestion by removing lignin and hemicellulose first.

Table 1.1. Impacts of microwave pretreatment on lignin, hemicellulose and cellulose contents in lignocellulosic biomass [116]

Substrate	Pretreatment	Lignin (%)	Hemicellulose (%)	Cellulose (%)	Ref
Sugarcane bagasse	1% NaOH (3 min)	X_C:18 X_P:4.9	X_C: 27 X_P: 26.5	Xc: 34 Xp:66.6	[117]
Sugarcane bagasse	0.2M H_2SO_4	X_C:14.1 X_P:10.7	Xc:26.0 Xp:0.6	Xc:52.5 Xp:68.4	[118]
Corn straw	Control	X_C:19.0	X_C:14.8	X_C:27.9	[115]
	MW+water	X_P:21.1	X_P:13.3	X_P: 28.9	
	MW+glycerol	X_P:13.4	X_P:11.5	X_P: 22.6	
	MW+ alk glycerol	X_P: 14.7	X_P:12.8	X_P: 23.1	
Rice straw	1% NaOH	X_C: 13.6 X_P: 4.9	X_C: 19.7 X_P: 10.2	X_C: 38.6 X_P: 69.2	[119]
Wheat straw	1% NaOH	X_C:21.3 X_P: 5.7	X_C: 25.8 X_P: 7.8	X_C: 41.2 X_P: 79.6	[120]
Rape straw	2%(v/v) H_2SO_4	X_C: 18.0 X_P: 15.4	X_C: 19.6 X_P: 23.6	X_C: 37.0 X_P: 42.3	[121]
Palm fiber	Control	X_C: 27.3	X_C: 19.9	X_C: 35.4	[122]
	MW+3.5% NaOH	X_P: 12.3	X_P: 15.5	X_P: 56.7	
	MW+3.5% H_2SO_4	X_P: 20.7	X_P: 14.5	X_P: 44.4	
	MW+2.0% Na_2CO_3	X_P: 20.3	X_P: 17.4	X_P: 44.4	
	MW+5.0% H_2O_2	X_P: 15.0	X_P: 15.8	X_P: 51.3	
Corn stover	0.2N H_2SO_4	X_C: 11.9 X_P: 12.2	X_C: 31.3 X_P: 15.6	X_C: 36.5 X_P: 38.5	[123]
Rice husk	Control	X_C: 16.3	X_C: 7.3	X_C: 22.5	[115]
	MW+water	X_P: 19.3	X_P: 6.3	X_P: 20.2	
	MW+glycerol	X_P: 14.4	X_P: 4.1	X_P: 19.1	
	MW+alkaline glycerol	X_P:17.1	X_P: 7.9	X_P: 22.5	
Wheat straw	2.75% (w/v) NaOH	X_C: 14.8 X_P: 5.8	X_C: 28.0 X_P: 31.0	X_C: 45. X_P: 51.0	[124]

In our study, microwave was used to produce sugars from walnut shells which were subsequently transformed (bio) catalytically to lactic acid, bioethanol, and bio jet precursors

1.15. Deep Eutectic Solvents

Deep eutectic solvents have been introduced as low-cost eutectic mixtures with comparable physical and chemical properties to ILs. They are produced by combining hydrogen bonding donors (HBDs) and acceptors (HBAs) to form eutectic mixtures. DESs are chosen over conventional ILs because they are simple to synthesize, and are cost-effective, and are environmentally benign [125]. The cost of producing a DES was only about 20% of that of producing an IL. The relationship between the molecular makeup of the resulting eutectic mixtures and their solvent characteristics; however, is not completely known. However, DES prospective applications can be found in medicines, electrochemistry, bio-industrial chemistry, fermentation, the food and feed sector, and the processing of biomass. The use of

DESs as an alternative to ILs in dissolving the polysaccharides (i.e., cellulose, xylose, arabinose, starch, chitin) and lignin contained in biomass has piqued the scientific community's attention worldwide to manufacture value-added products, biofuels, and commodity chemicals [126]. Certain pretreatments (hydrothermal, dilute acid, organosolv, dilute alkali, chemical pulping, and ionic liquids (ILs)), particularly under high-severity conditions, solubilize and degrade hemicelluloses and/or lignin to a degree, forming inhibitors such as hydroxymethyl furfural, furfural, hydroxy acids, and aliphatic carboxylic acids. Thus, an additional detoxification step may become unavoidable to minimize enzyme or microbe toxicity, while still achieving high product yields [127,128]. Under mild working circumstances, ionic liquids have demonstrated high efficacy in extracting lignin, lowering cellulose crystallinity, and increasing enzymatic digestibility. Their practical applicability, however, has been hampered by their high costs, incompatibility with enzymes and bacteria, and recycling issues [129]. Thus, multiple factors such as the nature of the feedstock (hardwood, softwood, agricultural residue, and grass), capital and operating costs, energy investment, yields, efficiency, and environmental sustainability all play a critical role in determining the most appropriate pretreatment approach for biomass. Thus, there is still much room for innovation and the development of unique and disruptive biomass pretreatment methods. DESs have several advantages over conventional solvents and ionic liquids, including the ease with which they can be synthesized without any purification or waste generation steps, their renewable nature, the wide availability and cost effectiveness of their constituents (for example, ChCl is available as chicken feed; whereas, urea is frequently used as fertilizer) [130].

1.16. Classification of DES

A eutectic mixture is a mixture of two or more phase immiscible solid components that undergoes a complete phase transition to liquid at a specified temperature [131]. This point is referred to as the eutectic point because it is the lowest melting point in the entire set of compositions (Figure 1.5). This phenomenon occurs when component atoms are small enough to fit into the interstitial spaces of a composite network created by larger atoms, breaking the network's crystalline pattern and thus lowering the freezing point of the eutectic mixture.

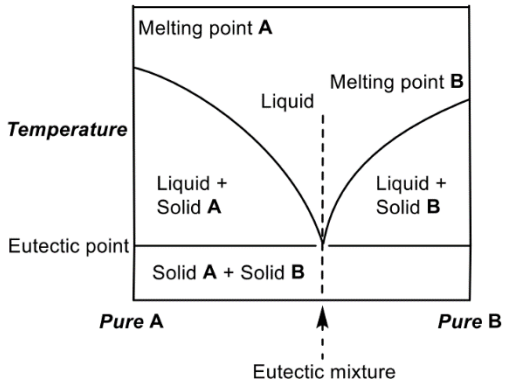

Figure 1.5. Phase diagram of a eutectic point on a two component phase [131].

The classic example of a DES is the eutectic mixture formed by choline chloride (ChCl) and urea at a molar ratio of 1:2, which has a freezing point of 12 degrees Celsius, considerably lower than the freezing points of ChCl (302 °C) and urea (133°C) [132]. DESs are formed by mixing hydrogen bonding donors (HBDs, such as amines, amides, carboxylic acids, and polyols) and hydrogen bonding acceptors (HBAs, such as the counterion of quaternary ammonium salt). Typically, this occurs as a result of the interaction of these components: the higher the interaction is, the greater the variation in melting point relative to the mixture's ideal melting temperature (Figure 1.6).

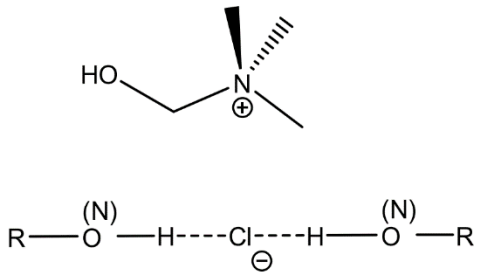

Figure 1.6. Interaction of HBD onto the counterion of HBA (ChCl in this case) [133]

The melting point of DESs varies according to the source materials and their reciprocal molar ratios. The melting point drop of DESs is ascribed to charge delocalization caused by hydrogen bonding between HBD and HBA. A mixture with a higher hydrogen bonding capacity will result in a more dramatic drop in the melting point of the DES. DESs are classified into four categories by Abbott [134].

Table 1. 2. General formula for the classification of DESs. Cat^+, any ammonium, phosphonium, or sulfonium cation; X, a Lewis base, generally a halide anion; Y, a Lewis or Bronsted acid; z, number of y molecules that interact with the anion [135]

Type	Components	General Formula	Example
I	Metal salt organic salt	$Cat^+ X^-$ zMClx; M=Zn Sn, Fe, Al, Ga. In	$ZnCl_2$ + ChCl
II	Metal salt hydrate + organic salt	$Cat^+ X^-$ zMClx.yH2O; M=Cr, Co, Cu, Ni, Fe	$CoCl_2$.6H2O+ChCl
III	HBD+organic salt	$Cat^+ X^-$ zRZ; Z=$CONH_2$, COOH, OH	Urea + ChCl
IV	Zinc/aluminium chloride+HBD	MClx + RZ=MCl_{x-1}^+ Zn & Z=$CONH_2$,OH	$ZnCl_2$+urea

DESs have been categorized according to the chemical constituents they contain (Table 1.2). Due to the high melting points of the non-hydrated metal halides, Type I DESs have limited use in biomass processing, but Type II DESs are more practical for industrial processes due to the relatively lower costs of their hydrated metal halides [135]. However, Type III DESs are investigated most due to their ease of synthesis, inertness to water, biodegradability, and low cost [130,135]. Finally, Type IV DESs employ inorganic transition metals with urea to create eutectic mixtures, although metal salts do not ordinarily ionize in non-aqueous mediums [130,135]. It is critical to understand the physicochemical properties of DESs to apply them in industry. Density, viscosity, and conductivity of DESs are briefly discussed.

1.17. Density

Most of DESs are denser than water, with densities ranging from 1.0 to 1.35 g/cm^3, although those based on metallic salts, such as $ZnCl_2$:urea and $ZnCl_2$:ethylene glycol, have densities in the range of 1.3–1.6 g/cm^3 [136]. The DESs' density is determined by the molecular components' packing pattern and the testing temperature [136]. As expected, increasing the temperature or the water content of DESs decreases density [136,137]. In addition, as the alkyl chain length of DES components increases, the density drops, as does the relative ratio of salt to HBD [138,139]

1.18. Viscosity

The viscosity of DESs is dictated by their intermolecular interactions, which are impacted by various factors, including the chemical composition of their constituents, such as the kind of HBD and HBA, their molar ratio, temperature, and water content [135]. For example, in certain composition ranges, the viscosity of ChCl-based DESs reduces with increased temperature

and ChCl content [135,140]. The DESs with reduced viscosity are desirable for industrial and biomass processing applications [130].

1.19. Conductivity

It is generally recognized that the molar conductivity of DESs and their fluidity (reciprocal of viscosity) have a linear relationship [135]. DESs are in increasing demand as substitutes for conventional organic solvents due to their exceptional stability and biodegradability despite their low conductivity [135,141]. Thus, it is observed that highly viscous DESs have a low conductivity, increasing with temperature [140].

1.20. DES application as a biomass pre-treatment process

The principal application of DESs for lignocellulosic biomass valorization is based on their capacity to separate components effectively. Due to the intrinsic ionic character, the supramolecular H-bond that stabilizes the hemicellulose-lignin complex in lignocellulosic biomasses is destroyed, allowing the covalent link to be dissolved more easily. With this approach, the various components can be rearranged under extremely mild circumstances without forming inhibitors of the subsequent depolymerization of cellulose to create glucose [142]. Pretreatment with DES is commonly used to fractionate biomass [143,144], particularly to solubilize and remove lignin [145], resulting in a residual cellulose-rich substrate that is more amenable to enzymatic hydrolysis than the beginning lignocellulosic biomass [146]. This approach to biomass fractionation using the DES is used to remove lignin from cellulose. Unlike cellulose, which has a well-defined sequence of monomeric units connected by regular β-1,4-glycosidic linkages, lignin has a range of discrete and chemically diverse bonding patterns, each requiring a unique set of circumstances for cleavage during targeted depolymerization. While lignin is physically more complex than polysaccharides or holocelluloses, its higher carbon concentration and lower oxygen content make it an appealing feedstock for the synthesis of biofuels and chemicals. Notably, lignin's highly functionalized, and aromatic nature enables the direct manufacture of aromatic specialty and fine chemicals, obviating the need for complete de-functionalization to "BTX" (benzene, toluene, and xylenes) and subsequent re-functionalization to required platform chemicals. Nevertheless, hemicellulose is critical for valorizing the initial biomass. As a hydrolyzable polymer is composed primarily of C5 and C6 sugars, it can be chemically exploited by isolating it from other biomass components such as hydrolyzed sugars. The quantitative solubilization

of the hemicellulose fraction enables the recovery of xylans along with lignin for subsequent conversion to other high-value chemicals.

As noted previously, lignocellulosic biomass is often pretreated with DESs to solubilize lignin and hemicellulose while leaving the cellulose intact. The comparison of pretreatment methods utilizing various DESs is hampered by the enormous number and complexity of the biomasses investigated, each of which can interact differently with the same type of DES. Three experimental measures, however, such as delignification yields, hemicellulose solubilization, and cellulose recovery, can be used to assess and compare the efficacy of a DES treatment.

Findings of a multivariate study of characteristics revealed that the hydrophilic ability, polarity, acidity, and ability of HBDs to establish hydrogen bonds were the most important qualities related to DESs in terms of delignification yields. The three key factors were, in order of importance: (1) the oil-water partition coefficient (logP), (2) the acidity coefficient (pKa), and (3) the number of hydrogen bond donors in HBD. In comparison, the three critical operating variables affecting biomass pretreatment were the temperature (T-R), the reaction severity factor (R factor), and the ratio of HBD to HBA (DES ratio) [147]. As mentioned earlier, fractionation of lignocellulosic biomass occurs as a result of the displacement of the initial H-bond, which confers supramolecular contacts in the lignocellulose, by new ones with the DES's components, as well as the breaking of covalent bonds in the LCC.

1.21. Mechanocatalysis

Numerous single and combined pretreatment treatments have been extensively investigated and evaluated in terms of their relative merits and drawbacks. [71] Mechanocatalysis is a solvent-free reaction that combines mechanical forces and chemical reactions (through ball milling and acid catalysis). Briefly, mechanocatalysis is the process of activating chemical bonds using mechanical forces[148]. To depolymerize cellulose, mechanocatalysis is performed. Cellulose is a three-dimensional network of intra-molecular and inter-molecular hydrogen bonds that generate a refractory crystalline phase that prohibits catalysts from reaching the β-(1-4) glycoside bonds. Homogeneous catalysts have shown important promise in depolymerizing cellulose to sugar monomers. However, homogeneous catalysts have several disadvantages in lignocellulosic biomass deconstruction, including (i) their corrosive nature, (ii) their recovery difficulty, and (iii) their reusability.

Heterogeneous catalysts that were less corrosive and easier to recover had a reduced cellulose surface-to-catalyst contact, resulting in low glucose yields. Catalyst recovery and reusability are critical for the feasibility and sustainability of biorefining setups. Due to the ease, with which heterogeneous catalysts may be recovered, they are more favorable than homogeneous catalysts. However, proper interaction between the heterogeneous catalysts and the cellulose is required. Hick et al. developed a mechanical procedure that entailed grinding cellulose with a solid catalyst to create a solid-solid contact that deconstructs the cellulose [149]. With mechanical forces acting as the reaction initiator, kaolinite converted 84% cellulose into a water-soluble fraction (cellobiose, glucose, levoglucosan, etc.) [149]. Meine et al. showed a considerable improvement in mechanocatalytic processes [150]. Milling acid-impregnated cellulose produced completely water-soluble products. The impregnation technique is often done using strong acids with pka>1.8 (H_2SO_4, HCl). Following hydrolysis of these water-soluble products at 130°C for 1 hour without the need of an external catalyst, the mechanocatalytic process becomes a formidable and realistic alternative to enzymatic digestion in the deconstruction of lignocellulosic biomass in a biorefining setup.

1.22. Combination of pre-treatment methods

As previously stated, many pretreatment procedures have several limitations restricting their applications. Combining pretreatment approaches has lately been regarded as a viable approach for overcoming these obstacles as it increases sugar production efficiency, decreases inhibitor development, and shortens the processing time.

1.23. Downstream process

Downstream processing of biofuels and bio-based chemicals is generally a stumbling block to the economic and sustainable development of new technologies. Moreover, it is a challenging topic for process design and optimization, owing to the intrinsically non-ideal thermodynamics of the liquid mixes formed during the (bio)chemical conversion of biomass.

1.24. Production of Lactic acid

Lactic acid can be synthesized chemically or biotechnologically. Lactic acid generated chemically often yields a racemic combination of L- and D-lactic acid isomers (Figure 1.7). The chemical method includes the hydrolysis of lactonitrile with strong acids. Other chemical approaches for lactic acid production have been explored but have been determined to be

commercially unfeasible[155]. Microbial fermentation of sugar streams derived from renewable feedstock to produce optically active isomers of D-lactic acid or L-lactic acid increases the feasibility and economic sustainability of biological operations[156]. Numerous materials have been explored as viable alternative substrates and renewable resources, including by-products of agriculture and food sectors, as well as natural unutilized biomasses. Moreover, depending on the strain used, biotechnological techniques can be used to produce optically pure L- or D-lactic acid.

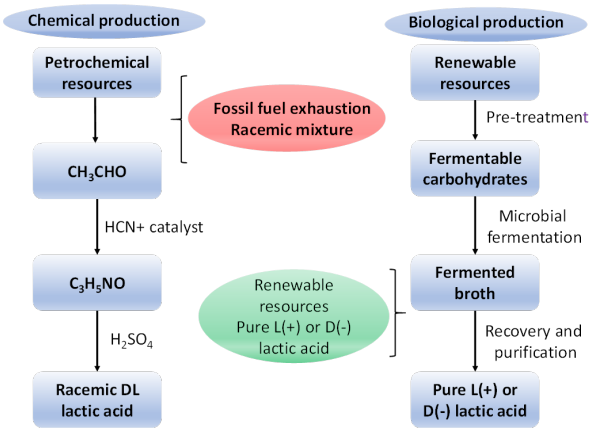

Figure 1.7. Schematic processes of chemical and biological route to lactic acid production

1.25. Biosynthesis of lactic acid

Sugars are fermented to produce lactic acid by lactic acid-producing bacteria, either naturally derived or bioengineered in the laboratory. *Corynebacterium glutamicum*, *Escherichia coli*, *Bacillus strains*, and Lactic Acid Bacteria (LAB) are the best-known divisions of microorganisms capable of making lactic acid (LA).

While the biological route is a more superior and feasible process for lactic acid fermentation than the non-fermentation route, it has some drawbacks: (i) byproduct formation and low yield; (ii) use of the nutrition-rich medium; and (iii) high risk of bacteriophage infection, which results in cell lysis and halts lactic acid production[157,158]. To overcome these obstacles, bioengineering techniques have been utilized to (i) increase lactic acid output by inhibiting byproduct synthesis. [159] (ii) and, engineering bacteria strains capable of producing lactic acid [160].

While the heterofermentative pathway results in equimolar levels of LA and other byproducts such as acetic acid, carbon dioxide, and ethanol, the homofermentative route results in solely LA[161]. Due to the possibility of LAB forming byproducts other than lactic acid during heterofermentation, the maximum yield of LA to glucose is 0.5 g/g or 1.0 mol/mol[156]. Heterofermentation of glucose to LA by LAB utilizes the alternative pentose monophosphate route, mediated by many enzymes, which converts C6 sugars (hexoses) to C5 sugars (pentoses) and CO_2 [162].

Then, the resulting C5 is attached to glyceraldehyde 3-phosphate and acetyl phosphate by phosphoketolase [162]. Homofermentative LAB produces LA as the single end product and use the Embden-Meyerhof-Parnas pathway. Glucose is converted into pyruvic acid, and this is further reduced to LA. The theoretical maximum yield of the homofermentative process is 2 mol of LA per gram of glucose consumed (1 g of product per gram of substrate). It is a reality that theoretical yields are not always achieved due to the utilization of carbon sources in the biomass generation process. The yields obtained in experiments range between 0.74 and -0.99 g/g [46].

1.26. Challenges of LA production through biosynthesis

Most LAB are sophisticated organisms that require complicated nutrients to develop and produce LA. As fermentation occurs at such a low temperature, there is a possibility of contamination. To address this issue, thermotolerant bacteria *Bacillus* have been identified and cultured specifically for the generation of LA. Some Bacillus species, including *Bacillus coagulans*, *Bacillus subtilis*, *Bacillus stearothermophilus*, and *Bacillus sp*., have also been found to produce lactic acid via the homofermentative process. *Bacillus ssp*. has several benefits over LAB: (i) *Bacillus ssp* can replicate and generate LA on mineral salt media with a minimum amount of nitrogen[163], (ii) *Bacillus ssp.* can produce LA at high fermentation temperature (≥50 °C), and this ability of *Bacillus spp* may create the possibility of open fermentation and non-sterilized media [164]. Bacillus strains are capable of fermenting both C6 and C5 sugar streams or lignocellulosic biomass hydrolysate to LA.

However, to utilize lignocellulosic biomass successfully, many obstacles must be overcome: (i) a green and efficient pretreatment procedure is required to deconstruct the biomass's resistive nature. (ii) hydrolysate that contains fewer inhibiting chemicals needs to be generated (iii) the pretreatment procedure should be regulated to obtain a single-sugar

hydrolysate to avoid the inhibition of carbon catabolite activity produced by the heterogeneity of the hydrolysate-sugar composition.

1.27. Fermentation of sugar into ethanol

Zymomonas mobilis, Saccharomyces cerevisiae, and Clostridium thermocellum, Escherichia coli, have established themselves as ubiquitous bioethanol fermentation microorganisms. *S. cerevisiae* is industrial yeast with a lengthy history of fermentation and a high tolerance for ethanol [165]. *Z. mobilis* is a bacterium that produces ethanol 2.5 times faster than *S. cerevisiae* and can achieve greater than 90% of the theoretical yield [166]. E. coli, the conventional bacterial production host, is also used due to its low nutritional requirements for growth and maintenance and its long history of use in recombinant technologies. Similarly, *C. thermocellum*, a thermophilic gram-positive bacterium, is employed because of its unusual ability to spontaneously produce enzymes capable of hydrolyzing a wide variety of plant components and fermenting hydrolysis products formed from cellulose. Each of these microbes offers distinct advantages in the manufacturing of ethanol. None, however, is capable of expressing all of the perfect ethanol production features naturally.

For example, yeasts such as *S. cerevisiae* can ferment at moderate pH and have historically been easier to separate from fermentation substrate than bacteria. Although thermophilic microorganisms such as *C. thermocellum* can ferment at higher temperatures, lowering viscosities, increasing potential substrate loadings, and minimizing the need for cooling, they have less genetic tractability and are less well characterized than *S. cerevisiae* or *E. coli* [166,167].

Compared with certain ethanologenic bacteria, *E. coli* can metabolize pentose carbohydrates but has growth constraints in the presence of glucose due to pentose catabolism inhibition. Additionally, it is less tolerant of ethanol than yeast and more susceptible to environmental factors such as temperature and pH[166]. These flaws do not preclude any of these microorganisms as bioethanol production hosts, but they necessitate the development of novel toxicological mitigation strategies to improve their growth and ethanol synthesis characteristics if they are to usher in a new era of commercially viable bioethanol production.

1.28. Bio jet fuel precursors production pathways

Biomass-derived jet fuel has the potential for a near-term, if not long-term, solution for the aviation and military, while having a lesser environmental impact than petroleum-based jet fuel. Regardless of their stage of development, demonstration, or commercialization, numerous bio jet fuel conversion methods have been documented in the literature. The upgrading paths are based on the feedstocks and conversion techniques: (i) sugar-to-jet (STJ), (iii) alcohol-to-jet (ATJ), and (iv) oil-to-jet (OTJ)[65].

(i) Alcohol-to-jet (ATJ)

Catalytic dehydration can be used to convert alcohols to their alkene counterparts. The carbon chain is stretched to the range of jet fuel by oligomerizing the alkenes. Hydrocarbon fuels that are compatible with jet engines are produced through further hydrogenation [168]. Short C2 and C4 molecules, such as ethanol and butanol are frequently employed in the ATJ pathway.

However, this strategy has run into several challenges, the most notable of which are the efficient release of fermentable sugars from lignocelluloses, the cheap cost of sugar conversion to alcohols, and the precise regulation of oligomerization to reach carbon lengths comparable to jet fuel.

(ii) Gas-to-jet (GTJ)

Fischer Tropsch is a catalytic process for converting syngas (CO and H_2) produced during biomass gasification to liquid straight-chain hydrocarbon fuels [172]. The catalyst, the process pressure, and the temperature all affect the range of hydrocarbons produced [173]. Jet fuel produced using the FT technique from various feedstocks shares several characteristics, such as a lack of sulfur and aromatics [174]. However, The GTJ route's high complexity is an impediment to commercialization. Indeed, this technique is only economically viable at large scales, which is detrimental when employing low energy density feedstocks like biomass [178].

(iii) Oil-to-jet (OTJ)

The OTJ conversion pathway includes three processes: hydro-treated depolymerized cellulosic jet (HRJ), also known as HEFA; catalytic hydro-thermolysis (CH), also known as hydrothermal liquefaction; and hydro-treated depolymerized cellulosic jet (HDCJ), also known as fast pyrolysis with upgrading to jet fuel. Catalytic hydrotreating is a process that transforms

vegetable oils and related feedstocks to jet fuel-grade liquid hydrocarbon fuels [179]. This approach allows the progressive removal of oxygen from biomass feedstocks through catalytic reactions conducted at moderate to high temperatures (250–400°C) and high hydrogen pressures (20–100 bar).

While promising results have been obtained using relatively pure vegetable oils and free fatty acids, hydrotreating less expensive waste feedstocks poses a challenge due to the presence of impurities (e.g., sulfur, nitrogen, alkali, and phosphorus) that can deactivate the catalysts. While hydrotreating yields linear and slightly branched alkanes, it typically fails to yield essential components of jet fuel such as cyclo-alkanes and aromatics.

(iv) Sugar-to-jet (STJ)

Transforming biomass into platform chemicals, then chemically or biologically converting the chemicals into hydrocarbon molecules in the range of jet fuel, is the platform chemical pathway to bio-jet fuel generation. The following factors should be included or considered in the procedure for manufacturing bio-jet fuel using the platform chemicals pathway: (1) Pretreatment to break down the cross-linked structure of lignocellulose to fractionate the biomass components; (2) Enzymatic, biological, or chemical conversion of cellulose, hemicellulose, and lignin into monomers such as hexoses, pentoses, and phenols; (3) Transformation of the resultant monomers into platform chemicals such as furfural, HMF, and phenols [181], levulinic acid [182], and γ-valerolactone [183]. (4) carbon chain extension processes such as HAA, aldol condensation, and ketonization are used because the carbon atoms in lignocellulose-based platform chemicals are often insufficient to meet the needs of jet fuel. [184], and oligomerization [185] should be used to obtain oxygenate precursors;

(5) The oxygen-containing precursors must then be treated through hydrodeoxygenation (HDO) to produce hydrocarbon liquid products; and (6) the resulting hydrocarbon liquid products may not fully meet the physical and chemical properties of existing fossil-based jet fuel, which requires further upgrading. Non-alcoholic compounds created from lignocellulosic biomass, such as HMF, furfural, and γ-valerolactone, are referred to as "platform chemicals" and can be used to make jet fuel.

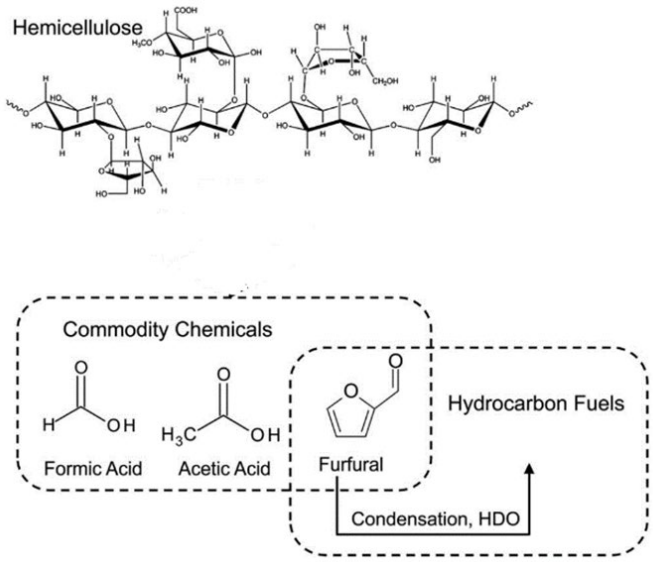

Figure 1.8. Commodity chemical and transportation fuel production from xylans

Furfural generation: however, is the preferred option for jet fuels as furfural can be converted to high-yielding jet fuel range alkanes (Figure 1.8). Mixed heterocyclic oxygenates with high octane values that are well suited for gasoline mixing, yet mixed heterocyclic species are difficult to convert to jet fuel-appropriate hydrocarbons. Furfural can be converted to a variety of range alkanes for use in aviation fuel[186,187]. Hydroalkylation (HAA) followed by hydrodeoxygenation can also be used to upgrade furfural to diesel fuel range components [186,188]. To expand the carbon backbone of precursor compounds, 2-methyl furan derived from furfural is hydroalkylated with aldehydes and ketones such as furfural or acetone. These precursor molecules can then be hydrodeoxygenated to create hydrocarbons in the diesel fuel spectrum.

In this study, model furfural and cyclopentanone into jet fuel precursors such as 2, 5-bis(2-furylmethylidene) cyclopentanone (F_2Cp) and 2-(2-furylmethylidene) cyclopentanone (FCp) through aldol condensation was performed as a proof of concept (Figure 1.9). The success gained in this work will pave the way for valorizing furfural from lignocellulosic biomass into bio jet fuel precursors.

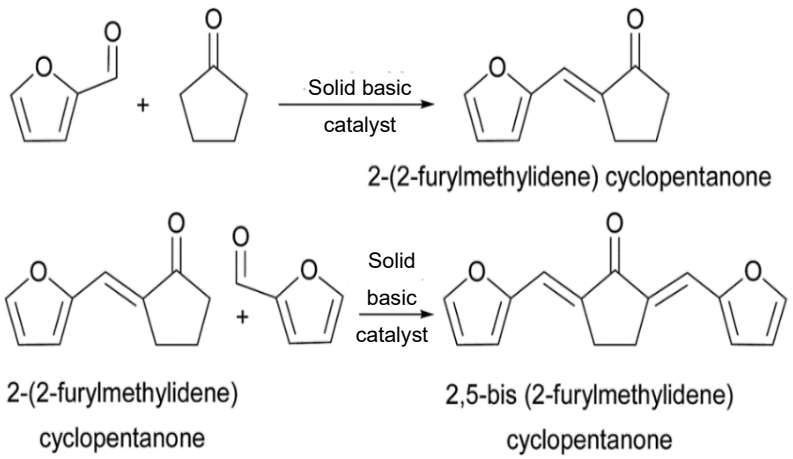

Figure 1.9. Aldol condensation of furfural and cyclopentanone

1.29. Aldol condensation

Aldol condensation catalyzed by acid or alkali, is a crucial stage in the organic synthesis process. The transition of molecules with active α-hydrogen atoms is involved (such as carboxylic acid, aldehyde, ketone, and ester), followed by nucleophilic addition to making β-hydroxyl compounds, and further dehydration to form α, β-unsaturated carbonyl compounds.The number of carbonyl groups in two species combining to form aldol adducts is governed by equilibrium; however, dehydration favors the reaction and accelerates the creation of the α, β-unsaturated aldehyde. Aldol condensations are particularly useful for biomass upgrading because they easily remove oxygen, increase the carbon to oxygen ratio, and aid in the conversion of oxygenates generated by biomass to liquid hydrocarbons[189]. Consequently, this coupling reaction is widely used to transform bio-derived carbonyl compounds into larger products that may be hydrogenated to produce jet and diesel fuels or lubricants. In the presence of a homogeneous or heterogeneous acid, base, or amphoteric catalyst, aldol condensations are usually conducted at mild reaction temperatures (273–473K) (e.g., alkali metals, [190,191] metal oxides, [192,193] amines grafted onto supports,[194] mixed metal oxides, [195,196] and hydroxyapatite) [196]. Stabilization of transition states on acid-base pair sites has resulted in enhanced reaction rates in heterogeneous catalysis systems with acid-base bifunctionality. The reactant molar ratio, [191] the structure of the reactant molecules [197], reaction temperature, [192,198] and the catalyst type [194] all affect the process selectivity toward heavier compounds.

1.30. Solid basic catalyst

Solid metal hydroxides, such as $Mg(OH)_2$, hydrotalcites, and rehydrated hydrotalcites, have been extensively used in a variety of heterogeneous catalytic systems. Hydrotalcites (also known as layered double hydroxides, LDHs) and rehydrated hydrotalcites have demonstrated excellent catalytic performance in various reactions (e.g., aldol, Knoevenagel, and Claisen–Schmidt condensations) due to their abundant surface hydroxyl content (Bronsted–type alkaline sites located in the brucite–like layers)[199]. The structure of base sites can be altered due to varied elements composition and structural design.

1.31. Mixed metal oxides

Compared to single-component metal oxides, mixed metal oxides have shown promise in heterogeneous basic catalytic processes. The use of magnesium and zirconium mixed oxides (Mg-Zr) as solid basic catalysts in the aqueous phase aldol condensation of 5-hydroxymethylfurfural (5-HMF) and acetone for the generation of fuel precursors was examined [203]. Mg-Zr mixed oxide catalyst is the best catalytic performance for the generation of aldol condensation products (yield: 37%), notably for the formation of the second adduct (C15) (yield: 16%). Furthermore, the Mg-Zr catalyst exhibited higher kinetic constants (k_1 and k_2) and a higher concentration of medium-strength alkaline sites than the Mg-Al catalyst.

Due to the heterogeneous structure/property of alkaline sites, many mixed metal oxides exhibit a wide range of behaviors in alkaline-catalyzed processes such as acetone and furfural aldol condensation. It was discovered that the activity and selectivity of three distinct mixed metal oxide catalysts (Mg–Zr, Mg-Al, and Ca–Zr) for aldol condensation of acetone and furfural were related to their physicochemical properties [204]. The Mg–Zr mixed oxide catalyst containing the highest concentration of alkaline sites (especially medium-strength alkaline sites) exhibits the maximum activity and selectivity for the C13 fraction; whereas acetone/furfural exhibits a molar ratio of 1:1 (atomic yield more than 60%).

The final products and their kinetic dependence on the reactant concentration are consistent with a catalytic mechanism, where enolate species formation is the rate-determining step. The researchers have discovered that the rates of C8 formation are first-order dependent on the concentration of acetone and zeroth-order depending on the concentration of furfural;

whereas, the rates of C13 creation are first and zeroth-order dependent on the concentration of C8 and furfural, respectively.

1.32. References

[1] Carus M, Dammer L. The Circular Bioeconomy - Concepts, Opportunities, and Limitations. Industrial Biotechnology 2018; 14:83–91. doi: 10.1089/ind.2018.29121.mca.

[2] Foundation EM. Towards a Circular Economy: Business Rationale for an Accelerated Transition. Ellen MacArthur Foundation (EMF) 2015:20.

[3] Merli R, Preziosi M, Acampora A. How do scholars approach the circular economy? A systematic literature reviews. Journal of Cleaner Production 2018; 178:703–22. doi: 10.1016/j.jclepro.2017.12.112.

[4] Andersen MS. An introductory note on the environmental economics of the circular economy. Sustainability Science 2007; 2:133–40. doi:10.1007/s11625-006-0013-6.

[5] European Commission. An EU action plan for the Circular Economy. Http://Eur-Lexeuropaeu/Resourcehtml?Uri=cellar:8a8ef5e8-99a0-11e5-B3b7-01aa75ed71a1001203/DOC_1&format=HTML&lang=EN&parentUrn=COM:2015:614:FIN2015. http://repositorio.unan.edu.ni/2986/1/5624.pdf.

[6] Augustsson A, Sörme L, Karlsson A, Amneklev J. Persistent Hazardous Waste and the Quest Toward a Circular Economy: The Example of Arsenic in Chromated Copper Arsenate–Treated Wood. Journal of Industrial Ecology 2017; 21:689–99. doi:10.1111/jiec.12516.

[7] McCormick K, Kautto N. The Bioeconomy in Europe: An Overview. Sustainability (Switzerland) 2013; 5:2589–608. doi:10.3390/su5062589.

[8] Pfau SF, Hagens JE, Dankbaar B, Smits AJM. Visions of sustainability in bioeconomy research. Sustainability (Switzerland) 2014; 6:1222–49. doi:10.3390/su6031222.

[9] Hetemäki L, Aho E, Narbona Ruiz C, Persson G, Potočnik J. Leading the way to a European circular bioeconomy strategy. 2017.

[10] European Commission. Expert Group Report: Review of the EU Bioeconomy Strategy and its Action Plan. vol. Publicatio. 2017.

[11] Davis CB, Aid G, Zhu B. Secondary Resources in the Bio-Based Economy: A Computer Assisted Survey of Value Pathways in Academic Literature. Waste and Biomass Valorization 2017; 8:2229–46. doi:10.1007/s12649-017-9975-0.

[12] Lange L. The importance of fungi and mycology for addressing major global challenges. IMA Fungus 2014; 5:463–71. doi:10.5598/imafungus.2014.05.02.10.

[13] Daioglou V, Wicke B, Faaij APC, van Vuuren DP. Competing uses of biomass for energy and chemicals: implications for long-term global CO_2 mitigation potential. GCB Bioenergy 2015; 7:1321–34. doi:10.1111/gcbb.12228.

[14] Worm B, Lotze HK, Jubinville I, Wilcox C, Jambeck J. Plastic as a Persistent Marine Pollutant. Annual Review of Environment and Resources 2017;42:1–26. doi:10.1146/annurev-environ-102016-060700.

[15] Geyer R, Jambeck JR, Law KL. Production, use, and fate of all plastics ever made. Science Advances 2017;3:25–9. doi:10.1126/sciadv.1700782.

[16] Rillig MC. Microplastic in terrestrial ecosystems and the soil? Environmental Science and Technology 2012;46:6453–4. doi:10.1021/es302011r.

[17] Ellen MacArthur Foundation. The New Plastics Economy: Rethinking the future of plastics. Ellen MacArthur Foundation 2016:120.

[18] Zink T, Geyer R, Startz R. Toward Estimating Displaced Primary Production from Recycling: A Case Study of U.S. Aluminum. Journal of Industrial Ecology 2018;22:314–26. doi:10.1111/jiec.12557.

[19] Hidalgo-Ruz V, Gutow L, Thompson RC, Thiel M. Microplastics in the marine environment: A review of the methods used for identification and quantification. Environmental Science and Technology 2012;46:3060–75. doi:10.1021/es2031505.

[20] Wright SL, Kelly FJ. Plastic and Human Health: A Micro Issue? Environmental Science and Technology 2017;51:6634–47. doi:10.1021/acs.est.7b00423.

[21] Yang D, Shi H, Li L, Li J, Jabeen K, Kolandhasamy P. Microplastic Pollution in Table Salts from China. Environmental Science and Technology 2015;49:13622–7. doi:10.1021/acs.est.5b03163.

[22] GESAMP Joint Group of Experts on the Scientific Aspects of Marine Environmental Protection. Sources, fate and effects of microplastics in the marine environment: part 2 of a global assessment. (IMO, FAO/UNESCO-IOC/UNIDO/WMO/IAEA/UN/UNEP/UNDP). In: Kershaw, P.J. (Ed.), Rep. Stud. GESAMP No. 90 (96 pp). Reports and Studies GESAMP, No 93, 96 P 2016;93.

[23] Dris R, Gasperi J, Saad M, Mirande C, Tassin B. Synthetic fibers in atmospheric fallout: A source of microplastics in the environment? Marine Pollution Bulletin 2016;104:290–3. doi:10.1016/j.marpolbul.2016.01.006.

[24] Gall SC, Thompson RC. The impact of debris on marine life. Marine Pollution Bulletin 2015;92:170–9. doi:10.1016/j.marpolbul.2014.12.041.

[25] Werner S, Budziak A, Van Franeker J, Galgani F, Hanke G, Maes T, et al. Harm caused by Marine Litter. 2016. doi:10.1590/S1517-83822014005000038.

[26] Koelmans AA, Besseling E, Foekema E, Kooi M, Mintenig S, Ossendorp BC, et al. Risks of Plastic Debris: Unravelling Fact, Opinion, Perception, and Belief. Environmental Science and Technology 2017;51:11513–9. doi:10.1021/acs.est.7b02219.

[27] Hussain N, Jaitley V, Florence AT. Recent advances in the understanding of uptake of microparticulates across the gastrointestinal lymphatics. Advanced Drug Delivery Reviews 2001;50:107–42. doi:10.1016/S0169-409X(01)00152-1.

[28] Revel M, Châtel A, Mouneyrac C. Micro(nano)plastics: A threat to human health? Current Opinion in Environmental Science and Health 2018;1:17–23. doi:10.1016/j.coesh.2017.10.003.

[29] Powell JJ, Thoree V, Pele LC. Dietary microparticles and their impact on tolerance and immune responsiveness of the gastrointestinal tract. British Journal of Nutrition 2007;98:59–63. doi:10.1017/S0007114507832922.

[30] Karl TR, Trenberth KE. Modern Global Climate Change. Science 2003;302:1719–23. doi:10.1126/science.1090228.

[31] Wuebbles DJ, Jain AK. Concerns about climate change and the role of fossil fuel use. Fuel Processing Technology 2001;71:99–119. doi:10.1016/S0378-3820(01)00139-4.

[32] Ravishankara AR, Rudich Y, Pyle JA. Role of Chemistry in Earth's Climate. Chemical Reviews 2015;115:3679–81. doi:10.1021/acs.chemrev.5b00226.

[33] IPCC. IPCC CLIMATE CHANGE 2013 Climate Change 2013. 2013. doi:10.1017/CBO9781107415324.Summary.

[34] Doney SC, Fabry VJ, Feely RA, Kleypas JA. Ocean acidification: The other CO2 problem. Annual Review of Marine Science 2009;1:169–92. doi:10.1146/annurev.marine.010908.163834.

[35] Chapman L. Transport and climate change: a review. Journal of Transport Geography 2007;15:354–67. doi:10.1016/j.jtrangeo.2006.11.008.

[36] Potter S. Transport energy and emissions: urban public transport. In: Hensher, D.A., Button, K.J. (Eds.), Handbooks in Transport 4: Handbook of Transport and the Environment. 2003.

[37] IEA. IEA, 2000. International Energy Agency. CO2 Emissions From Fuel Combustions 1971 – 1998., 2000, p. Edition OECD, Paris.

[38] Cairns S, Newson C. Predict and decide: aviation, climate change and policy, 2006.

[39] IPCC. Climate Change 2014: Synthesis Report. Contribution of Working Groups I, II and III to the Fifth Assessment Report of the Intergovernmental Panel on Climate Change. Ipcc 2014:151.

[40] Axsen J, Plamp P, Wolinetz M. Crafting strong, integrated policy mixes for deep CO2 mitigation in road transport. Nature Climate Change 2020. doi:10.1038/s41558-020-0877-y.

[41] Biddy MJ, Scarlata CJ, Kinchin CM. Chemicals from biomass: A market assessment of bioproducts with near-term potential. NREL Report 2016. doi:10.2172/1244312.

[42] Grandview R. Grand View Research : Lactic Acid Market Growth & Trends https://www.grandviewresearch.com/press-release/global-lactic-acid-and-poly-lactic-acid-market accessed on 9/25/2020 2020:2020.

[43] Thongwai R. Production of L- (+) Lactic Acid From Blackstrap Molasses by Lactobacillus Casei Subspecies Rhamnosus ATCC 11443 1999:15–22.

[44] Islam Aljundi. Fermentation and Separation of lactic acid. 2000.

[45] M. Dworkin, S. Falkow, E. Rosenberg, K. H. Schleifer ES. Organic Acid and Solvent Production, Springer, New York, 2006, pp. 2006.

[46] Castillo Martinez FA, Balciunas EM, Salgado JM, Domínguez González JM, Converti A, Oliveira RP de S. Lactic acid properties, applications and production: A review. Trends in Food Science and Technology 2013;30:70–83. doi:10.1016/j.tifs.2012.11.007.

[47] John RP, Nampoothiri KM, Pandey A. Simultaneous saccharification and fermentation of cassava bagasse for L-(+)-lactic acid production using Lactobacilli. Applied Biochemistry and Biotechnology 2006;134:263–72. doi:10.1385/ABAB:134:3:263.

[48] Anders Sodergard MS. Properties of polylactic acid fiber based polymers and their correlation with composition. Progress in Polymer Science 2007;27:1123–63.

[49] Papagaroufalis K, Fotiou A, Egli D, Tran L-A, Steenhout P. A Randomized Double Blind Controlled Safety Trial Evaluating D-Lactic Acid Production in Healthy Infants Fed a Lactobacillus reuteri -containing Formula . Nutrition and Metabolic Insights 2014;7:NMI.S14113. doi:10.4137/nmi.s14113.

[50] John RP, Nampoothiri KM, Pandey A. Fermentative production of lactic acid from biomass: An overview on process developments and future perspectives. Applied Microbiology and Biotechnology 2007;74:524–34. doi:10.1007/s00253-006-0779-6.

[51] Vink ETH, Davies S, Kolstad JJ. The eco-profile for current Ingeo® polylactide production. Industrial Biotechnology 2010;6:212–24. doi:10.1089/ind.2010.6.212.

[52] Chum HLEWJEASICM. A comparison of commercial ethanol production systems from Brazilian sugarcane and US corn. Biofuels, Bioproducts and Biorefining 2014:205–23. doi:10.1002/bbb.

[53] Sims REH, Mabee W, Saddler JN, Taylor M. An overview of second generation biofuel technologies. Bioresource Technology 2010;101:1570–80. doi:10.1016/j.biortech.2009.11.046.

[54] Charles D. Corn-based ethanol flunks key test. Science 2009;324:587. doi:10.1126/science.324_587.

[55] Axelsson L, Franzén M, Ostwald M, Berndes G, Lakshmi G, Ravindranath NH. Perspective: Jatropha cultivation in southern India: Assessing farmers' experiences. Biofuels, Bioproducts and Biorefining 2012;6:246–56. doi:10.1002/bbb.

[56] Sun Y, Cheng J. Hydrolysis of lignocellulosic materials for ethanol production: A review. Bioresource Technology 2002;83:1–11. doi:10.1016/S0960-8524(01)00212-7.

[57] Kim S, Dale BE. Energy and greenhouse gas profiles of polyhydroxybutyrates derived from corn grain: A life cycle perspective. Environmental Science and Technology 2008;42:7690–5. doi:10.1021/es8004199.

[58] Kim S, Dale BE. Global potential bioethanol production from wasted crops and crop residues. Biomass and Bioenergy 2004;26:361–75. doi:10.1016/j.biombioe.2003.08.002.

[59] Cardona CA, Sánchez ÓJ. Fuel ethanol production: Process design trends and integration opportunities. Bioresource Technology 2007;98:2415–57. doi:10.1016/j.biortech.2007.01.002.

[60] Sánchez ÓJ, Cardona CA. Trends in biotechnological production of fuel ethanol from different feedstocks. Bioresource Technology 2008;99:5270–95. doi:10.1016/j.biortech.2007.11.013.

[61] HINMAN CEWND. Ethanol: Fundamentals of Production from Renewable Feedstocks and Use as a Transportation Fuel Fundamentals of Production from Renewable Feedstocks and Use as a Transportation Fuel. Applied Biochemistry and Biotechnology 1990;24/25:735–53. doi:10.1007/bf02920291.

[62] Kohse-Höinghaus K, Oßwald P, Cool TA, Kasper T, Hansen N, Qi F, et al. Biofuel combustion chemistry: From ethanol to biodiesel. Angewandte Chemie - International Edition 2010;49:3572–97. doi:10.1002/anie.200905335.

[63] Braun-Unkhoff M, Riedel U. Alternative fuels in aviation. CEAS Aeronautical Journal 2015;6:83–93. doi:10.1007/s13272-014-0131-2.

[64] Launch of the European Advanced Biofuels Flightpath. Available online: https://ec.europa.eu/energy/sites/ener/files/20110622_biofuels_flight_path_launch.pdf (accessed on 12/08.2021) n.d.

[65] Wang W-C, Tao L, Markham J, Zhang Y, Tan E, Batan L, et al. Review of Biojet Fuel Conversion Technologies. National Renewable Energy Laboratory, Technical Report NREL/TP-5100-66291. 2016:98.

[66] Agusdinata DB, Zhao F, Ileleji K, Delaurentis D. Life cycle assessment of potential biojet fuel production in the United States. Environmental Science and Technology 2011;45:9133–43. doi:10.1021/es202148g.

[67] Carlson TR, Cheng YT, Jae J, Huber GW. Production of green aromatics and olefins by catalytic fast pyrolysis of wood sawdust. Energy and Environmental Science 2011;4:145–61. doi:10.1039/c0ee00341g.

[68] Bond JQ, Alonso DM, Wang D, West RM, Dumesic JA. Integrated catalytic conversion of γ-valerolactone to liquid alkenes for transportation fuels. Science 2010;327:1110–4. doi:10.1126/science.1184362.

[69] Wright MM, Satrio JA, Brown RC, Daugaard DE, Hsu DD. Techno-economic analysis of biomass fast pyrolysis to transportation fuels. Technical Report NREL/TP-6A20-46586. Nrel 2010;89:463–9.

[70] Chandel AK, Singh O V. Weedy lignocellulosic feedstock and microbial metabolic engineering: Advancing the generation of "Biofuel." Applied Microbiology and Biotechnology 2011;89:1289–303. doi:10.1007/s00253-010-3057-6.

[71] Soltanian S, Aghbashlo M, Almasi F, Hosseinzadeh-Bandbafha H, Nizami AS, Ok YS, et al. A critical review of the effects of pretreatment methods on the exergetic aspects of lignocellulosic biofuels. Energy Conversion and Management 2020;212:112792. doi:10.1016/j.enconman.2020.112792.

[72] Sundararajan PR, Rao VSR. Conformational Studies of p-~-l,4'-Xylan* 1969;8:305–12.

[73] Dumitriu Severian. Polysaccharides structural diversity and functional versatility. 1998.

[74] Kondo T. Hydrogen Bonds in Cellulose and Cellulose Derivatives. Polysaccharides 2004. doi:10.1201/9781420030822.ch3.

[75] Pérez S, Mazeau K. Conformations, Structures, and Morphologies of Celluloses. Polysaccharides 2004. doi:10.1201/9781420030822.ch2.

[76] Tashiro K, Kobayashi M. Theoretical evaluation of three-dimensional elastic constants of native and regenerated celluloses: role of hydrogen bonds. Polymer 1991;32:1516–26. doi:10.1016/0032-3861(91)90435-L.

[77] Caffall KH, Mohnen D. The structure, function, and biosynthesis of plant cell wall pectic polysaccharides. Carbohydrate Research 2009;344:1879–900. doi:10.1016/j.carres.2009.05.021.

[78] Wolf WJ. Soybean proteins: Their production, properties, and food uses. A selected bibliography. Journal of the American Oil Chemists' Society 1974;51:51–4. doi:10.1007/BF02542093.

[79] Saha BC. Hemicellulose bioconversion. Journal of Industrial Microbiology and Biotechnology 2003;30:279–91. doi:10.1007/s10295-003-0049-x.

[80] Bobleter O. Hydrothermal degradation of polymers derived from plants. Progress in Polymer Science 1994;19:797–841. doi:10.1016/0079-6700(94)90033-7.

[81] G. Garrote. Hydrothermal processing of lignocellulosic materials. Holz Roh Werkst 1999;57:191–202.

[82] Feldman D. Wood—chemistry, ultrastructure, reactions, by D. Fengel and G. Wegener, Walter de Gruyter, Berlin and New York, 1984, 613 pp. Price: 245 DM. Journal of Polymer Science: Polymer Letters Edition 1985;23:601–2. doi:10.1002/pol.1985.130231112.

[83] LeVan SL, Ross RJ, Winandy JE. Effects of fire retardant chemicals on the bending properties of wood at elevated temperatures. Forest Product Laboratory, Forest Service 1990:26.

[84] Whetten RW, MacKay JJ, Sederoff RR. Recent advances in understanding lignin biosynthesis. Annual Review of Plant Biology 1998;49:585–609. doi:10.1146/annurev.arplant.49.1.585.

[85] Tao YZ GY. Study of chemical composition of lignin and its application. J Cellul Sci Technol 2003;11:42–55.

[86] H. V. Lee, S. B. A. Hamid and SKZ. Conversion of Lignocellulosic Biomass to Nanocellulose: Structure and Chemical Process. The Scientific World Journal 2014:1–20.

[87] Tarasov D, Leitch M, Fatehi P. Lignin-carbohydrate complexes: Properties, applications, analyses, and methods of extraction: A review. Biotechnology for Biofuels 2018;11:1–28. doi:10.1186/s13068-018-1262-1.

[88] Giummarella N, Pu Y, Ragauskas AJ, Lawoko M. A critical review on the analysis of lignin carbohydrate bonds. Green Chemistry 2019;21:1573–95. doi:10.1039/c8gc03606c.

[89] Gupta R, Khasa YP, Kuhad RC. Evaluation of pretreatment methods in improving the enzymatic saccharification of cellulosic materials. Carbohydrate Polymers 2011;84:1103–9. doi:10.1016/j.carbpol.2010.12.074.

[90] Mosier N, Wyman C, Dale B, Elander R, Lee YY, Holtzapple M, et al. Features of promising technologies for pretreatment of lignocellulosic biomass 2005;96:673–86. doi:10.1016/j.biortech.2004.06.025.

[91] Lynd LR, Wyman CE, Gerngross TU. Biocommodity engineering. Biotechnology Progress 1999;15:777–93. doi:10.1021/bp990109e.

[92] Mandal A, Chakrabarty D. Isolation of nanocellulose from waste sugarcane bagasse (SCB) and its characterization. Carbohydrate Polymers 2011;86:1291–9. doi:10.1016/j.carbpol.2011.06.030.

[93] Palmqvist E, Hahn-Hägerdal B. Fermentation of lignocellulosic hydrolysates. I: Inhibition and detoxification. Bioresource Technology 2000;74:17–24. doi:10.1016/S0960-8524(99)00160-1.

[94] Haque KE. Microwave energy for mineral treatment processes - A brief review. International Journal of Mineral Processing 1999;57:1–24. doi:10.1016/s0301-7516(99)00009-5.

[95] Gonzalez A, Hendriks ATWM, van Lier JB, de Kreuk M. Pre-treatments to enhance the biodegradability of waste activated sludge: Elucidating the rate limiting step. Biotechnology Advances 2018;36:1434–69. doi:10.1016/j.biotechadv.2018.06.001.

[96] Karlsson M, Carlsson H, Idebro M, Eek C. Microwave Heating as a Method to Improve Sanitation of Sewage Sludge in Wastewater Plants. IEEE Access 2019;7:142308–16. doi:10.1109/ACCESS.2019.2944210.

[97] Surat M a., Jauhari S, Desak KR. A brief review : Microwave assisted organic reaction. Applied Science Research 2012;4:645–61.

[98] Anthony G. Collins SM and SGP. Microwave Heating for Sludge Dewatering and Drying. Research Journal of the Water Pollution Control Federation 2014;63:921–4.

[99] Shah J, Mohanraj K. Comparison of conventional and microwave-assisted synthesis of benzotriazole derivatives. Indian Journal of Pharmaceutical Sciences 2014;76:46–53.

[100] de la Hoz A, Díaz-Ortiz À, Moreno A. Microwaves in organic synthesis. Thermal and non-thermal microwave effects. Chemical Society Reviews 2005;34:164–78. doi:10.1039/b411438h.

[101] Mokhtar NM, Omar R, Idris A. Microwave pyrolysis for conversion of materials to energy: A brief review. Energy Sources, Part A: Recovery, Utilization and Environmental Effects 2012;34:2104–22. doi:10.1080/15567036.2010.493923.

[102] Miura M, Kaga H, Sakurai A, Kakuchi T, Takahashi K. Rapid pyrolysis of wood block by microwave heating. Journal of Analytical and Applied Pyrolysis 2004;71:187–99. doi:10.1016/S0165-2370(03)00087-1.

[103] Wu TN. Environmental perspectives of microwave applications as remedial alternatives: Review. Practice Periodical of Hazardous, Toxic, and Radioactive Waste Management 2008;12:102–15. doi:10.1061/(ASCE)1090-025X(2008)12:2(102).

[104] Morgan HM, Bu Q, Liang J, Liu Y, Mao H, Shi A, et al. A review of catalytic microwave pyrolysis of lignocellulosic biomass for value-added fuel and chemicals. Bioresource Technology 2017;230:112–21. doi:10.1016/j.biortech.2017.01.059.

[105] Nüchter M, Ondruschka B, Bonrath W, Gum A. Microwave assisted synthesis – a critical technology overview. Green Chemistry 2004;6:128–41. doi:10.1039/b310502d.

[106] (Eds.) FK· AS. Broadband dielectric spectroscopy. 2003. doi:10.1016/b978-0-12-823518-8.00001-3.

[107] Kappe CO, Stadler A, Dallinger D. Microwaves in Organic and Medicinal Chemistry. Microwaves in Organic and Medicinal Chemistry 2012:1–668. doi:10.1002/9783527647828.

[108] Kappe CO. Controlled microwave heating in modern organic synthesis. Angewandte Chemie - International Edition 2004;43:6250–84. doi:10.1002/anie.200400655.

[109] Lam SS, Chase HA. A review on waste to energy processes using microwave pyrolysis. Energies 2012;5:4209–32. doi:10.3390/en5104209.

[110] Li Q, Guo C, Liu CZ. Dynamic microwave-assisted alkali pretreatment of cornstalk to enhance hydrogen production via co-culture fermentation of Clostridium thermocellum and Clostridium thermosaccharolyticum. Biomass and Bioenergy 2014;64:220–9. doi:10.1016/j.biombioe.2014.03.053.

[111] Fan YT, Zhang YH, Zhang SF, Hou HW, Ren BZ. Efficient conversion of wheat straw wastes into biohydrogen gas by cow dung compost. Bioresource Technology 2006;97:500–5. doi:10.1016/j.biortech.2005.02.049.

[112] Liu J, Takada R, Karita S, Watanabe T, Honda Y, Watanabe T. Microwave-assisted pretreatment of recalcitrant softwood in aqueous glycerol. Bioresource Technology 2010;101:9355–60. doi:10.1016/j.biortech.2010.07.023.

[113] Keshwani DR, Cheng JJ. Microwave-Based Alkali Pretreatment of Switchgrass and Coastal Bermudagrass for Bioethanol Production 2009. doi:10.1002/btpr.371.

[114] Sapci Z. Bioresource Technology The effect of microwave pretreatment on biogas production from agricultural straws. Bioresource Technology 2013;128:487–94. doi:10.1016/j.biortech.2012.09.094.

[115] Diaz AB, Maria M, Moretti DS, Bezerra-bussoli C, Carreira C, Blandino A, et al. Evaluation of microwave-assisted pretreatment of lignocellulosic biomass immersed in alkaline glycerol for fermentable sugars production. BIORESOURCE TECHNOLOGY 2015. doi:10.1016/j.biortech.2015.02.112.

[116] Bundhoo ZMA. Microwave-assisted conversion of biomass and waste materials to biofuels. Renewable and Sustainable Energy Reviews 2018;82:1149–77. doi:10.1016/j.rser.2017.09.066.

[117] Akhtar N, Goyal D, Goyal A. Characterization of microwave-alkali-acid pre-treated rice straw for optimization of ethanol production via simultaneous saccharification and fermentation (SSF). Energy Conversion and Management 2017;141:133–44. doi:10.1016/j.enconman.2016.06.081.

[118] Chen WH, Tu YJ, Sheen HK. Disruption of sugarcane bagasse lignocellulosic structure by means of dilute sulfuric acid pretreatment with microwave-assisted heating. Applied Energy 2011;88:2726–34. doi:10.1016/j.apenergy.2011.02.027.

[119] Zhu S, Wu Y, Yu Z, Liao J, Zhang Y. Pretreatment by microwave/alkali of rice straw and its enzymic hydrolysis. Process Biochemistry 2005;40:3082–6. doi:10.1016/j.procbio.2005.03.016.

[120] Zhu S, Wu Y, Yu Z, Chen Q, Wu G, Yu F, et al. Microwave-assisted Alkali Pre-treatment of Wheat Straw and its Enzymatic Hydrolysis. Biosystems Engineering 2006;94:437–42. doi:10.1016/j.biosystemseng.2006.04.002.

[121] Lu X, Xi B, Zhang Y, Angelidaki I. Microwave pretreatment of rape straw for bioethanol production: Focus on energy efficiency. Bioresource Technology 2011;102:7937–40. doi:10.1016/j.biortech.2011.06.065.

[122] Laghari SM, Isa MH, Laghari AJ. Delignification of palm fiber by microwave assisted chemical pretreatment for improving energy efficiency. Malaysian Journal of Science 2016;35:8–14. doi:10.22452/mjs.vol35no1.2.

[123] Liu CZ, Cheng XY. Improved hydrogen production via thermophilic fermentation of corn stover by microwave-assisted acid pretreatment. International Journal of Hydrogen Energy 2010;35:8945–52. doi:10.1016/j.ijhydene.2010.06.025.

[124] Singh A, Bishnoi NR. Enzymatic hydrolysis optimization of microwave alkali pretreated wheat straw and ethanol production by yeast. Bioresource Technology 2012;108:94–101. doi:10.1016/j.biortech.2011.12.084.

[125] Mbous YP, Hayyan M, Hayyan A, Wong WF, Hashim MA, Looi CY. Applications of deep eutectic solvents in biotechnology and bioengineering—Promises and challenges. Biotechnology Advances 2017;35:105–34. doi:10.1016/j.biotechadv.2016.11.006.

[126] Vigier KDO, Chatel G, Jérôme F. Contribution of deep eutectic solvents for biomass processing: Opportunities, challenges, and limitations. ChemCatChem 2015;7:1250–60. doi:10.1002/cctc.201500134.

[127] Agrawal R, Satlewal A, Gaur R, Mathur A, Kumar R, Gupta RP, et al. Pilot scale pretreatment of wheat straw and comparative evaluation of commercial enzyme preparations for biomass saccharification and fermentation. Biochemical Engineering Journal 2015;102:54–61. doi:10.1016/j.bej.2015.02.018.

[128] Akinosho H, Rydzak T, Borole A, Ragauskas A, Close D. Toxicological challenges to microbial bioethanol production and strategies for improved tolerance. Ecotoxicology 2015;24:2156–74. doi:10.1007/s10646-015-1543-4.

[129] Yoo CG, Pu Y, Ragauskas AJ. Ionic liquids: Promising green solvents for lignocellulosic biomass utilization. Current Opinion in Green and Sustainable Chemistry 2017;5:5–11. doi:10.1016/j.cogsc.2017.03.003.

[130] Loow YL, Wu TY, Yang GH, Ang LY, New EK, Siow LF, et al. Deep eutectic solvent and inorganic salt pretreatment of lignocellulosic biomass for improving xylose recovery. Bioresource Technology 2018;249:818–25. doi:10.1016/j.biortech.2017.07.165.

[131] Alonso DA, Baeza A, Chinchilla R, Guillena G, Pastor IM, Ramón DJ. Deep Eutectic Solvents : The Organic Reaction Medium of the Century 2016:612–32. doi:10.1002/ejoc.201501197.

[132] Zhao H, Baker GA. Ionic liquids and deep eutectic solvents for biodiesel synthesis: A review. Journal of Chemical Technology and Biotechnology 2013;88:3–12. doi:10.1002/jctb.3935.

[133] Scelsi E, Angelini A, Pastore C. Deep Eutectic Solvents for the Valorisation of Lignocellulosic Biomasses towards Fine Chemicals. Biomass 2021;1:29–59. doi:10.3390/biomass1010003.

[134] Abbott AP, Capper G, Davies DL, Rasheed RK, Tambyrajah V. Novel solvent properties of choline chloride/urea mixtures. Chemical Communications 2003:70–1. doi:10.1039/b210714g.

[135] Smith EL, Abbott AP, Ryder KS. Deep Eutectic Solvents (DESs) and Their Applications. Chemical Reviews 2014;114:11060–82. doi:10.1021/cr300162p.

[136] García G, Aparicio S, Ullah R, Atilhan M. Deep eutectic solvents: Physicochemical properties and gas separation applications. Energy and Fuels 2015;29:2616–44. doi:10.1021/ef5028873.

[137] Shahbaz K, Mjalli FS, Hashim MA, Alnashef IM. Prediction of deep eutectic solvents densities at different temperatures. Thermochimica Acta 2011;515:67–72. doi:10.1016/j.tca.2010.12.022.

[138] Chen Z, Greaves TL, Warr GG, Atkin R. Mixing cations with different alkyl chain lengths markedly depresses the melting point in deep eutectic solvents formed from alkylammonium bromide salts and urea. Chemical Communications 2017;53:2375–7. doi:10.1039/c7cc00201g.

[139] Van Osch DJGP, Kollau LJBM, Van Den Bruinhorst A, Asikainen S, Rocha MAA, Kroon MC. Ionic liquids and deep eutectic solvents for lignocellulosic biomass fractionation. Physical Chemistry Chemical Physics 2017;19:2636–65. doi:10.1039/c6cp07499e.

[140] Abo-Hamad A, Hayyan M, AlSaadi MAH, Hashim MA. Potential applications of deep eutectic solvents in nanotechnology. Chemical Engineering Journal 2015;273:551–67. doi:10.1016/j.cej.2015.03.091.

[141] Li M, Pu Y, Ragauskas AJ. Current understanding of the correlation of lignin structure with biomass recalcitrance. Frontiers in Chemistry 2016;4:1–8. doi:10.3389/fchem.2016.00045.

[142] Zulkefli S, Abdulmalek E, Abdul Rahman MB. Pretreatment of oil palm trunk in deep eutectic solvent and optimization of enzymatic hydrolysis of pretreated oil palm trunk. Renewable Energy 2017;107:36–41. doi:10.1016/j.renene.2017.01.037.

[143] Francisco M, Van Den Bruinhorst A, Kroon MC. Low-transition-temperature mixtures (LTTMs): A new generation of designer solvents. Angewandte Chemie - International Edition 2013;52:3074–85. doi:10.1002/anie.201207548.

[144] Liu Y, Chen W, Xia Q, Guo B, Wang Q, Liu S, et al. Efficient Cleavage of Lignin–Carbohydrate Complexes and Ultrafast Extraction of Lignin Oligomers from Wood Biomass by Microwave-Assisted Treatment with Deep Eutectic Solvent. ChemSusChem 2017;10:1692–700. doi:10.1002/cssc.201601795.

[145] Chen Y, Mu T. Application of deep eutectic solvents in biomass pretreatment and conversion. Green Energy and Environment 2019;4:95–115. doi:10.1016/j.gee.2019.01.012.

[146] Kim KH, Eudes A, Jeong K, Yoo CG, Kim CS, Ragauskas A. Integration of renewable deep eutectic solvents with engineered biomass to achieve a closed-loop biorefinery. Proceedings of the National Academy of Sciences of the United States of America 2019;116:13816–24. doi:10.1073/pnas.1904636116.

[147] Xu H, Kong Y, Peng J, Song X, Liu Y, Su Z, et al. Comprehensive analysis of important parameters of choline chloride-based deep eutectic solvent pretreatment of lignocellulosic biomass. Bioresource Technology 2021;319:124209. doi:10.1016/j.biortech.2020.124209.

[148] Beyer MK, Clausen-Schaumann H. Mechanochemistry: The mechanical activation of covalent bonds. Chemical Reviews 2005;105:2921–48. doi:10.1021/cr030697h.

[149] Hick SM, Griebel C, Restrepo DT, Truitt JH, Buker EJ, Bylda C, et al. Mechanocatalysis for biomass-derived chemicals and fuels. Green Chem 2010;12:468–74. doi:10.1039/b923079c.

[150] Meine N, Rinaldi R, Schüth F. Solvent-Free catalytic depolymerization of cellulose to water-soluble oligosaccharides. ChemSusChem 2012;5:1449–54. doi:10.1002/cssc.201100770.

[151] Schüth F, Rinaldi R, Meine N, Käldström M, Hilgert J, Rechulski MDK. Mechanocatalytic depolymerization of cellulose and raw biomass and downstream processing of the products. Catalysis Today 2014;234:24–30. doi:10.1016/j.cattod.2014.02.019.

[152] Loerbroks C, Rinaldi R, Thiel W. The electronic nature of the 1,4-β-glycosidic bond and its chemical environment: DFT insights into cellulose chemistry. Chemistry - A European Journal 2013;19:16282–94. doi:10.1002/chem.201301366.

[153] Banat. IMPNDSAPMU. Ethanol production at elevated temperatures and alcohol concentrations: Part I ± Yeasts in general. World Journal of Microbiology & Biotechnology 14, 2014;14:809–21. doi:10.1023/A.

[154] Ezeji T, Qureshi N, Blaschek HP. Production of acetone-butanol-ethanol (ABE) in a continuous flow bioreactor using degermed corn and Clostridium beijerinckii. Process Biochemistry 2007;42:34–9. doi:10.1016/j.procbio.2006.07.020.

[155] Gao C, Ma C, Xu P. Biotechnological routes based on lactic acid production from biomass. Biotechnology Advances 2011;29:930–9. doi:10.1016/j.biotechadv.2011.07.022.

[156] Abdel-Rahman MA, Tashiro Y, Sonomoto K. Lactic acid production from lignocellulose-derived sugars using lactic acid bacteria: Overview and limits. Journal of Biotechnology 2010;156:286–301. doi:10.1016/j.jbiotec.2011.06.017.

[157] Singh SK, Ahmed SU, Pandey A. Metabolic engineering approaches for lactic acid production. Process Biochemistry 2006;41:991–1000. doi:10.1016/j.procbio.2005.12.004.

[158] Budhavaram NK, Fan Z. Production of lactic acid from paper sludge using acid-tolerant, thermophilic Bacillus coagulan strains. Bioresource Technology 2009;100:5966–72. doi:10.1016/j.biortech.2009.01.080.

[159] Zhou S, Zhou S, Causey TB, Causey TB, Hasona a, Hasona a, et al. Production of Optically Pure. Society 2003;69:399–407. doi:10.1128/AEM.69.1.399.

[160] Zhou S, Shanmugam KT, Ingram LO. Functional replacement of the Escherichia coli D-(-)-lactate dehydrogenase gene (ldhA) with the L-(+)-lactate dehydrogenase gene (ldhL) from Pediococcus acidilactici. Applied and Environmental Microbiology 2003;69:2237–44. doi:10.1128/AEM.69.4.2237-2244.2003.

[161] Hofvendahl K. Factors affecting the fermentative lactic acid production from renewable resources 1 2000;26:87–107.

[162] Abdel-Rahman MA, Tashiro Y, Sonomoto K. Recent advances in lactic acid production by microbial fermentation processes. Biotechnology Advances 2013;31:877–902. doi:10.1016/j.biotechadv.2013.04.002.

[163] Wang Q, Zhao X, Chamu J, Shanmugam KT. Isolation, characterization and evolution of a new thermophilic Bacillus licheniformis for lactic acid production in mineral salts medium. Bioresource Technology 2011;102:8152–8. doi:10.1016/j.biortech.2011.06.003.

[164] Qin J, Zhao B, Wang X, Wang L, Yu B, Ma Y, et al. Non-sterilized fermentative production of polymer-grade L-lactic acid by a newly isolated thermophilic strain bacillus sp. 2-6. PLoS ONE 2009;4:2–6. doi:10.1371/journal.pone.0004359.

[165] GINLEY DSDC. Fundamentals of Materials for Energy and Environmental Sustainability. Cambridge University Press, New York: 2012.

[166] Weber C, Farwick A, Benisch F, Brat D, Dietz H, Subtil T, et al. Trends and challenges in the microbial production of lignocellulosic bioalcohol fuels. Applied Microbiology and Biotechnology 2010;87:1303–15. doi:10.1007/s00253-010-2707-z.

[167] Scully SM, Orlygsson J. Recent advances in second generation ethanol production by thermophilic bacteria. Energies 2015;8:1–30. doi:10.3390/en8010001.

[168] Zhao X, Sun X, Cui X, Liu D. Production of biojet fuels from biomass. Elsevier Inc.; 2019. doi:10.1016/B978-0-12-817654-2.00005-8.

[169] Zhan N, Hu Y, Li H, Yu D, Han Y, Huang H. Lanthanum-phosphorous modified HZSM-5 catalysts in dehydration of ethanol to ethylene: A comparative analysis. Catalysis Communications 2010;11:633–7. doi:10.1016/j.catcom.2010.01.011.

[170] Silvester L, Lamonier JF, Faye J, Capron M, Vannier RN, Lamonier C, et al. Reactivity of ethanol over hydroxyapatite-based Ca-enriched catalysts with various carbonate contents. Catalysis Science and Technology 2015;5:2994–3006. doi:10.1039/c5cy00327j.

[171] Bedia J, Barrionuevo R, Rodríguez-Mirasol J, Cordero T. Ethanol dehydration to ethylene on acid carbon catalysts. Applied Catalysis B: Environmental 2011;103:302–10. doi:10.1016/j.apcatb.2011.01.032.

[172] Sustainable Way for Alternative Fuels and Energy in Aviation: State of the Art on Alternative Fuels in Aviation. Web Version:Https://Edepotwurnl/180370 n.d.

[173] Demirbas MF. Biorefineries for biofuel upgrading : A critical review. Applied Energy 2009;86:S151–61. doi:10.1016/j.apenergy.2009.04.043.

[174] Hileman JI, Ortiz DS, Bartis JT, Wong HM, Donohoo, Pearl E, Weiss MA, et al. Near-Term Feasibility of Alternative Jet Fuels -Technical Report. RAND Corporation and MIT 2009:1–152.

[175] Kreutz TG, Larson ED, Liu G, Williams RH. Fischer-tropsch fuels from coal and biomass. 25th Annual International Pittsburgh Coal Conference, PCC - Proceedings 2008.

[176] Greg Hemighaus, Tracy Boval, Carol Bosley, Roger Organ, John Lind, Rosanne Brouette, Toni Thompson, Joanna Lynch JJ. Alternative Jet Fuels. Chevron Corporation 2006:pg 5-11.

[177] Roberts, William L (Dept of Mech & Aero Eng North NCSU. Bio Jet Fuels. Fuel 2011:1–31.

[178] Rebecca Mawhood, Evangelos Gazis, Sierk de Jong, Ric Hoefnagels RS. Production pathways for renewable jet fuel: a review of commercialization status and future prospects. Biofuels, Bioproducts and Biorefining 2016;6:246–56. doi:10.1002/bbb.

[179] Serrano-Ruiz JC, Ramos-Fernández E V., Sepúlveda-Escribano A. From biodiesel and bioethanol to liquid hydrocarbon fuels: New hydrotreating and advanced microbial technologies. Energy and Environmental Science 2012;5:5638–52. doi:10.1039/c1ee02418c.

[180] Gutiérrez-Antonio C, Gómez-Castro FI, de Lira-Flores JA, Hernández S. A review on the production processes of renewable jet fuel. Renewable and Sustainable Energy Reviews 2017;79:709–29. doi:10.1016/j.rser.2017.05.108.

[181] Chheda JN, Román-Leshkov Y, Dumesic JA. Production of 5-hydroxymethylfurfural and furfural by dehydration of biomass-derived mono- and poly-saccharides. Green Chemistry 2007;9:342–35. doi:10.1039/b611568c.

[182] Sheldon RA. Green and sustainable manufacture of chemicals from biomass: State of the art. Green Chemistry 2014;16:950–63. doi:10.1039/c3gc41935e.

[183] Zhang Z. Synthesis of γ-Valerolactone from Carbohydrates and its Applications. ChemSusChem 2016;9:156–71. doi:10.1002/cssc.201501089.

[184] Wu L, Moteki T, Gokhale AA, Flaherty DW, Toste FD. Production of Fuels and Chemicals from Biomass: Condensation Reactions and Beyond. Chem 2016;1:32–58. doi:10.1016/j.chempr.2016.05.002.

[185] Alonso DM, Bond JQ, Dumesic JA. Catalytic conversion of biomass to biofuels. Green Chemistry 2010;12:1493–513. doi:10.1039/c004654j.

[186] Li G, Li N, Wang Z, Li C, Wang A, Wang X, et al. Synthesis of high-quality diesel with furfural and 2-methylfuran from hemicellulose. ChemSusChem 2012;5:1958–66. doi:10.1002/cssc.201200228.

[187] Corma A, De La Torre O, Renz M. Production of high quality diesel from cellulose and hemicellulose by the Sylvan process: Catalysts and process variables. Energy and Environmental Science 2012;5:6328–44. doi:10.1039/c2ee02778j.

[188] Corma A, De La Torre O, Renz M, Villandier N. Production of high-quality diesel from biomass waste products. Angewandte Chemie - International Edition 2011;50:2375–8. doi:10.1002/anie.201007508.

[189] Anbarasan P, Baer ZC, Sreekumar S, Gross E, Binder JB, Blanch HW, et al. Integration of chemical catalysis with extractive fermentation to produce fuels. Nature 2012;491:235–9. doi:10.1038/nature11594.

[190] O'Lenick AJ. Guerbet Chemistry. Journal of Surfactants and Detergents 2001;4:311–5. doi:10.1007/s11743-001-0185-1.

[191] West RM, Liu ZY, Peter M, Dumesic JA. Liquid alkanes with targeted molecular weights from biomass-derived carbohydrates. ChemSusChem 2008;1:417–24. doi:10.1002/cssc.200800001.

[192] Ji W, Chen Y. Vapour phase aldol condensation of acetaldehyde catalysed by some oxide catalysts. Chinese Journal of Catalysis 1997;18:56–9.

[193] Di Cosimo JI, Díez VK, Ferretti C, Apesteguía CR. Basic catalysis on MgO: Generation, characterization and catalytic properties of active sites. Catalysis 2014;26:1–28. doi:10.1039/9781782620037-00001.

[194] Sankaranarayanapillai S, Sreekumar S, Gomes J, Grippo A, Arab GE, Head-Gordon M, et al. Catalytic Upgrading of Biomass-Derived Methyl Ketones to Liquid Transportation Fuel Precursors by an Organocatalytic Approach. Angewandte Chemie - International Edition 2015;54:4673–7. doi:10.1002/anie.201412470.

[195] Faba L, Díaz E, Ordóñez S. Gas phase acetone self-condensation over unsupported and supported Mg-Zr mixed-oxides catalysts. Applied Catalysis B: Environmental 2013;142–143:387–95. doi:10.1016/j.apcatb.2013.05.043.

[196] Gabriëls D, Hernández WY, Sels BF, Van Der Voort P, Verberckmoes A. Review of catalytic systems and thermodynamics for the Guerbet condensation reaction and challenges for biomass valorization. Catalysis Science and Technology 2015;5:3876–902. doi:10.1039/c5cy00359h.

[197] Climent MJ, Corma A, Iborra S, Velty A. Synthesis of methylpseudoionones by activated hydrotalcites as solid base catalysts. Green Chemistry 2002;4:474–80. doi:10.1039/b205532p.

[198] Salvapati GS, Ramanamurty K V., Janardanarao M. Selective catalytic self-condensation of acetone. Journal of Molecular Catalysis 1989;54:9–30. doi:10.1016/0304-5102(89)80134-8.

[199] Hora L, Kikhtyanin O, Čapek L, Bortnovskiy O, Kubička D. Comparative study of physico-chemical properties of laboratory and industrially prepared layered double hydroxides and their behavior in aldol condensation of furfural and acetone. Catalysis Today 2015;241:221–30. doi:10.1016/j.cattod.2014.03.010.

[200] León M, Faba L, Díaz E, Bennici S, Vega A, Ordóñez S, et al. Consequences of MgO activation procedures on its catalytic performance for acetone self-condensation. Applied Catalysis B: Environmental 2014;147:796–804. doi:10.1016/j.apcatb.2013.10.014.

[201] Liu Z, Li W, Pan C, Chen P, Lou H, Zheng X. Conversion of biomass-derived carbohydrates to methyl lactate using solid base catalysts. Catalysis Communications 2011;15:82–7. doi:10.1016/j.catcom.2011.08.019.

[202] Sutradhar N, Sinhamahapatra A, Pahari SK, Pal P, Bajaj HC, Mukhopadhyay I, et al. Controlled synthesis of different morphologies of MgO and their use as solid base catalysts. Journal of Physical Chemistry C 2011;115:12308–16. doi:10.1021/jp2022314.

[203] Jennifer Cueto, Laura Faba, Eva Díaz SO. Performance of basic mixed oxides for aqueous-phase 5-hydroxymethylfurfural-acetone aldol condensation. Applied Catalysis B: Environmental 2017;201:221–31. doi:10.1016/j.apcatb.2016.08.013.

[204] Faba L, Díaz E, Ordóñez S. Aqueous-phase furfural-acetone aldol condensation over basic mixed oxides. Applied Catalysis B: Environmental 2012;113–114:201–11. doi:10.1016/j.apcatb.2011.11.039.

[205] Granados-Reyes J, Salagre P, Cesteros Y. Effect of the preparation conditions on the catalytic activity of calcined Ca/Al-layered double hydroxides for the synthesis of glycerol carbonate. Applied Catalysis A: General 2017;536:9–17. doi:10.1016/j.apcata.2017.02.013.

Chapter 2.
Research scope, structure, and justification

The scope of this thesis is to valorize walnut shell as case study in the framework of circular bioeconomy using and integrated biorefinery as a tool see figure 2.1 and 2.2

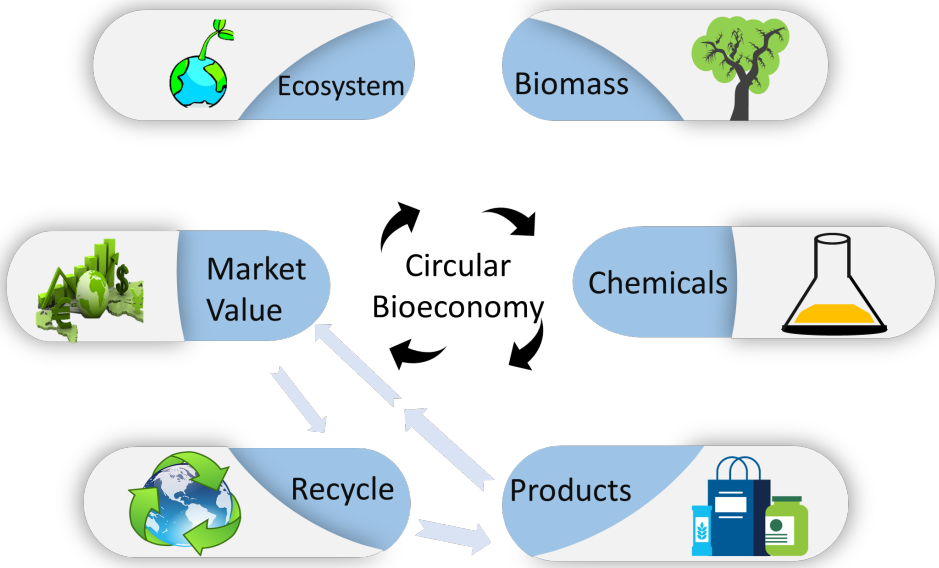

Figure 2. 1. Schematic diagram of circular bioeconomy with vegetal biomass as the feedstock

In the literature, one could find one upstream technique (process) being applied to a particular biomass to obtain platform chemicals. Due to the intrinsic recalcitrance of biomass, we began by addressing the recalcitrance issue by isolating the least recalcitrant hemicellulose from walnut shell in a form of C5 utilizing a universal solvent (H_2O) and microwave. We also presented a second possibility called a lignin-first strategy, in which the most recalcitrant lignin was extracted from walnut shell using an environmentally benign solvent (deep eutectic solvent) and ball milling. To overcome particularly cellulosic recalcitrate and liberate C6 sugars, a mechanocatalytic technique was used. Bacillus coagulans was used to convert the C5 monomer to L+lactic acid (bioplastic feedstock), whilst *Saccharomyces cerevisiae* was used to convert the C6 monomer to bioethanol. Apparently, the upstream processes were efficient at releasing monomers of sugars while producing a small amount of breakdown products such as 5-hydroxymethyl furfural and furfural. These breakdown products might readily be identified and used as feedstock for the production of biojet fuel. As a proof of concept, we attempted to synthesize 2,5-bis(2-furylmethylidene) cyclopentanone (F2Cp) and 2-(2-furylmethylidene) cyclopentanone (FCp) from commercial furfural and cyclopentanone by aldol condensation in the presence of a metal oxide catalyst. Thus, we established a closed-loop utilization of biomass (walnut shell/poplar wood) in proof-of-concept study to

support a circular bioeconomy approach. This proof-of-concept study was undertaken in accordance with Anastas's suggested twelve principles of green chemistry (see picture). by Anastas, see figure 3.

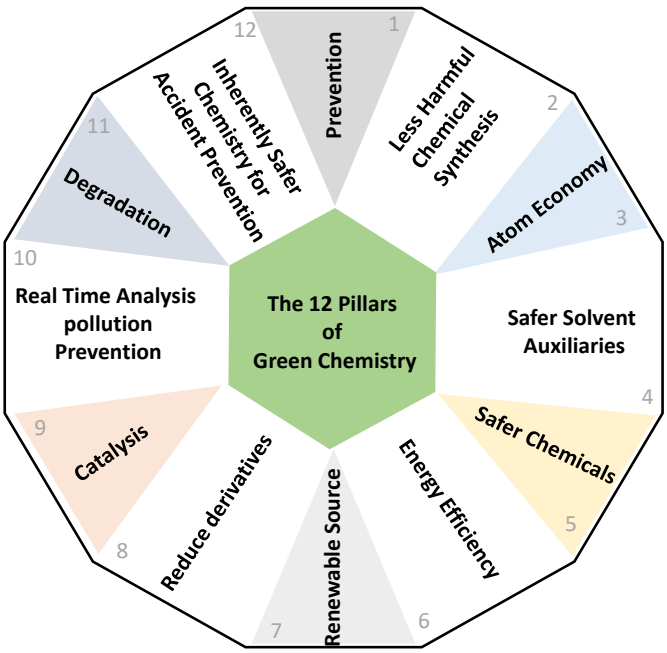

Figure 2. 2. The twelve principles of green chemistry , adapted and modified from reference [1]

This is a journal format thesis structured into 8 chapters.

Chapter 1. **Introduction**. This chapter gives an insight into biorefineries processes (both upstream and downstream) with introduction to integrating circular bioeconomy principle.

Chapter 2. **Thesis justification and structure**. This chapter gives a concise objective and the arrangement of the chapters of the thesis.

Chapter 3. Microwave processes: A viable technology for obtaining xylose from walnut shell to produce lactic acid by *Bacillus coagulans*; the effects of temperature and residence time on deconstruction of walnut shell, the yield of xylose and glucose obtained. The production of L lactic acid with *Bacillus coagulans DSM 2314*.

Chapter 4. Lignin as a viable substrate for immobilization of Bacillus coagulans; The aim of this chapter was to assess the viability of lignin as a potential substrate for immobilization. We demonstrated that the lignin obtained after deconstruction of walnut shell

in chapter 3 (cellulose and hemicellulose) was a sustainable material for Bacillus coagulans immobilization in lactic acid fermentation process.

Chapter 5. Synergy of ball milling, microwave irradiation and Deep Eutectic Solvents for a rapid and selective delignification: Walnut shells as model for lignin-enriched recalcitrant biomass; Here we assess the impact of ball milling, microwave and deep eutectic solvents on lignin yield and quality. Various reaction parameters such as temperature and residence time were evaluated. High lignin yield and quality obtained could serve an entry-point feedstock for lignin-first approach in biorefineries.

Chapter 6. Towards zero-waste biorefineries: Hypercrosslinked benzene polymer as a task-specific reusable adsorbent for detoxification of lignocellulosic hydrolysates for downstream fermentation: In this chapter we attempt to test the fermentability of sugars streams from a highly efficient mechanocatalytic process through a novel neutralization and purification step. Conversion of the purified sugar streams from mechanocatalytic processes to bioethanol was achieved.

Chapter 7. Catalytic cross-aldol condensation of furanics to produce C10 and C15 bio-jet fuel precursors with microwave-assisted process; In this chapter, furfural and cyclopentanone were used as representative compounds from deconstruction of biomass to produce 2,5-bis(2-furylmethylidene) cyclopentanone (F2Cp) and 2-(2-furylmethylidene) cyclopentanone (FCp). Temperature and residence time on product yield were studied. Product yield and selectivity of catalyst were also assessed.

Chapter 8: General conclusions; the last chapter gives the conclusion and future perspectives of both upstream and downstream processes.

2.1 Justification of research

1. To use a renewable feedstock (walnut shell) as replacement for the dwindling petroleum resources.

2.To reverse effects of climate change on the environment by producing net-zero carbon biofuels.

3. To mitigate plastic pollution by reversing linear economy practices into circular bioeconomy.

4. To produce biodegradable polymers/chemicals/materials from sustainable resources.

5. To enhance and increase the market share of bio-based products of high value to compete with fossil-based products.

6. To test the viability and reliability of pretreatment techniques in biorefinery processes against the conventional petroleum refineries.

[1] Anastas P, Eghbali N. Green Chemistry: Principles and Practice. Chemical Society Reviews 2010;39:301–12. doi:10.1039/b918763b.

Chapter 3.
Microwave processes: A viable technology for obtaining xylose from walnut shell to produce lactic acid by *Bacillus coagulans*

Journal of Cleaner Production 2019; 231:1171–81.

3.1. Introduction

The unique chemical and physical properties of 2-hydroxypropanoic acid (Lactic acid, LA) make it an important industrial platform chemical. Recently, there has been increased demand for LA because of its usefulness as a precursor for biodegradable plastic (polylactic acid, PLA) production and in many applications in the pharmaceutical sector [1,2]. Biodegradable polylactic acid offers a better alternative to petrochemical-derived plastics [3]. Lactic acid has been used to synthesize biodegradable green solvents [4], graphene-enhanced PLA filaments for 3D printing, PLA formulation for 3D printing and PLA resin from second-generation feedstock [5]. In 2016, the demand for lactic acid reached 1220.0 kt. This demand is expected to reach 1960 kt by 2025, an annual growth of 16.2% with a cash value of $9.8 billion [5]. So, lactic acid production and usage has both environmental and economic benefits. LA can be synthesized through a chemical route (from petrochemical sources) or by microbial fermentation [6]. At present, high-grade sugars or consumable crops are used for the production of LA [7] thereby circumventing the cost of pretreatment and some material balance challenges. Since the availability of food has been limited by an upsurge in the world population, a readily available and sustainable carbohydrate substrate must be found. The alternative to these highly competitive and expensive high-grade sugars is lignocellulosic biomass, an inexpensive and readily accessible renewable substrate that has no competing food value [8] and which is also an alternative to petrochemical sources. The valorization of lignocellulosic biomass into platform chemicals consolidates the circular economy, a regenerative framework in which resources are used for their maximum value in the production chain. The EU defined the concept of the bioeconomy as encompassing “the production of renewable biological resources and the conversion of these resources and waste streams into value-added products such as feed, food, biobased products and bioenergy” [9]. For many years, the world has practiced a straightforward, crude industrial behavior - ‘produce, use, dispose’ - which deteriorates the environment. The recent introduction of the circular economy and its useful resource management practices will help lessen this environmental impact. In the USA, the bio- economy reached an estimated value of $415 billion in revenues in 2015 [10]. The EU bioeconomy turnover in 2015 was 2.29 trillion [11]. Integrating and implementing a circular bioeconomy will retain material value. The circular economy promotes employment and reverses the trend of unrecycled biowaste so the successful conversion of lignocellulosic biomass into platform chemicals is of immense importance. Lignocellulosic biomass consists of cellulose, hemicellulose, and lignin. Cellulose

is a highly crystalline homopolymer linked by β- (1,4)-glycosidic bonds. Cellulose and hemicellulose are encapsulated in a sophisticated matrix of phenolic lignin [8]. Hemicelluloses are heteropolymers and can be made up of xylan, glucuronoxylan, arabinoxylan, glucomannan, xyloglucan and uronic acid. The composition of hemicellulose depends on the lignocellulosic material: hardwoods contain mostly xylan, softwoods contain mostly glucomannans, and many agricultural wastes or byproducts are made up of backbone chains of 1-4-linked - β D-xylopyranose units substituted with arabinose, uronic acid moieties (or their 4-O-methyl ether), and acetic, ferulic, or coumaric acid [12]. Walnut shell (WS) is agricultural waste that has the potential to be used in biorefining processes and produce xylose from its hemicellulose component. In 2017, world walnut production hit 2.2 million metric tones [13]. Walnuts have considerable nutritional value and demand is on the rise. This demand could lead to increased cultivation and a greater amount of waste. The threat of waste in the environment cannot be overlooked so all sorts of agriculture feedstock must be given the necessary attention and subject to thorough scientific investigation. Walnut shell is no exception to this. The physicochemical properties of biomass and its resistance to hydrolysis have a considerable influence on the choice of the pretreatment process that will be used. The enzymatic conversion of cellulose and hemicellulose has been widely studied [14,15]. Enzymatic hydrolysis usually involves enzyme cocktails that lead to high pretreatment costs. However, hemicellulose can be depolymerized by autohydrolysis to pentose and hexose and other chemical platforms without the aid of solid catalysts, acid catalysts or enzymes. The residual solid lignin, on the other hand, can be used as a source of phenolic and aromatic building blocks from the perspective of a quantitative hydrolysis of the whole matrix [16]. Autohydrolysis pretreatment is cost effective and gives significant benefits to hydrolysis processes for the following reasons: (1) it does not require the addition and recovery of any chemicals other than water, (2) the corrosion of the equipment is limited, (3) it is simple and economically prudent and (4) it is environmentally friendly [17]. Without the assistance of a solid or acid catalyst in the hydrolysis of hemicellulose and with water as a solvent, conditions need to be subcritical if the unique acidic property of water is to be activated. The decrease in the dielectric constant of water when the temperature increases in subcritical conditions coupled with the cleavage of acetyl groups bonded to hemicellulose generates hydronium ions, which tend to help dissolve the branched polysaccharides into oligosaccharides and sugar monomers (autohydrolysis). The element that most directly affects the initiation of autohydrolysis is how energy is supplied to the reaction medium. The most commonly used heating mode is the conventional heating methodology in which hot plate, heating mantles

and burners integrate into batch reactor systems, and the heat transfer rate is relatively low [16]. However, in the pretreatment process microwave heating has these advantages: (1) there is a wide range of feedstock for valorization and higher quality products; (2) heating is non-contact and volumetric; (3) energy is transferred not heat; (4) energy is saved; (5) heating is rapid and efficient; (6) material is selectively heated; (7) start-up start-up and shut down are quick; (8) there is a higher level of safety and automation [18]. Microwave processes depolymerize cellulose by generating hot spots which break up its crystalline structure under mild conditions [19]. This process has also shown significant promise in achieving xylo-oligosacharide yields from various types of biomass [20]. Lignocellulosic biomass is regarded as a viable feedstock for sugar production. It's depolymerization leads to a heterogeneous hydrolysate of hexoses and pentoses. This heterogeneity presents a bottleneck called carbon-catabolite repression in which the mixed sugars in the hydrolysate ferment in a sequential order. The glucose is usually utilized first, which then represses the utilization of other sugars. This phenomenon has been observed with most lactic acid bacteria (LAB) [21,22]. The sequential consumption of mixed sugars results in the low yield and productivity of lactic acid [23]. Other bacteria can only ferment pentose sugars through the phosphoketolase pathway, yielding equal molar amounts of acetic acid and lactic acid with a theoretical yield of 60% [24]. To achieve economic balance, product yield and productivity need to be enhanced by complete utilization of sugars [25,26]. Therefore, it is vital to create genetically modified strains, or to identify a new strain so that the heterogeneous hydrolysate can be efficiently converted into lactic acid. In this regard, we used *Bacillus coagulans DSM 2314* which is a moderate thermophilic bacterium that can grow in slightly acidic environments and simultaneously convert glucose and xylose homo-fermentatively. Conversion of glucose and xylose to lactic acid can exceed 90% on a w/w basis and lactic acid productivity can be as high as 5 g/L/h [8]. *Bacillus coagulans DSM 2314* is extremely efficient at producing optically pure L- (+) lactic acid. Because it is thermophilic, the medium does not need to be sterilized, so the energy cost associated with the fermentation process decreases.

In this study, microwave-assisted autohydrolysis, a cleaner, more cost-efficient technology in the context of biorefining [27], was used to obtain free xylose and glucose from WS. The composition of the liquid fraction (hydrolysate) at different temperatures and residence times was analyzed. The operation condition in which the yield of xylose was highest was selected for fermentation processes to produce lactic acid. The effects of treatment conditions on WS were investigated to reveal both physical and chemical changes. The goal of this study is to

evaluate the efficacy of microwave-assisted autohydrolysis in processes of non- woody agriculture feedstock such as WS and to evaluate the convertibility of the hydrolysates from WS to lactic acid through a batch fermentation process.

3.2. Materials and methods

3.2.1. Raw material

The raw walnut used in this study was grown in Southern California. The hard shells were broken with a shell nutcracker in the laboratory and the shells were separated from the walnut. The shells were mechanically reduced by using a small blade coffee blender (KunFT GTM-8803120W 30 g capacity) to an estimated size of 4mm or less. The sieve (CISA) was applied to further segregate the ground walnut shell into diameters of 1-2 mm, 0.5 mm, 0.3 mm, 0.2mm and 0.1 mm. WS were dried in an oven at 105 °C for 24 h. A moisture content of less than 2% was obtained for all WS, which were kept in an airtight vial that was stored in a desiccator for further usage.

3.2.2. Compositional analysis

In this study, extractives were separated through Soxhlet extraction, and an ethanol-toluene mixture was used as solvent in accordance with the protocol set by the American Society of Testing Material (ASTM) D 1107-84. The percentage of ash in the original, non-extracted material was measured using the protocol ASTM D 1102-84. The hydrolyzed WS was analyzed for carbohydrates and Klason lignin with protocol ASTM D 1106-84. Analysis was performed by quantitative hydrolysis of the solid WS in 72% wt H_2SO_4 at 30 °C for 60 min. The solution was then diluted to 4% wt sulfuric acid, and the reaction continued at 121 °C for 60 min in autoclave. A sample of this acidic solution was filtered through a 0.45 mm nylon syringe filter. HPLC analyses were performed with an Agilent 1100 series chromatograph using an ICSep ICE-COREGEL 87H3 (Column serial n_12525124). The temperature of the column was 50 °C, and the mobile phase was a solution of 0.005M H_2SO_4 at a flow rate of 0.6 ml min^{-1}. An Agilent 1100-DAD ultraviolet, diode-array (UV) detector and an Agilent 1100-RID refractive index (RI) detector were connected in series. The UV detector was used to quantify furfural and HMF in the samples that had low concentrations of these compounds. The RI detector was used for samples with high concentrations of furfural and HMF and also to quantify acetic acid and carbohydrates. The HPLC system was calibrated with standards of known concentration prepared from xylose, levulinic acid, furfural and 5-

hydroxymethylfurfural, all from Sigma- Aldrich. Glucose and acetic acid were purchased from Panreac and Scharlau, respectively. All chemicals were used without further modification.

3.2.3 Autohydrolysis

Several autohydrolysis conditions were studied. The hydrolysis experiments were carried out in a Milestone Synthwave Single Reaction Chamber (SRC), which comes with a rack configuration of five reactors. For each experiment, 1 g of raw walnut shell (diameter 1-2mm) with a humidity of less than 2% was loaded into a glass vial with 15 ml of Milli-Qwater. Vials containing WS in Milli-Q water were fitted with loose PTFE caps to ensure pressure balance. The reaction chamber was filled with 300ml of Milli-Q water. The chamber was pre-pressurized with nitrogen at 30 bar to prevent the mixture from boiling. An agitation of 600 rpm was ensured throughout the experiment. Experiments were carried out at temperatures between 150 °Cand 210 °C for 10, 25, 40, and 55 min of reaction time and at a microwave power of 1200W. This power was only used to reach the desired reaction temperature and it automatically dropped to 550-600W during the rest of the reaction, hence making it more energy efficient. The microwave cavity was water cooled, which significantly reduced the reaction cooling time and increased productivity. The severity factor, calculated with the equation below, quantified the autohydrolysis process:

(Kinetic Severity Factor) $KFs=\log_{10}[t_1 . \exp(T_1 - 100/14.75)]$ ……..[1]

Where t_1 and T_1 are cumulative treatment time (minute) and temperature (°C), respectively. The value of 14.75 is an empirical parameter related to temperature and activation energy (Aparecida et al., 2015; Overend et al., 1987). After autohydrolysis, the hydrolysate was vacuum filtered to separate the solid residue from the solubilized carbohydrates in solution. The solid residue was washed twice and dried in an oven at 105 °C for 16 h. A portion of the hydrolysate was filtered through a PTFE filter of 0.45 mm which was used for HPLC analysis to detect and quantify the following compounds: glucose, xylose, acetic acid, levulinic acid, 5-hydroxymethylfurfural, and furfural. The conversion of hemicellulose was calculated on mass basis, g/g;

$$Conversion\ of\ hemicellulose\ (\%) = \frac{Initial\ weight\ of\ xylan\ in\ reactor\ (g) - final\ weight\ of\ xylan\ recovered\ (g)}{(weight\ of\ initial\ xylan\ in\ the\ reactor\ (g))}\ x100 \ldots\ldots 2$$

$$Xylose\ yield\ (\%) = \frac{weight\ of\ xylose\ formed\ (g)}{(weight\ of\ initial\ xylan\ in\ the\ reactor\ (g))}\ x\ 100 \ldots \ldots 3$$

3.2.4 Physical and chemical characterization

ESEM (environmental scanning electron microscopy with a Quanta 600) was used to study the physical changes in the hydrolyzed residue of the walnut shell, which was directly loaded onto the sample holder and imaged at 15kV. FTIR (Fourier transform infrared spectroscopy) was used to analyze the functional group changes that occurred after hydrolysis. The FTIR spectra were recorded with a Jasco FT/IR-600 Plus equipped with ATR Specac Golden Gate, which directly measures the sample. The sample spectra were recorded with 32 scans using 2cm^{-1} resolution. Thermogravimetric analysis. The thermal degradation of the samples was studied by a Sen Sysevo TG-DSC analyzer. Samples of ~10mg were heated from 25 to 800 °C at a rate of10 °C min^{-1}, using a constant argon flow at 50 ml min^{-1} to generate an inert atmosphere during the experiments.

3.3. Results and discussion

3.3.1 Biochemical composition of walnut shell

Bacillus coagulans DSM 2314 was acquired as freeze-dried stock from the German collection of microorganisms and cell cultures (DSMZ, Germany). Cells were suspended for 30 min in 5ml of PYPD medium, consisting of 5 g/L yeast extract, 10 g/L peptone, 10 g/L xylose and 10 g/L 2- [Bis (2-hydroxyethyl) amino] -2-(hydroxymethyl) propane-1,3-dio (bis-Tris methane) pre-sterilized for 20 min at 121 °C. An isolated colony of *Bacillus coagulans DSM 2314* grown on agar was used to inoculate a 25-ml PYPD medium. The culture was incubated overnight at 55 °C, and then used as the inoculum for the fermentation process. Non-sterilized PYPD medium, at twice the concentration (no commercial xylose added), and hydrolysate from WS (fermentation matrix) in a 50:50 proportion was filtered through a sterilized PTFE filter into a pre- sterilized 25 ml batch reactor. Xylose and glucose in the hydrolysate were used as the carbon source. The pH of the fermentation matrix was adjusted to 7 with 0.2M potassium phosphate buffer, and then the reactor was sealed and capped. The containing the fermentation matrix was put on a hot plate to reach a temperature of 50 °C. Argon was passed through the fermentation matrix for 45 min to create an anaerobic environment. On the basis of several tests carried out using Resazurin as an indicator to establish the absence of oxygen

(not shown), this anaerobic environment was created in the traditional time of 45 min. The deoxygenated fermentation matrix was inoculated with 10% (v/v) of the overnight culture as described above. The inoculated fermentation matrix was incubated at 55 °C with an agitation of 150 rpm. Samples were taken at different time intervals. Fermentation was performed in triplicate, and the mean value was reported. Absorbance was measured at 600nm to determine the optical density (OD), and the remaining sample was filtered through a 0.45 mm filter and used for HPLC analysis. D-Lactic acid was measured with an Oenolab enzymatic kit. The optical purity (OP) of L-lactic acid was calculated with the equation below

$$Optical\ purity\ (\%) = \frac{[L-lactic\ acid]-[D-lactic\ acid]}{[L-lactic\ acid]+[D-lactic\ acid]} x\ 100 \ldots\ldots 4$$

The biochemical constituents of WS were estimated as shown in Table 1 which are consistent with those of other authors [28,29]. Some variations were observed in the biochemical composition of WS, which could be due to the degree of recalcitrance of WS which varies as a function of the thickness distribution of the shell being analyzed. The thickness distribution is predisposed by intrinsic variations in age, climate and soil conditions, and the extent of drying. On the basis of the biochemical composition

Table 3.1. Biochemical composition of walnut shell

Biopolymer	Dry matter (w/w %)
Cellulose	26.7
Hemicellulose	23.4
Klason Lignin	49.8
Extractives	4.1
Ash	0.9

of the WS, this lignocellulosic biomass can be classified as Lignin-Cellulose- Hemicellulose (LCH) [30]. The hemicellulose component of 23.4 % wt means that WS is a viable source of cheap agricultural feedstock from which xylose can be extracted for fermentation processes to produce lactic acid. The low ash content of 0.9 % wt has numerous advantages for fermentations associated with microbial cultures [31].

3.3.2. Effect of autohydrolysis on pH (acidity)

Autohydrolysis was also triggered when acetyl groups were cleaved from the β-(1,4)-linked xylan backbone to form acetic acid, which acted as a catalyst for the hydrolysis of

hemicellulose. Also, hydronium ions generated from water autoionization and the ionization of acidic species (uronic and formic acids) further catalyzed autohydrolysis reaction processes [32]. The pH of the hydrolysate for experiments 1-16 decreased from 4.1 to 2.6, respectively (see Table 3.2). The pH was highest for 150 °C and 10 min of reaction time, and lowest at 210 °C. It is also clear that higher pH values gave less acetic acid and lower pH values gave more (see Table 3.2). This also suggests that during autohydrolysis higher severity promoted the cleavage of acetyl groups into acetic acid. This trend is also supported by previous studies [33–35]. The effects of autohydrolysis on acetic acid, HMF, and furfural (byproducts) can be seen in Table 3.2. The increase in concentration of these byproducts gave lower pH values and a corresponding higher severity.

2.1.3. Effects of temperature and residence time on walnut shell autohydrolysis

A walnut shell (WS) diameter of 1-2mm was used in all microwave-assisted autohydrolysis experiments. Xylans are polyoses made up of a homopolymer backbone of xylose units [36]. Temperature and residence time (severity factor) have a considerable influence on xylose yield. A shorter residence time is one of the most significant advantages that microwave processes have over conventional heating techniques. Microwaves directly transfer energy to reactive species and provide highly effective and rapid heating of the reaction medium [37]. Biomass subjected to a low severity factor generates xylo- oligosaccharides as significant products of the depolymerization of the xylan in solution [38,39]. On the other hand, biomass subjected to a higher severity factor can reduce xylose to furfural, which can further degrade to other products [40]. Fig. 3.1 (a) shows the formation of xylose from the autohydrolysis of WS at 150 °C for 10, 25, 40 and 55 min and a xylose yield of 2.8%, 3.1%, 5% and 8.2%, respectively.

Table 3. 2. The composition of solubilized compounds from autohydrolysis of walnut shell. nd = not detected, Glu=glucose, Xyl=xylose, AceA=acetic acid, LevA=levulinic acid, HMF=hydroxymethylfurfural, Fur=furfural

Exp run No	Temp ^{O}C	Time min	Log KSF	pH	Glu g/L	Xyl g/L	AceA g/L	LevA g/L	HMF g/L	Fur g/L
1	150	10	2.47	4.1	0.17	0.51	0.08	nd	nd	nd
2	150	25	2.8	3.6	0.20	0.58	0.22	nd	0.01	nd
3	150	40	3.07	3.4	0.29	0.85	0.38	nd	0.02	nd
4	150	55	3.21	3.05	0.39	1.39	0.66	nd	0.03	nd
5	170	10	3.06	3.2	0.34	0.98	0.48	nd	0.03	0.02
6	170	25	3.46	3.1	0.41	5.45	1.80	nd	0.08	0.17
7	170	40	3.66	3.1	0.41	8.20	2.84	nd	0.12	0.47
8	170	55	3.8	3.02	0.45	10.14	4.28	nd	0.18	1.02
9	190	10	3.65	3.03	0.46	9.45	3.49	0.24	0.12	0.77
10	190	25	4.04	2.9	0.60	12.40	5.28	0.40	0.20	0.99
11	190	40	4.25	2.8	0.77	4.46	6.29	0.34	0.35	3.39
12	190	55	4.39	2.8	1.01	1.98	6.64	0.39	0.53	3.49
13	210	10	4.24	2.7	2.14	1.94	7.24	0.46	0.75	1.86
14	210	25	4.64	2.7	1.87	2.16	6.86	0.45	0.60	2.14
15	210	40	4.84	2.63	0.30	0.46	8.15	0.85	2.24	1.01
16	210	55	4.98	2.61	nd	0.47	7.50	0.72	0.91	0.40

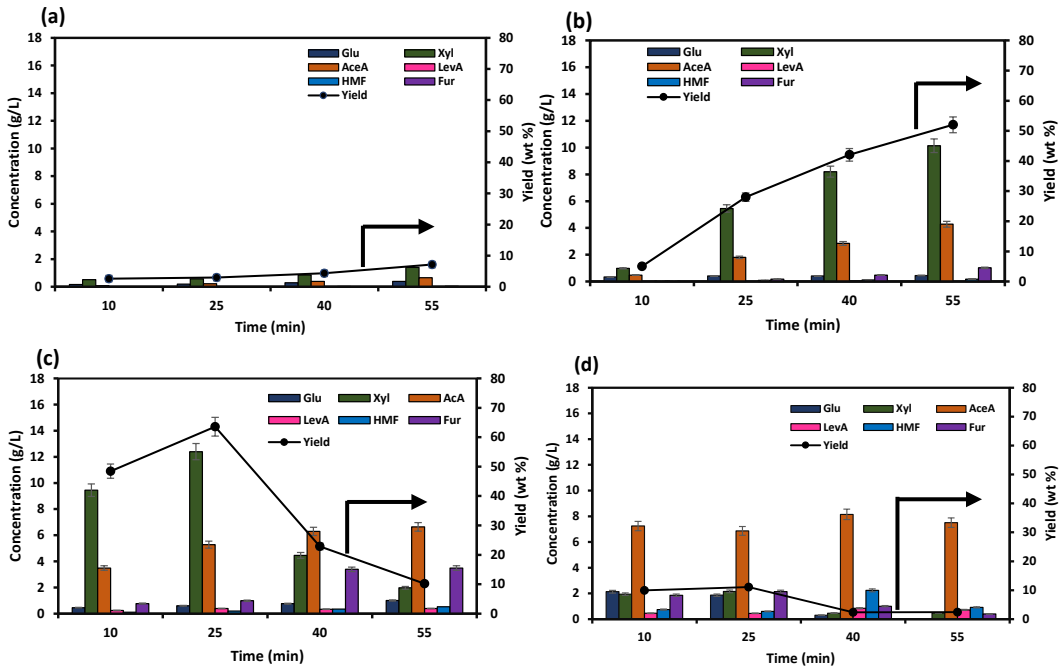

Figure 3. 1. Effects of autohydrolysis on solubilized compounds at (a) 150 °C, (b) 170 °C, (c) 190 °C and (d) 210 °C at different time intervals.

The xylose yield at the highest residence time of 55 min at 150 °C indicated incomplete depolymerization of the hemicellulose in relation to xylose conversion. Xylose yield was observed to increase with increasing residence time in these reaction conditions, 150 °C for 10, 25, 40 and 55 min. The amount of glucose and acetic acid also increased with increasing time. 5-Hydroxymethyfurfural (HMF) and furfural were not detected, and these products gave no indication of glucose and xylose degradation. At 170 °C and increasing residence time, xylose yield also increased with increasing residence time (see Figure 3.1b). This phenomenon was also consistent with the glucose and acetic acid produced at 170 °C. Longer reaction times resulted in a moderate xylose yield at reaction temperatures of 150 °C and 170 °C, which suggests that xylan can only be generated from WS at higher temperatures and longer reaction times. However, when the reaction temperature was raised to 190 °C, the xylose yield increased to the highest value, 63 % wt for 25 min of residence time, and then decreased when the reaction time was prolonged, indicative that the xylose produced was subsequently converted to other compounds like furfural (see Figure 3.1 c). This trend was consistent with the results obtained by other authors. At 170 °C for 55 min, xylose yield was

57.4% and the amount of furfural was 1.49 g/L. In comparison, the reaction at 190 °C and 25 min yielded more xylose with less furfural. When the reaction temperature was further increased to 210 °C with varying residence times, the xylose yield decreased significantly. The amounts of other compounds such as furfural, acetic acid, HMF, and levulinic acid increased (see Figure. 3.1d). A small amount of glucose was obtained in all reaction conditions but this was due to the depolymerization of the amorphous region of cellulose since amorphous cellulose thermally transforms at subcritical temperatures between 180 °C and 230 °C [41]. Hydrogen bonding is heavily involved in polysaccharide structure, and depolymerization depends on the hydrogen bond network made up of inter-sheet, inter- chain and intra-chain hydrogen bonds which impart rigidity and stability to the cellulose structure but which can be broken at high temperatures [42,43]. Below the softening temperature of 180 °C [16] a lower amount of glucose was obtained because the severity was not sufficient to completely depolymerize the amorphous cellulose. However, the amount of glucose was highest (2.1 g/L) at 210 °C, 10 min and a high significantly decreased the glucose concentration. severity factor log KFs =4. Increasing the residence time to 55 min After the highest yield of xylose had been achieved at 190 °C for 25 min (see Figure 3.2), the residence time was set to 25 min for the subsequent experiments with varying temperatures of 150 °C, 170 °C,190 °C and 210 °C as shown in Figure 3.2. A comparative study was done to select the hydrolysate with a lower inhibitory product such as furfural for the fermentation process. Figure 3.2 shows that the conversion of WS's hemicellulose at 190 °C was 96.4% with a xylose yield of 12.40 g/L.

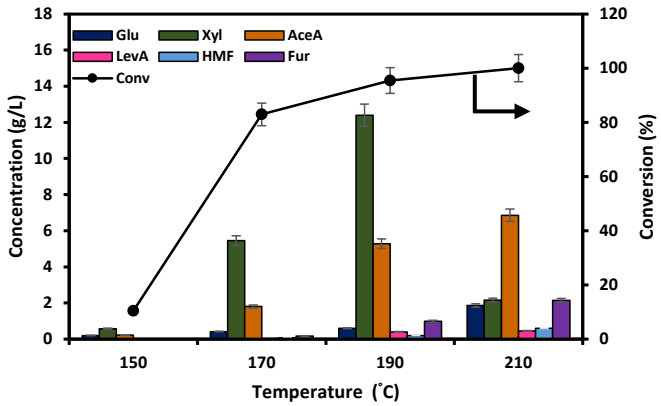

Figure 3. 2. Compositional analysis of hydrolysate in relation to conversion at 150 °C, 170 °C, 190 °C and 210 °C for 25 min.

Hemicellulose conversion was lowest at 150 °C and highest at 210 °C for 55 min, but xylose production was lower at 210 °C. These results revealed that temperature had a major influence on the process of converting hemicellulose into xylose. The change in the amount of xylose in different reaction conditions can be attributed to the presence of acetic acid and the activation energy at high temperatures. The physical and chemical properties of water vary when it is heated above its boiling point in a closed system. The reaction medium becomes more compatible because the polarity of water decreases and water at 180 °C gains the properties of subcritical conditions and acts like an organic solvent [44].

3.3.4. Morphological changes of walnut shell

Figure 3.3 shows the ESEM images of untreated WS, and WS subject to hydrothermal and microwave-assisted treatment at 150 °C, 170 °C, 190 °C and 210 °C at a fixed residence time of 25 min. The surface of untreated walnut shell had an irregular pattern and breakages which were caused mechanically during size reduction. Both untreated and treated WS at 150 °C for 25 min showed similar morphologies. For WS treated at 170 °C for 25 min, spherical and oval droplets were observed on the surface (See S1 in Annex A). From evidence provided in a previous study, these droplets were thought to be composed of lignin [45,46]. Other authors have hypothesized that droplets developed from pseudo- lignin from the dehydrated carbohydrates during severe hydro- thermal pretreatment [47–49]. However, WS treated at 190 °C with a severity factor of log KFs =4.04 developed no droplets on its sur- face, but the surface was rougher than untreated WS, and WS treated at 150 °C for 25 min (severity factor Log KFs =2.8). A microwave-assisted autohydrolysis (see Figure 3.3e), greater severity factor of log KFs=4.64 generated a char after WS did not increase the droplets on the WS surface, which might be due to the different biomass compositions studied by different authors.

2.1.5. Chemical changes in walnut shell

Structural changes were observed when untreated and microwave-assisted autohydrolyzed WS were analyzed with FTIR (Fourier transform infrared spectroscopy) (see Figure 3.4). Pure bands typical of wood were identified around 3390 cm^{-1}, 2921 cm^{-1}, 1800-900 cm^{-1} and the fingerprint region, 1740 cm^{-1} and 1510 cm^{-1}. A broad absorption band in the region of 3390 cm^{-1} can be assigned to O-H stretching groups in the cellulosic and lignin components [50]. The absorption band located around the region of 2921 cm^{-1} can be attributed to C-H stretching vibrations in the CH_3 and CH_2 groups of lignin. These pure bands (3390 cm^{-1}, 2921 cm^{-1}) showed no major changes in intensity. The decrease in band intensity observed at 1740

cm^{-1} and 1371 cm^{-1} is attributed to the C=O and C-O stretching vibrations associated with the acetyl ester in the hemicellulose of WS [51,52]. The decrease in the intensity of these bands was indicative of the dissolution of acetyl groups bonded to the hemicellulose in the WS. This was consistent with the fact that the acetic acid content of the hydrolysates increased significantly as the severity factor increased (see Table 3.2). The intensity of absorption band 1510 cm^{-1} attributed to the aromatic skeletal vibration of aromatic lignin rings increased as the severity factor became stronger. So, while the hemicellulose component was being solubilized, the lignin component became more pronounced. The absorption band around 1096 cm^{-1} assigned to C-O stretching in cellulose and hemicellulose increased in intensity probably due to the solubilization of hemicellulose. Also, the band intensity at 900 cm^{-1} ascribed to cellulose increased as the severity factor increased. This is further evidence of hemicellulose removal.

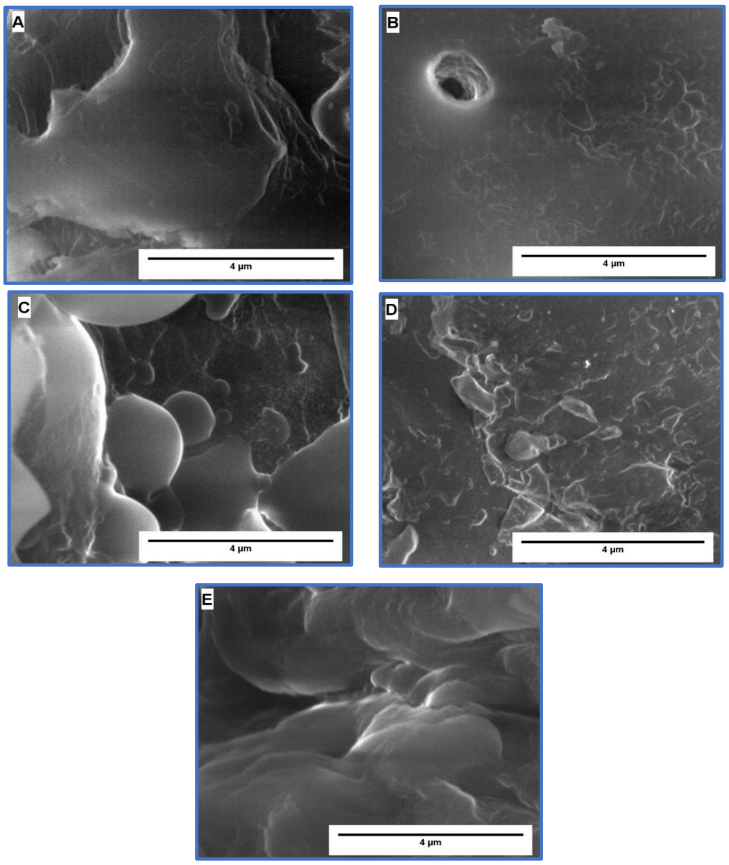

Figure 3. 3. ESEM images of (A) untreated WS, and WS treated for 25 min at (B) 150 °C (C) 170 °C (D) 190 °C (E) 210 °C.

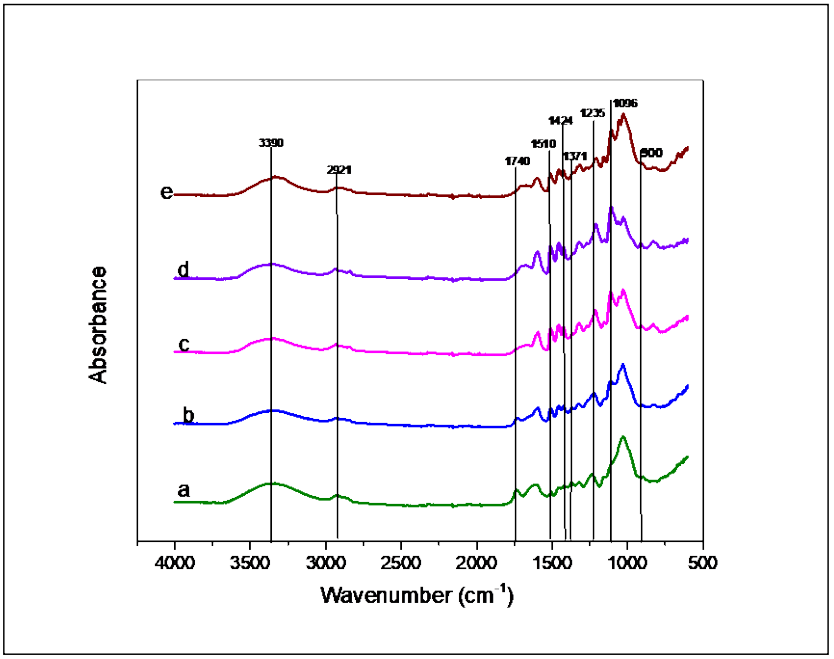

Figure 3. 4. FTIR spectra of (a) untreated WS, and WS treated for 25 min at (b) 150 °C (c) 170 °C (d) 190 °C (e) 210 °C.

2.1.6. Thermal analysis of walnut shell

TGA thermograms of the treated WS, untreated WS and pure xylan have shown differences in temperature after thermal reactions and the accompanying decompositions (see Figure 3.5). Moisture content was removed at around 90 °C for untreated WS, and WS treated at 150 °C, 170 °C and 190 °C with the corresponding weight loss of 7.7% wt, 4.3% wt, 5.3% wt and 3.8 % wt. The trend of decreasing moisture content with increasing severity in WS treated at 150 °C, 170 °C and 190 °C was interrupted at 170 °C, at which temperature moisture loss was 5.3% wt. This anomaly could be due to the heterogeneity of WS particle size. Pure xylan and WS treated at 210 °C did not show any significant moisture loss. At high temperatures, 240 °C, pure xylan began to decompose and showed a thermogram with a sharper shoulder and a weight loss of 96% wt. Untreated WS, and WS treated at 150 °C, 170 °C, 190 °C and 210 °C started to decompose at 240 °C, 280 °C, 169 °C and 163 °C, respectively. Similar weight losses of 60% wt, 65% wt, 63% wt and 65 % wt were recorded at these decomposition temperatures, respectively. WS treated at 150 °C showed a decomposition temperature of 218 °C because the pretreatment exposed a moderate hemicellulose component which decomposes between 200 °C and 300 °C [53]. However, at 170 °C and 190 °C, all or

significant amounts of hemicellulose components were removed, thereby exposing the lignin and cellulose components. Because there was a higher percentage of lignin in WS than cellulose, lignin decomposition dominated, so there were broad thermogram shoulders for WS treated at 170 °C and 190 °C [54]. The effect of the microwave-assisted autohydrolysis of hemicellulose, as shown in TGA analysis, complements FTIR analysis. It shows that removing hemicellulose contributed to enhancing the intensities of lignin and cellulose at 1510 cm^{-1} and 900 cm^{-1}, respectively. The thermogram of WS treated at 210 °C showed a more overlapped decomposition of lignin and cellulose, and, hence, a much broader shoulder. The DTG profile (see Figure 3.5 (b)) also complements TGA behavior and shows a typical 3-stage decomposition. The reference hemicellulose used was xylan from birchwood. It decomposed at a maximum temperature of 345 °C but decomposition started at 305 °C. The decomposition of xylan was different from that of the first stage, which usually involves the loss of moisture and other volatile compounds, possibly because of the absence of cellulose. Untreated WS and WS treated at 150 °C, 170 °C, 190 °C and 210 °C showed moisture decomposition below 200 °C. The DTG profile of WS treated at 150 °C showed decomposition between 250 °C and 350 °C. WS treated at 190 °C and 210 °C did not show any decomposition in the temperature range 250 °C to 345 °C. These temperature ranges are associated with hemicellulose decomposition, but in both cases, decomposition took place at 380 °C. This is an indication of the decomposition of their cellulosic component, which makes them more stable than xylan and un-treated WS. Therefore, it can be concluded that all hemicelluloses in WS treated at 190 °C and 210 °C were depolymerized during microwave-assisted hydrolysis. This phenomenon is consistent with TGA profiles. Overall, the TGA/DTG profile agrees with what is found in the literature: hemicellulose, cellulose and lignin decompose in the temperature ranges 210 °C to 324 °C, 310 °C to 400 °C and 160 °C to 900 °C), respectively, [55].

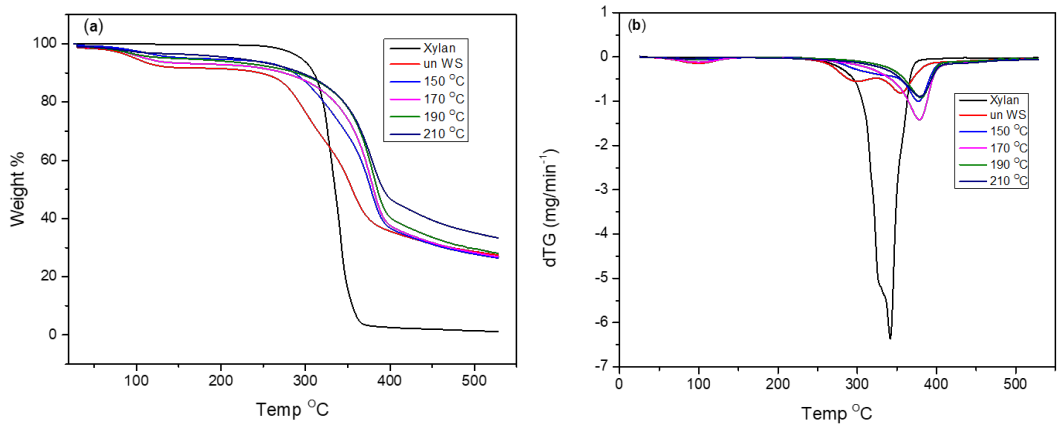

Figure 3. 5. Thermogram of (A) Xylan (B) untreated WS, and WS treated for 25 min at (C) 150 °C (D) 170 °C (E) 190 °C (F) 210 °C

2.1.7. Lactic acid (LA) production by *Bacillus coagulans DSM 2314*

Many microorganisms have been used to produce LA from lignocellulosic hydrolysates containing mixed sugars, including *Lactobacillus brevis* and *Lactobacillus plantarum* [56], *Bacillus coagulans IPE22* [57], *Lactobacillus rhamnosus* and *Lactobacillus brevis* [58], *Rhizopus oryzae* [59] and *Lactobacillus pentosus* [60]. *L. pentosus* achieved the highest LA productivity of 3.10 g/L/h from vine-shoot hydrolysates in a continuous fermentation process, which usually leads to incomplete utilization of the carbon sources. So, the subsequent separation of LA from residual sugars increases the costs of production [57]. *Bacillus coagulans DSM 2314* was suitable for producing LA from mixed sugars in a lignocellulosic hydrolysate because of its tendency to give high yields. Moreover, thermophilic *Bacillus coagulans DSM 2314* has robust property to resist contamination. The non-sterilized fermentation process adopted simplified the operation and reduced the costs of LA production. One of the major obstacles in using lignocellulosic biomass as a feedstock is the inherent heterogeneity of its sugar composition. Therefore, in this study, various cocktails of fermentation media were tested (not shown) to select the optimum and cheapest medium for fermentation processes to achieve maximum LA yield and productivity and utilize these sugars to the full. The fermentation medium with a pH of 5 gave a low LA amount, (1.1 g/ L), with a xylose-to-LA conversion of 4% (see Figure 3.6a). The low lactic acid conversion rate might be due to the poor growth of *B. coagulans* at low pHs. The pH of the hydrolysate (2.9) was a major factor that reduced the pH of the fermentation medium. However, when the

medium was buffered with 0.2M phosphate buffer and controlled at pH 7, there was a significant, simultaneous conversion of both glucose and xylose. Carbon catabolite repression was not observed (see Figure 3.6 b). The initial pH of the medium was a critical factor for microbial growth and the high rate of lactic acid production. There was a complete conversion of glucose and a 93% conversion of xylose into LA, which translates into a yield value of 81% while productivity gained 0.2 g/L/h.

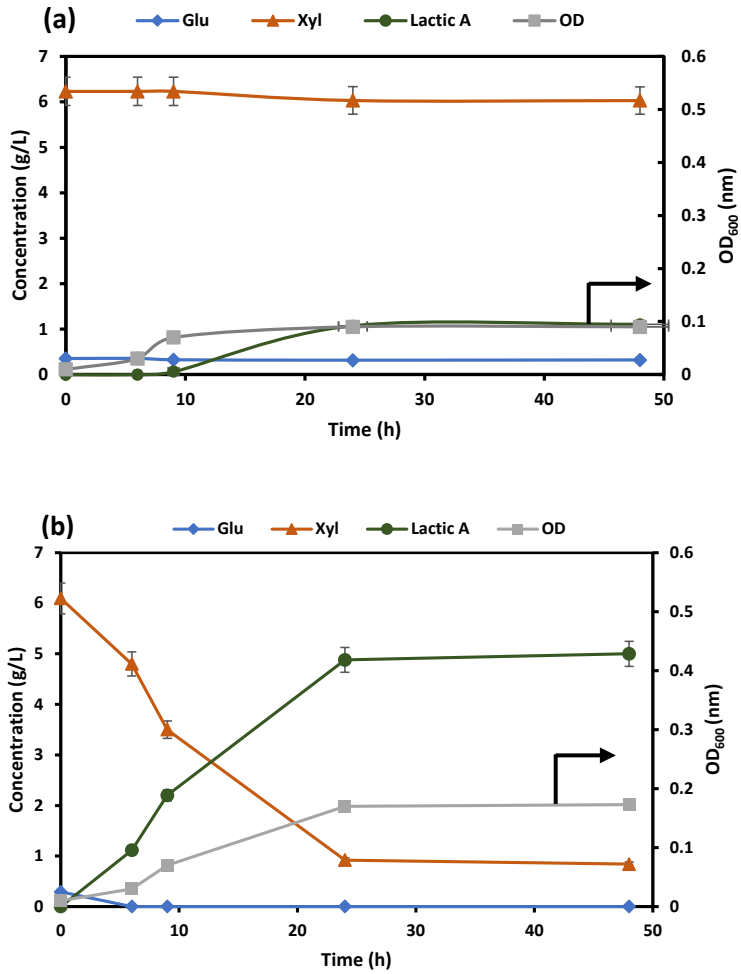

Figure 3. 6 L-lactic acid production by Bacillus coagulans DSM 2314 in batch fermentation at (a) pH 5 and (b) pH 7

This productivity is lower than the productivities obtained during the production of LA using high-grade sugars and continuous fermentation [8]. As seen in Figure 3.6 (b), there was no lag phase during the growth period of *Bacillus coagulans DSM 2314* because the overnight adaptation technique was used. Bacillus coagulans adapted to the medium and enhanced the fermentation of xylose and glucose to LA. The LA yield of 81% is higher than the theoretical yield of 60% resulting from a heterolactic fermentation process. Therefore, we suggest that *Bacillus coagulans DSM 2314* converted xylose from WS into LA through homolactic acid fermentation [61]. A furfural concentration of 0.45 g/L and an acetic acid concentration of 2.42 g/L in the hydrolysate were not detrimental to LA production by *Bacillus coagulans DSM 2314*. The optical purity of L- (+) LA produced by *Bacillus coagulans DSM 2314* was calculated to be 97.4%. This is in agreement, slightly in disagreement, with what other authors obtained: 98.9% [62], 99.4%, 97.2% [8] and 96.7-99.7% for the following strains *DSM 2314*, *DSM 2319, B. smithii DSM 459* and *DSM 460* [61](“Otto (2004).

3.4. Conclusions and economic outlook

In biorefining, the pretreatment of lignocellulosic biomass, the cost of the biomass, and the final cost of the lactic acid are vital in determining the economic feasibility of the conversion process. The enzymatic conversion of cellulose and hemicellulose has been widely studied. Nevertheless, the excessive amount of enzyme required to hydrolyze pre-treated biomass pushes up the cost of producing lactic acid. However, autohydrolysis is a much more efficient process than enzymatic treatment and such other technologies as dilute acid pretreatment, lime treatment, and ammonium fiber expansion. In this study, microwave-assisted autohydrolysis was used to selectively hydrolyze non-woody WS to obtain a hydrolysate containing xylose and glucose (from amorphous cellulose). *Bacillus coagulans DSM 2314* homo-fermentatively converted the glucose and xylose in the hydrolysate in the simple medium into LA under non-sterilized conditions and with no purification step. This led to considerable savings in both time and labor, which makes it easy to scale up for industrialization. LA yield and productivity were moderate in batch fermentations. The remarkable efficiency and resilience of *Bacillus coagulans DSM 2314* makes it a very promising strain for the industrial production of L- lactic acid from lignocellulose. The efficiency of the microwave- assisted autohydrolysis pretreatment of WS to xylose was optimum at 190 °C for 25 min although there were lower amounts of inhibiting byproducts in the hydrolysate. The results of this study have shown the potential of the microwave-assisted autohydrolysis pretreatment of lignocellulose biomass. The study demonstrates a plausible approach to

pretreating lignocellulose biomass without the use of additional solid or liquid catalysts in various biorefining processes.

3.5 References

[1] Gavilà L, Constantí M, Medina F. d-Lactic acid production from cellulose: dilute acid treatment of cellulose assisted by microwave followed by microbial fermentation. Cellulose 2015;22:3089–98. doi:10.1007/s10570-015-0720-1.

[2] Payot T, Chemaly Z, Fick M. Lactic acid production by Bacillus coagulans — Kinetic studies and optimization of culture medium for batch and continuous fermentations 1999;0229:191–9.

[3] Drumright RE, Gruber PR, Henton DE. Polylactic acid technology. Advanced Materials 2000;12:1841–6. doi:10.1002/1521-4095(200012)12:23<1841::AID-ADMA1841>3.0.CO;2-E.

[4] Kozlovskiy R, Shvets V, Kuznetsov A. Technological aspects of the production of biodegradable polymers and other chemicals from renewable sources using lactic acid. Journal of Cleaner Production 2017;155:157–63. doi:10.1016/j.jclepro.2016.08.092.

[5] Alves de Oliveira R, Komesu A, Vaz Rossell CE, Maciel Filho R. Challenges and opportunities in lactic acid bioprocess design—From economic to production aspects. Biochemical Engineering Journal 2018;133. doi:10.1016/j.bej.2018.03.003.

[6] Hu J, Zhang Z, Lin Y, Zhao S, Mei Y, Liang Y, et al. Bioresource Technology High-titer lactic acid production from NaOH-pretreated corn stover by Bacillus coagulans LA204 using fed-batch simultaneous saccharification and fermentation under non-sterile condition. BIORESOURCE TECHNOLOGY 2015;182:251–7. doi:10.1016/j.biortech.2015.02.008.

[7] Van Der Pol EC, Eggink G, Weusthuis RA. Production of L(+)-lactic acid from acid pretreated sugarcane bagasse using Bacillus coagulans DSM2314 in a simultaneous saccharification and fermentation strategy. Biotechnology for Biofuels 2016;9:1–12. doi:10.1186/s13068-016-0646-3.

[8] Maas RHW, Bakker RR, Jansen MLA, Visser D, Jong E De. Lactic acid production from lime-treated wheat straw by Bacillus coagulans : neutralization of acid by fed-batch addition of alkaline substrate 2008:751–8. doi:10.1007/s00253-008-1361-1.

[9] Henrike Gebhardt 1, Peter Na gler 2 S an B 2, Stef an Cornelissen 1, Edda Schulze 1 and AM 1. EVONIK: BIOECONOMY AND BIOBASED PRODUCTS. vol. 91. 2016.

[10] Guo M, Song W. The growing U.S. bioeconomy: Drivers, development and constraints. New Biotechnology 2018. doi:10.1016/j.nbt.2018.08.005.

[11] Hassan SS, Williams GA, Jaiswal AK. Emerging technologies for the pretreatment of lignocellulosic biomass. Bioresource Technology 2018;262:310–8. doi:10.1016/j.biortech.2018.04.099.

[12] Ramos LP. The Chemistry involved in the steam treatment of lignocellulosic materials. Quim Nova 2003;26:863–71.

[13] USDA Office of Global Analysis. Tree Nuts : World Markets and Trade 2013:0–2.

[14] Lin Y, Tanaka S. Ethanol fermentation from biomass resources: Current state and prospects. Applied Microbiology and Biotechnology 2006;69:627–42. doi:10.1007/s00253-005-0229-x.

[15] M. Taniguchi, M. Hoshina, S. Tanabe, Y. Higuchi, K. Sakai, S. Ohtsubo, K. Hoshino TT. Production of L-Lactic Acid by Simultaneous Saccharification and Fermentation Using Unsterilized Defatted Rice Bran as a Carbon Source and Nutrient Components. Food Science and Technology Research 2005;11:400–6. doi:10.3136/fstr.11.400.

[16] Galia A, Schiavo B, Antonetti C, Galletti AMR, Interrante L, Lessi M, et al. Autohydrolysis pretreatment of Arundo donax: A comparison between microwave-assisted batch and fast heating rate flow-through reaction systems. Biotechnology for Biofuels 2015;8:1–18. doi:10.1186/s13068-015-0398-5.

[17] Romaní A, Garrote G, Alonso JL, Parajó JC. Bioethanol production from hydrothermally pretreated Eucalyptus globulus wood. Bioresource Technology 2010;101:8706–12. doi:10.1016/j.biortech.2010.06.093.

[18] Zhang X, Rajagopalan K, Lei H. Sustainable Energy & Fuels An overview of a novel concept in biomass pyrolysis : microwave irradiation. Sustainable Energy & Fuels 2017;00:1–36. doi:10.1039/C7SE00254H.

[19] Ahorsu R, Medina F, Constantí M. Significance and Challenges of Biomass as a Suitable Feedstock for Bioenergy and Biochemical Production: A Review. Energies 2018;11:3366. doi:10.3390/en11123366.

[20] Luo Y, Fan J, Budarin VL, Hu C, Clark JH. Microwave-assisted hydrothermal selective dissolution and utilisation of hemicellulose in Phyllostachys heterocycla cv. Pubescens. Green Chemistry 2017;19:4889–99. doi:10.1039/c7gc02300f.

[21] Kim JH, Block DE, Shoemaker SP, Mills DA. Conversion of rice straw to bio-based chemicals: An integrated process using Lactobacillus brevis. Applied Microbiology and Biotechnology 2010;86:1375–85. doi:10.1007/s00253-009-2407-8.

[22] Stülke J, Hillen W. Carbon catabolite repression in bacteria. Current Opinion in Microbiology 1999;2:195–201. doi:10.1016/S1369-5274(99)80034-4.

[23] Bothast RJ, Nichols NN, Dien BS. Fermentations with new recombinant organisms. Biotechnology Progress 1999;15:867–75. doi:10.1021/bp990087w.

[24] Patel MA, Harbrucker R, Aldrich HC, Ou MS, Ingram LO, Buszko ML, et al. Isolation and Characterization of Acid-Tolerant, Thermophilic Bacteria for Effective Fermentation of Biomass-Derived Sugars to Lactic Acid. Applied and Environmental Microbiology 2006;72:3228–35. doi:10.1128/aem.72.5.3228-3235.2006.

[25] Kim JH, Block DE, Mills DA. Simultaneous consumption of pentose and hexose sugars: An optimal microbial phenotype for efficient fermentation of lignocellulosic biomass. Applied Microbiology and Biotechnology 2010;88:1077–85. doi:10.1007/s00253-010-2839-1.

[26] Saha BC. Hemicellulose bioconversion. Journal of Industrial Microbiology and Biotechnology 2003;30:279–91. doi:10.1007/s10295-003-0049-x.

[27] Abaide ER, Mortari SR, Ugalde G, Valério A, Amorim SM, Di Luccio M, et al. Subcritical water hydrolysis of rice straw in a semi-continuous mode. Journal of Cleaner Production 2019;209:386–97. doi:10.1016/j.jclepro.2018.10.259.

[28] Kambarova GB, Sarymsakov S. Preparation of activated charcoal from walnut shells. Solid Fuel Chemistry 2008;42:183–6. doi:10.3103/S0361521908030129.

[29] Zhu D, Li X, Liao X, Shi B. Immobilization of Saccharomyces cerevisiae using polyethyleneimine grafted collagen fibre as support and investigations of its fermentation performance. Biotechnology and Biotechnological Equipment 2018;32:109–15. doi:10.1080/13102818.2017.1389302.

[30] Vassilev S V., Baxter D, Vassileva CG. An overview of the behaviour of biomass during combustion: Part I. Phase-mineral transformations of organic and inorganic matter. Fuel 2013;112:391–449. doi:10.1016/j.fuel.2013.05.043.

[31] Pandey A, Soccol CR, Nigam P, Soccol VT. Biotechnological potential of agro-industrial residues. I: sugarcane bagasse. Bioresource Technology 2000;74:69–80.

[32] Aparecida L, Batalha R, Han Q, Jameel H, Chang H, Luiz J, et al. Bioresource Technology Production of fermentable sugars from sugarcane bagasse by enzymatic hydrolysis after autohydrolysis and mechanical refining. BIORESOURCE TECHNOLOGY 2015;180:97–105. doi:10.1016/j.biortech.2014.12.060.

[33] Bouchard J, Nguyen TS, Chornet E, Overend RP. Analytical methodology for biomass pretreatment. Part 2: Characterization of the filtrates and cumulative product distribution as a function of treatment severity. Bioresource Technology 1991;36:121–31. doi:10.1016/0960-8524(91)90169-K.

[34] Lee JM, Shi J, Venditti RA, Jameel H. Autohydrolysis pretreatment of Coastal Bermuda grass for increased enzyme hydrolysis. Bioresource Technology 2009;100:6434–41. doi:10.1016/j.biortech.2008.12.068.

[35] Liu C, Wyman CE. Partial flow of compressed-hot water through corn stover to enhance hemicellulose sugar recovery and enzymatic digestibility of cellulose. Bioresource Technology 2005;96:1978–85. doi:10.1016/j.biortech.2005.01.012.

[36] Nabarlatz D, Ebringerová A, Montané D. Autohydrolysis of agricultural by-products for the production of xylo-oligosaccharides. Carbohydrate Polymers 2007;69:20–8. doi:10.1016/j.carbpol.2006.08.020.

[37] Hayes BL. Recent Advances in Microwave- Assisted Synthesis n.d.:66–76.

[38] Carvalheiro F, Silva-Fernandes T, Duarte LC, Gírio FM. Wheat straw autohydrolysis: Process optimization and products characterization. Applied Biochemistry and Biotechnology 2009;153:84–93. doi:10.1007/s12010-008-8448-0.

[39] Gullón B, Yáñez R, Alonso JL, Parajó JC. Production of oligosaccharides and sugars from rye straw: A kinetic approach. Bioresource Technology 2010;101:6676–84. doi:10.1016/j.biortech.2010.03.080.

[40] Garrote G, Dom H, Paraj JC. Autohydrolysis of corncob : study of non-isothermal operation for xylooligosaccharide production 2002;52:211–8.

[41] Fan J, De Bruyn M, Budarin VL, Gronnow MJ, Shuttleworth PS, Breeden S, et al. Direct microwave-assisted hydrothermal depolymerization of cellulose. Journal of the American Chemical Society 2013;135:12728–31. doi:10.1021/ja4056273.

[42] Kovalenko VI. Crystalline cellulose: structure and hydrogen bonds. Russian Chemical Reviews 2010;79:231–41. doi:10.1070/RC2010v079n03ABEH004065.

[43] Matthews JF, Bergenstråhle M, Beckham GT, Himmel ME, Nimlos MR, Brady JW, et al. High-temperature behavior of cellulose i. Journal of Physical Chemistry B 2011;115:2155–66. doi:10.1021/jp1106839.

[44] Siskin M, Katritzky AR. Reactivity of organic compounds in hot water: Geochemical and technological implications. Science 1991;254:231–7. doi:10.1126/science.254.5029.231.

[45] Donohoe BS, Decker SR, Tucker MP, Himmel ME, Vinzant TB. Visualizing lignin coalescence and migration through maize cell walls following thermochemical pretreatment. Biotechnology and Bioengineering 2008;101:913–25. doi:10.1002/bit.21959.

[46] Selig MJ, Viamajala S, Decker SR, Tucker MP, Himmel ME, Vinzant TB. Deposition of lignin droplets produced during dilute acid pretreatment of maize stems retards enzymatic hydrolysis of cellulose. Biotechnology Progress 2007;23:1333–9. doi:10.1021/bp0702018.

[47] Ko JK, Kim Y, Ximenes E, Ladisch MR. Effect of liquid hot water pretreatment severity on properties of hardwood lignin and enzymatic hydrolysis of cellulose. Biotechnology and Bioengineering 2015;112:252–62. doi:10.1002/bit.25349.

[48] Kumar R, Hu F, Sannigrahi P, Jung S, Ragauskas AJ, Wyman CE. Carbohydrate derived-pseudo-lignin can retard cellulose biological conversion. Biotechnology and Bioengineering 2013;110:737–53. doi:10.1002/bit.24744.

[49] Sannigrahi P, Ragauskas AJ, Miller SJ. Effects of Two-Stage Dilute Acid Pretreatment on the Structure and Composition of Lignin and Cellulose in Loblolly Pine. BioEnergy Research 2008;1:205–14. doi:10.1007/s12155-008-9021-y.

[50] Andrei I, Roxana G, Ghitescu E, Catalin A, Valentin P. Preparation of lignin nanoparticles by chemical modification 2014:355–63. doi:10.1007/s13726-014-0232-0.

[51] Bodîrlău R, Teacă CA. Fourier transform infrared spectroscopy and thermal analysis of lignocellulose fillers treated with organic anhydrides. Romanian Reports of Physics 2009;54:93–104.

[52] Nitsos CK, Matis KA, Triantafyllidis KS. Optimization of hydrothermal pretreatment of lignocellulosic biomass in the bioethanol production process. ChemSusChem 2013;6:110–22. doi:10.1002/cssc.201200546.

[53] Xiao B, Sun XF, Sun R. Chemical , structural , and thermal characterizations of alkali-soluble lignins and hemicelluloses , and cellulose from maize stems , rye straw , and rice straw 2001;74:307–19.

[54] Gani A, Naruse I. Effect of cellulose and lignin content on pyrolysis and combustion characteristics for several types of biomass. Renewable Energy 2007;32:649–61. doi:10.1016/j.renene.2006.02.017.

[55] Xiao B, Sun XF, Sun R, Zeng Y, Yarbrough JM, Mittal A, et al. Isolation of nanocellulose from waste sugarcane bagasse (SCB) and its characterization. Biotechnology for Biofuels 2011;74:1–12. doi:10.1016/j.biortech.2009.10.066.

[56] Zhang Y, Vadlani P V. Lactic acid production from biomass-derived sugars via co-fermentation of Lactobacillus brevis and Lactobacillus plantarum. Journal of Bioscience and Bioengineering 2015;119:694–9. doi:10.1016/j.jbiosc.2014.10.027.

[57] Zhang Y, Chen X, Luo J, Qi B, Wan Y. Bioresource Technology An efficient process for lactic acid production from wheat straw by a newly isolated Bacillus coagulans strain IPE22. Bioresource Technology 2014;158:396–9. doi:10.1016/j.biortech.2014.02.128.

[58] Cui F, Li Y, Wan C. Bioresource Technology Lactic acid production from corn stover using mixed cultures of Lactobacillus rhamnosus and Lactobacillus brevis. Bioresource Technology 2011;102:1831–6. doi:10.1016/j.biortech.2010.09.063.

[59] Bai DM, Li SZ, Liu ZL, Cui ZF. Enhanced L-(+)-lactic acid production by an adapted strain of Rhizopus oryzae using corncob hydrolysate. Applied Biochemistry and Biotechnology 2008;144:79–85. doi:10.1007/s12010-007-8078-y.

[60] Bustos G, de la Torre N, Moldes AB, Cruz JM, Domínguez JM. Revalorization of hemicellulosic trimming vine shoots hydrolyzates trough continuous production of lactic acid and biosurfactants by L. pentosus. Journal of Food Engineering 2007;78:405–12. doi:10.1016/j.jfoodeng.2005.10.008.

[61] Goldschmid O. Phenolic Hydroxyl Content. Analytical Chemistry 1954;26:1421–3.

[62] Glaser R, Venus J. Model-based characterisation of growth performance and L-lactic acid production with high optical purity by thermophilic Bacillus coagulans in a lignin-supplemented mixed substrate medium. New Biotechnology 2017;37:180–93. doi:10.1016/j.nbt.2016.12.006.

Chapter 4: Lignin as a viable substrate for immobilization of *Bacillus coagulans*

4.1. Introduction

Lactic acid (2-hydroxypropanoic acid, CH3–CH(OH)–COOH) is an organic acid that has found use in the food, cosmetics, and pharmaceutical sectors, as well as in the production of specialty chemicals [1]. Currently, there is rising demand for lactic acid as a feedstock for the synthesis of the biopolymer poly-lactic acid (PLA), which is a promising biodegradable, biocompatible, and ecologically friendly alternative to petrochemical-derived plastics. Almost all lactic acid produced on a worldwide scale nowadays is produced via fermentation [2]. Many studies have been conducted in comparison to other microorganisms on the production of lactic acid by lactic acid bacteria (LAB). The demand for lactic acid has increased significantly as a result of its wide range of applications; however, the high cost of raw materials, such as starch and refined sugars, which account for the lion's share of production costs, represents one of the most significant impediments to fermentative production of lactic acid competing with chemical synthesis [3]. Cheap raw materials are critical for biotechnological lactic acid production to be feasible, as polymer makers and other industrial customers typically require large volumes of lactic acid at a low cost.

Immobilization of cells has a number of advantages, including increased volumetric output, reduced process costs, ease of handling, and improved operational stability [4]. Catalytic activity is a critical attribute of a variety of biological materials collectively referred to as biocatalysts, which include complete cells, cell components, and enzymes. Microorganisms typically develop as aggregates connected to solid surfaces or in microbial films (biofilms) on a range of materials under natural settings. Microorganisms in rivers are rarely found in free suspension; instead, they are connected with solid surfaces (e.g. silt particles)[5] . Immobilization of biologically active materials enables their repeated or continuous usage in a controlled setting [6]. In comparison to gel entrapment, microencapsulation, or membrane retention, surface adsorption appears to be a successful approach that has a negligible effect on bacteria growth [7]. Nonetheless, the development of immobilized cell reactors is hampered by the scarcity of matrices, their high cost, and the immobilization technique's efficiency. The use of synthetic polymers has a number of disadvantages, including high cost, low physical strength, difficulties with substrate and product diffusion, and trouble with recycling operations. As a result, it is necessary to research natural renewable biomaterials with cell binding properties. Due to their abundance, ease of use, low cost, high porosity, and minimal toxicity to cells, lignocellulosic substrates have a significant deal of potential for use as immobilization carriers [8]. Walnut shell (WS) is a lignocellulosic biomass that is renewable

and relatively inexpensive. Walnut output in the world was 4.5 million metric tons [9]. This could result in the production of low-cost agricultural waste that must be valorized. Pretreatment, on the other hand, is required to transform the holocellulosic component (59%) into sugar streams. Typically, residual lignin from the pretreatment process of walnut is used as a source of heat. We are attempting to immobilize LA-producing bacteria using lignin as a matrix. Lignin is well-known for its adhesion to the substrate and its stability and stiffness. These properties make immobilization matrices appealing. To our knowledge, this is the first report of bacteria generating LA being immobilized on lignin for the purpose of manufacturing LA. To begin, holocellulose was deconstructed into sugar streams using a microwave-assisted autohydrolysis technique. In the immobilization process, the residue (lignin) was utilized as a solid substrate as step to eliminate wastage, improve LA production and recycle the bacteria.

4.2. Materials and Methods

Glucose (panreac), xylose, peptone casein, peptone soy, potassium dihydrogen phosphate, and dipotassium hydrogenphosphate were purchased from sigma Aldrich. Lignin was obtained as a residue after hydrolysis of walnut shell with microwave process.

4.2.1. Preparation of inoculum

Bacillus coagulans DSM 2314 was acquired as freeze-dried stock from the German collection of microorganisms and cell cultures (DSMZ, Germany). Cells were suspended for 30 min in 5ml of PYPD medium, consisting of 5 g/L yeast extract, 10 g/L peptone, 10 g/L xylose and 10 g/L 2- [Bis (2-hydroxyethyl) amino] -2-(hydroxymethyl) propane-1,3-dio (bis-Tris methane) pre-sterilized for 20 min at 121 °C. An isolated colony of *Bacillus coagulans DSM 2314* grown on agar was used to inoculate a 25-ml PYPD medium. The culture was incubated overnight at 55 °C, and then used as the inoculum for the fermentation process. Non-sterilized PYPD medium, at twice the concentration (no commercial xylose added), and hydrolysate from WS (fermentation matrix) in a 50:50 proportion was filtered through a sterilized PTFE filter into a pre- sterilized 25 ml batch reactor. Xylose and glucose in the hydrolysate were used as the carbon source. The pH of the fermentation matrix was adjusted to 7 with 0.2M potassium phosphate buffer, and then the reactor was sealed and capped. Argon was passed through the fermentation matrix for 45 min to create an anaerobic environment. On the basis of several tests carried out using Resazurin as an indicator to establish the absence of oxygen (not shown), this anaerobic environment was created in the traditional time of 45 min.

4.2.2. Immobilization procedure

0.5g of lignin was sterilized and used as the support for immobilization of *Bacillus coagulans DSM 2314*. The immobilization medium was filtered through a previously sterilized pvdf filter of 0.25um pore size into a sterilized 50ml reactor. A total 0.5g of the sterilized lignin was carefully added to the immobilization media and inoculated with 10v/v % of overnight culture. The inoculated immobilization media was incubated at 50 °C with an agitation speed of 120 rpm for 24 hours. The immobilized bacteria were filtered through a sterilized quartz filter paper with 25μm retention. The filtrate was collected and plated. The difference between bacteria growth before filtration and filtrate was considered as the immobilized bacteria. The inoculated fermentation matrix was incubated at 55 °C with an agitation of 150 rpm. Samples were taken at different time intervals. Fermentation was performed in triplicate, and the mean value was reported.

4.2.3. Environmental scanning electron microscopy

Sample preparation: Bacteria in broth was dropped on filter membrane (0.45 micron or 0.2 micron) and air dried. The bacteria and content were fixed in 2.5% glutaraldehyde in the presence PBS buffer for 45 min- 1 h, and rinsed with PBS for 3—15 min.

The prepared bacteria sample was later refixed in 1% OsO_4 in PBS buffer for 1h followed by series dehydration with ethanol, 10 min each rinse (30%, 50%, 70%, 80%, 100% ethanol). Bacteria sample was fixed again in absolute ethanol (15 min approx.). Critical-point drying was carried out followed by attaching bacteria to ESEM platform. The bacteria sample was sputter coated with gold. Finally, ESEM was performed.

ESEM (environmental scanning electron microscopy with a Quanta 600) was used to study the physical changes in the hydrolyzed residue of the walnut shell, which was directly loaded onto the sample holder and imaged at 15kV

4.2.4. Surface area measurement

The specific surface area of lignin was determined by Brunauer–Emmett–Teller method using the nitrogen adsorption approach (Quantachrom apparatus).

4.3.4. Results and Discussion

Identifying good and natural substrate for biocatalytic activity is necessary in consolidating renewability of biorefineries. ESEM image of raw lignin revealed a moderate rough surface

with visible holes/crevices (Figure 4.1a). Additionally, the shape of the support's surface has a significant effect on cell adsorption: a rough and porous surface with a suitable pore size is required [10,11].Even though the pore diameter 3.6 nm was smaller to serve as anchorage for cells, these visible holes/crevices could serve as base to help cell growth. Lower surface area was recorded for lignin support (Table 4.1).

Table 4. 1. Physical properties of lignin substrate

Material	Surface area BET m^2/g	Pore volume cc/g pore size nm	
Raw nutshell	0.228	0.017	3.308
Lignin	0.124	0.037	3.672

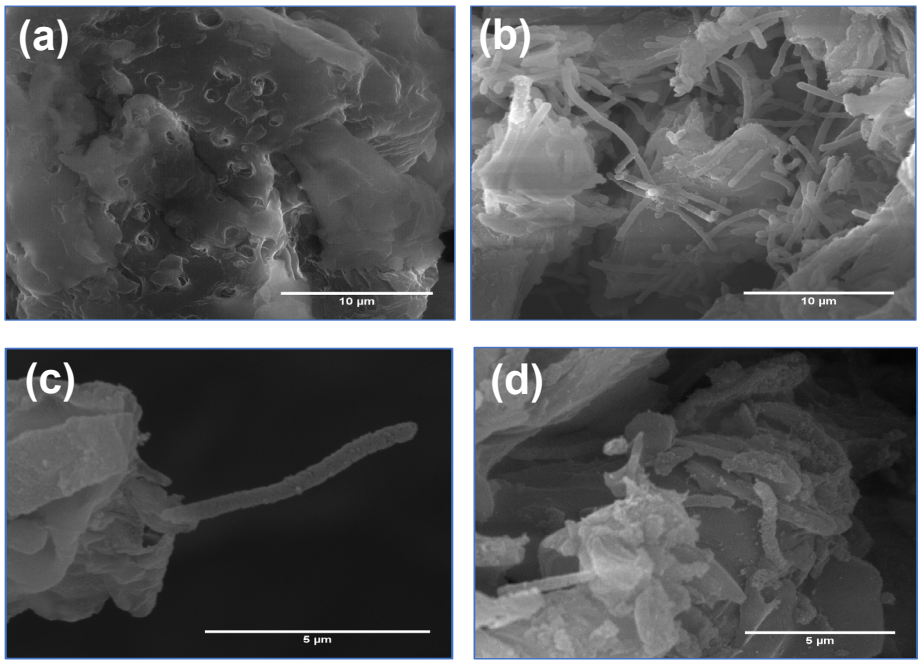

Figure 4. 1. ESEM image of lignin surface (a), Bacillus coagulans DSM 2314 immobilized on lignin surface (b), an edge view of *Bacillus coagulans DSM 2314* immobilized on lignin substrate (c), Bacillus coagulans on lignin substrate after fermentation (d)

However, the lignin support with a natural phenylpropanoid serves as cheap, rigid and low toxicity risk compared to inorganic substrate [12] . This characteristics makes it more compelling to be investigated, as other natural substrates such as bacterial cellulose, sugarcane bagasse, grape skins have shown promising results [13–15]. ESEM images also revealed detailed adsorption of BC onto lignin support and BC attachment to the lignin support

after fermentation, Figure 4.1c and 4.1d respectively. This adsorption could be due weak linkages formed through electrostatic interaction. Colonization of the surface and crevices/holes leads to formation biofilm generated through secretions from the bacteria [16].

Comparative studies between immobilized cells (IC) and free cells were tested as shown in Figure 4.2a and 4.2b. The IC showed cell multiplication at fermentation to the 6th hour. This high cell growth could be due to the cells finding preferred locus to binding at the surface and edges of the lignin where the conditions for growth are favorable. There was no lag phase observed in the IC fermentation profile while the contrast was observed with free cells. Efficiency of both IC and free cells were compared to ascertain the productivity. It was observed that, both immobilized and free cells converted xylose to lactic acid at rate of, 0.72 g/l/h and 0.56 g/l/h respectively. It also revealed that cell density was higher in the immobilized fermentation profile compared to free cells. However, recovered bacteria had a low cell density which could be as a result of cell leakage but gave a productivity value of 0.4 g/l/h, Figure 4.2c. This could suggest that a critical density of bacteria was required to convert sugar to lactic acid based on concentration of sugar source available. This recovered cell usage in lactic acid production also demonstrated the applicability of lignin as viable substrate to be considered in immobilization process. In terms of xylose conversion to lactic acid both IC and free cells gave with similar value, 84.6 % and 83.87 % at 6 h and 9 h respectively. To test the stability and longevity of IC, fed batch fermentation was carried out for 49 h. In the first 3hr of the fermentation, there was minimal conversion of xylose to lactic acid with slight growth of bacteria. The xylose conversion process continued into the 6hr with slow rate. Xylose was then injected at this 6h to make available sugar for conversion throughout the night. On the 18h there was about 72.7 % conversion of xylose to lactic acid. The bacteria growth decreased significantly after 18h. At 18h, 0.2M NaOH was added to increase the pH to 6.0. This increased the bacteria growth at 25h. But no growth was observed at this hour. So, xylose was added to increase the sugar source. At 43hrs there was only 22.25 % of xylose conversion between the 25h and 43h. The growth of bacteria also ceased at this hour.

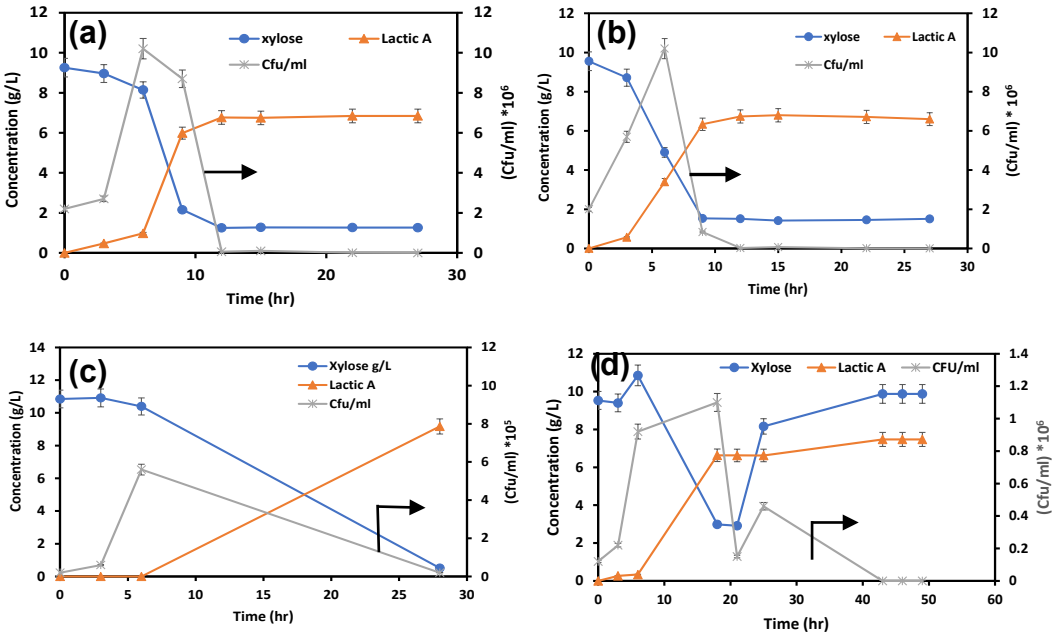

Figure 4. 2. LA production with Bacillus coagulans DSM 2314 (BC) through batch fermentation with non-immobilized profile (a) profile immobilized BC on lignin (b) profile of recovered immobilized BC after 14 h of previous batch fermentation (c) profile of fed-batch fermentation

4.5. Conclusions

Our findings indicate that lignin may be used as a biocompatible support for BC immobilization. Numerous improvements, including increased cell loading and reusability were realized, resulting in steady operation in both batch and fed-batch fermentation processes. In this view, it could be recommended that, utilizing lignin as a support to improve lactic acid yield could be considered in achieving circular bioeconomy strategy. However, further studies to understand the interaction between the cell and support is necessary to fully harness and utilize lignin as matrix in immobilization.

4.6. Reference

[1] Abdel-Rahman MA, Tashiro Y, Sonomoto K. Lactic acid production from lignocellulose-derived sugars using lactic acid bacteria: Overview and limits. Journal of Biotechnology 2011;156:286–301. doi:10.1016/j.jbiotec.2011.06.017.

[2] Abdel-Rahman MA, Tashiro Y, Sonomoto K. Lactic acid production from lignocellulose-derived sugars using lactic acid bacteria: Overview and limits. Journal of Biotechnology 2010;156:286–301. doi:10.1016/j.jbiotec.2011.06.017.

[3] Datta R, Tsai S, Bonsignore P, Moon S, Frank JR. and Lactic Acid Derivatives 1995;16:221–31.

[4] Honigberg SM. Cell signals, cell contacts, and the organization of yeast communities. Eukaryotic Cell 2011;10:466–73. doi:10.1128/EC.00313-10.

[5] Heukelekian, H N. D, editor. Principles and Applications in Aquatic Microbiology. 1964. doi:10.1016/S0006-4971(20)69330-2.

[6] Qadir F, Ejaz U, Sohail M. Co-culturing corncob-immobilized yeasts on orange peels for the production of pectinase. Biotechnology Letters 2020;42:1743–53. doi:10.1007/s10529-020-02897-y.

[7] Yñiguez-Balderas B, Ortiz-Muñiz B, Gómez-Rodríguez J, Gutierrez-Rivera B, Aguilar-Uscanga M. Ethanol production by Pichia stipitis immobilized on sugarcane bagasse. Bioethanol 2016;2:44–50. doi:10.1515/bioeth-2016-0001.

[8] Heris Anita S, Mangunwardoyo W, Yopi Y. Sugarcane Bagasse as a Carrier for the Immobilization of Saccharomyces cerevisiaein Bioethanol Production. Makara Journal of Technology 2016;20:73. doi:10.7454/mst.v20i2.3059.

[9] https://www.tridge.com/intelligences/walnut/production n.d.

[10] Saeed A, Iqbal M. Loofa (Luffa cylindrica) sponge: Review of development of the biomatrix as a tool for biotechnological applications. Biotechnology Progress 2013;29:573–600. doi:10.1002/btpr.1702.

[11] Kilonzo P, Margaritis A, Bergougnou M. Effects of surface treatment and process parameters on immobilization of recombinant yeast cells by adsorption to fibrous matrices. Bioresource Technology 2011;102:3662–72. doi:10.1016/j.biortech.2010.11.055.

[12] Zhu D, Li X, Liao X, Shi B. Immobilization of Saccharomyces cerevisiae using polyethyleneimine grafted collagen fibre as support and investigations of its fermentation performance. Biotechnology and Biotechnological Equipment 2018;32:109–15. doi:10.1080/13102818.2017.1389302.

[13] Aggelis, Athanasios Mallouchos. George. AAKK. Grape skins as a natural support for yeast immobilization. Biotechnology Letters 2002;24:1331–5. doi:10.1023/A.

[14] Singh A, Sharma P, Saran AK, Singh N, Bishnoi NR. Comparative study on ethanol production from pretreated sugarcane bagasse using immobilized Saccharomyces cerevisiae on various matrices. Renewable Energy 2013;50:488–93. doi:10.1016/j.renene.2012.07.003.

[15] Baldikova E, Pospiskova K, Ladakis D, Kookos IK, Koutinas AA, Safarikova M, et al. Magnetically modified bacterial cellulose: A promising carrier for immobilization of affinity ligands, enzymes, and cells. Materials Science and Engineering C 2017;71:214–21. doi:10.1016/j.msec.2016.10.009.

[16] Junter G-A, Jouenne T. Immobilized Viable Cell Biocatalysts: A Paradoxical Development ☆. Reference Module in Life Sciences 2017:1–16. doi:10.1016/b978-0-12-809633-8.09086-5.

Chapter 5: Synergy of ball milling, microwave irradiation and Deep Eutectic Solvents for a rapid and selective delignification: Walnut shells as model for lignin-enriched recalcitrant biomass

Submitted to chemical Engineering Journal

5.1 Introduction

Valorization of lignocellulosic biomass via an integrated biorefining process has rekindled interest in environmentally friendly and sustainable chemistry[1]. Walnut shells (WS) are typically discarded as agricultural feedstock or used in low-value, large-volume applications such as abrasives and heating. Walnuts (in Shells, WS) are produced in ca. 3.8 million metric tons per year [2]. With a remarkably high lignin content (49-52%)[3,4], WS have potential to be an appealling raw material, particularly when it comes to “lignin-first“ biorefinery concepts, in which the potential of lignin is put forefront, and prior to the subsequent valorziation of the polysaccharide fractions[5]. In more classic approches for biomass valorization, emphasis lies on the obtention of fermentable sugar streams for biofuel production, while lignin is underutilized (e.g. combustion)[6]. Importantly, lignin, an integral component of the cell wall of plant fibers,[7] remains elusive to be extracted in high-purity while preserving the native structure [8]. Pretreatment techniques to deconstruct biomass include steam explosion, dilute acid, ionic liquids, and alkaline assisted hydrolysis. The recently introduced OrganoCat approach intends to efficiently process lignocellulose while addressing environmental concerns associated with other methods[9].

When emphasis is put on a (non-reductive) “lignin-first“ approach, pretreatments for selective delignification – while leaving the polysaccharide fractions as intact as possible, are desired. Recently, Deep Eutectic Solvents (DES) derived from the combination of hydrogen-bond donors (HBDs) and hydrogen-bond acceptors (HBAs) have garnered interest in biomass delignification[6,10], being DESs typically cost-effective and environmentally benign solvents [11]. DES trigger the partial cleavage of ether bonds among lignin phenylpropane units, contributing to the depolymerization[12], and generating shorter molecular weight lignin distributions, while maintaining many of the structural bonds of native lignin. In this area, for instance, Jablonsky et al. successfully employed several DES such as lactic acid:alanine (9:1 molar ratio), lactic acid:glycine (9:1 molar ratio), lactic acid:betaine (2:1 molar ratio), choline chloride:ethylene glycol (1:2 molar ratio), or choline chloride:glycolic acid (1:3 molar ratio) at 60 °C for 24 h on beechwood and straw. Of all of them, lactic acid: alanine (9:1 molar ratio) and choline chloride:glycolic acid (1:3 molar ratio) DES resulted the most efficient ones for a broad delignification [13]. In general, the lignin yield and purity was dependent on reaction temperature, (long) residence times, DES composition and type of biomass. Other more recalcitrant (but potentially useful) derivatives containing higher lignin contents (e.g. walnut shells), have not been broadly assessed with DES, and examples are scarce[14].

Remarkably, those derivatives are typically non-edible and present a high energy density, what may be advantageous for future biorefineries[14].

Envisioning the need of more efficient approaches by means of the DES as promising alternative for delignification, this paper explores strategies with largely diminished residence times (ultimately, reducing them to a matter of *minutes*), with promising biomass loadings (100-200 g L^{-1}), and valorizing recalcitrant raw materials, particularly with high lignin content (WS). If successul, those approaches may pave the way for continuous delignification processes, what could certainly improve the economic figures and the overall sustainability. To that end, a combination of a Ball Milling (BM) step, together with microwave irradiation (MI), and DES-mediated delignification is demonstrated (Scheme 1). To our knowledge the joint combination of BM with MI in DES has never been assessed in the area, and only one paper describes the separation of polyprenyl acetates from *Gingko biloba* leaves[15]. Mechanical approaches can improve performance in biomass pretreatment[16–18]. With respect to use MI with DES, some publications evidence the residence time reduction, yet typically using lower biomass loadings[19,20], and materials with less lignin contents. MI has the following advantages over conventional heating during the pretreatment: (i) heating is non-contact and volumetric; (ii) energy is transferred not heat; (iii) energy is conserved; (iv) heating is rapid and efficient; (v) material is selectively heated [21].

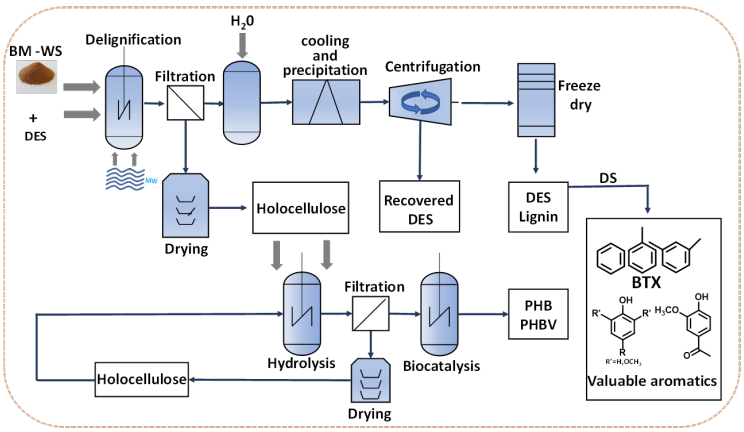

Scheme 5.1 Envisioned flow to integrate a synergistic multiple pretreatment process as biorefinery, using WS as prototypical biomass with high recalcitrance due to their high lignin content. The polysaccharide fractions are envisioned as fermentable sugars to produce polyhydroxybutyrate, but other valorization routes can be considered as well. DS = Downstream process, BM= planetary ball mill, WS=walnut shell. MW=microwave, BM= Ball milling, DES=Deep eutectic solvent, PHB=Polyhydroxybutyrate

5.2.1 Methods and Materials

Materials: Choline chloride (CC), formic acid (FA), lactic acid, L-alanine (AL) and glycolic acid (GA) were purchased from sigma Aldrich. Glucose, Xylose, acetic acid, levulinic acid, furfural, and arabinose was purchased from Scharlab. Nylon filter was purchased from Scharlab.

5.2.2 Walnut shell preparation: The walnut used in this study was grown in Southern California. The shells reduced by using a small blade coffee blender (KunFT GTM-8803120W 30 g capacity). The sieve (CISA) was applied to segregate the ground walnut shell into WS particle of 0.5 mm, 0.3 mm, 0.2mm and 0.1 mm. WS were dried in an oven at 105 °C for 24 h until constant weight. A moisture content of less than 2% was obtained for all WS, which were kept in an airtight vial that was stored in a desiccator for further usage.

5.2.3 DES preparation: Each DES system was prepared by weighing the required quantity computed from their molar ratios. Each system was heated at 60 °C for 24hr. A clear mixture formed was cooled down to room temperature in desiccator. Three Different DES systems were prepared in various molar ratios Lactic acid :alanine (9:1), formic acid: choline chloride (2:1), glycolic acid :choline chloride (3:2).

5.2.4 Procedure for WS delignification via DES: Extract-free WS of 10 wt% (100g/1000g) or 20 wt% (200g/1000g) were studied. The appropriate amount of WS of various diameter (0.1mm, 0.3mm and 0.5mm) was placed in clear mixture and reacted at 60 °C 90, 120 °C and 150 °C either with conventional heating (oil bath) or microwave reactor (milestone). Extractive free ball milled WS were also tested at 60 °C, 90 °C, 120 °C and 150 °C. In microwave heating, temperature was elevated from room temperature to 60 °C, 90 °C, 120 °C and 150 °C with a power of 1000W over 5 min to reach set-point temperature and held at set-point temperature for the appropriate residence time, (either 5, 15, 35, and 55 min). 1000W was used to reach the set-point temperature and it automatically dropped to 500-600W until the reaction ended.. After each reaction with DES-WS system, the system was cooled down. 0.5 mL of distilled water added and stirred vigorously for 5 minutes and then filtered through nylon filter. Lignin was then precipitated from the liquid fraction by addition of 20 mL of distilled water. The precipitated lignin was separated by centifugation at 5000 rpm and subsequent decantation. The lignin was lyophilized for 24 h and the yield was calculated as reported elsewhere[22]. The solid fraction was washed with distilled water until neutral pH was reached and further dried at 105 °C for 16h. The yield of residual solids were calculated as reported in the literature [22].

5.2.4 Biochemical analysis of solid residue: The pretreated WS residue was analyzed for carbohydrates and Klason lignin with protocol ASTM D 1106-84[23].Analysis was performed by quantitative hydrolysis of the residue in 72% wt H_2SO_4 at 30 °C for 60 min. The solution was then diluted to 4% wt H_2SO_4, further hydrolysis at 121 °C for 60 min in autoclave. A sample of this acidic solution was filtered through a 0.45 mm nylon syringe filter. HPLC analyses were performed with an Agilent 1100 series chromatograph using an ICSep ICE-COREGEL 87H3 (Column serial n_12525124). The temperature of the column was 50 °C, and the mobile phase was a solution of 5 mM H_2SO_4 at a flow rate of 0.6 mL min^{-1}. An Agilent 1100-DAD ultraviolet, diode-array (UV) detector and an Agilent 1100-RID refractive index (RI) detector were connected in series to quantify furfural, HMF and carhydrate/carboxylic acids respectively. Klason lignin content was estimated as the residue after sulfuric acid hydrolysis of the pre-extracted material, corrected for ash.

5.2.5 MWL and MAL: MWL (milled wood lignin) was isolated with Björkman method [24]. For 24 hours, the ball-milled wood sample was suspended in 96 % dioxane at a solid-to-liquid ratio of 1:10 (g/mL) and stirred continuously at room temperature. Filtration and washing with the same solvents were performed until the filtrate was clear. These operations were carried out twice. MAL and purification steps were adopted from literaure [25].

5.2.6 FTIR (Fourier transform infrared spectroscopy): was used to study and intepret the chemical changes that occurred pretreated WS and lignin obtained. The FTIR spectra were recorded with a Jasco FT/IR-600 Plus equipped with ATR Specac Golden Gate, which directly measures the sample. The sample spectra were recorded with 32 scans using 2 cm^{-1} resolution.

5.2.7 ESEM (environmental scanning electron microscopy with Quanta 600): was used to evaluate the morphology of pretreated WS. Samples were sputtered with gold nanoparticles prior to analysis. Images were taken at 3kV.

5.2.8 Viscosity measurement: Calibrated Ubbelohde viscometer (K=0.09989 cst/s, 10-100mm^2/D) was applied in measuring the kinematic viscosity of each DES. The viscometer was charged with 20 mL DES and placed in temperature bath for 20 min. to allow for DES to adjust bath temperature. Three valve rubber suction bulb was applied to raise the DES to the small upper reseviour. The efflux time was recorded for when the DES traveled between the set-marked distances. Kinematic viscosity (v)= C*t, where C denotes the viscometer

constant. t denotes flux time. The density of each DES was measured with a pycnometer at different temperatures (25 °C, 60 °C and 90 °C). The dynamic viscosity was calculated from the relation $v=\eta/\rho$, where v is kinematic viscosoty, η is dynamic viscosity and ρ is density.

Table 5. 1. Provides an overview of the experiments performed with WS in different DES and conditions, including conventional heating, microwave irradiation and ball milling. Processing time varied from hours to just minutes, when synergies appear and processing results fast (BM+MI+DES) .

Des	Temp (°C)	Time (minutes)	Heating source	Acronym
Lactic acid: alanine (LAAL)	60	480 minutes (8h)	Conventional	LAAL-8
Formic acid: choline chloride (FACC)	60	480 minutes (8h)	Conventional	FACC-8
Glycolic acid: choline chloride (GACC)	60	480 minutes (8h)	Conventional	GACC-8
Lactic acid: choline chloride (LAAL)	60	960 minutes (16h)	Conventional	LAAL-16
Formic acid: choline chloride (FACC)	60	960 minutes (16h)	Conventional	FACC-16
Glycolic acid: choline chloride (GACC)	60	960 minutes (16h)	Conventional	GACC-16
Lactic acid: alanine (LAAL)	60	1440 minutes (24h)	Conventional	LAAL-24
Formic acid: choline chloride (FACC)	60	1440 minutes (24h)	Conventional	FACC-24
Glycolic acid: choline chloride (GACC)	60	1440 minutes (24h)	Conventional	GACC-24
Formic acid: choline chloride (FACC)	60	60 minutes	Microwave	M6060
Formic acid: choline chloride (FACC)	90	20 minutes	Microwave and Ball milled	MB9020
Formic acid: choline chloride (FACC)	90	40 minutes	Microwave and Ball milled	M(B)9040
Formic acid: choline chloride (FACC)	90	60 minutes	Microwave and Ball milled	M(B)9060
Formic acid: choline chloride (FACC)	90	20 minutes	Conventional and Ball milled	C(B)9020
Formic acid: choline chloride (FACC)	90	40 minutes	Conventional and Ball milled	C(B)9040
Formic acid: choline chloride (FACC)	90	60 minutes	Conventional and Ball milled	C(B)9060
Formic acid: choline chloride (FACC)	120	10 minutes	Microwave and Ball milled	M(B)12010

Formic acid: choline chloride (FACC)	150	10 minutes	Microwave and Ball milled	M(B)15010

5.3. Results and Discussion

Typically, lignin obtained from kraft, sulfite, and organosolv processes is modified. During kraft and sulfite processes, lignin obtained aryl ethers and benzylic esters undergoes rearrangement and displacements by sulfides and sulfites, rendering the lignin less reactive to post-processing[26] as illustrated scheme 2. The presence of sulfur poisons catalysts in an attempt to utilize kraft lignin for downstream processes. Delignification with alkali and sulphates process reduces β-O-4 aryl ether linkages and subsequent formation of stable C-C bonds, complicating the utilization of lignin for downstream process [27]. However, lignin derived from DES has high amount of OH groups, which are readily available for functionalization or other downstream processes such as reductive degradation to yield BTX aromatics or reductive oxidation to yield other high-value aromatics[12].

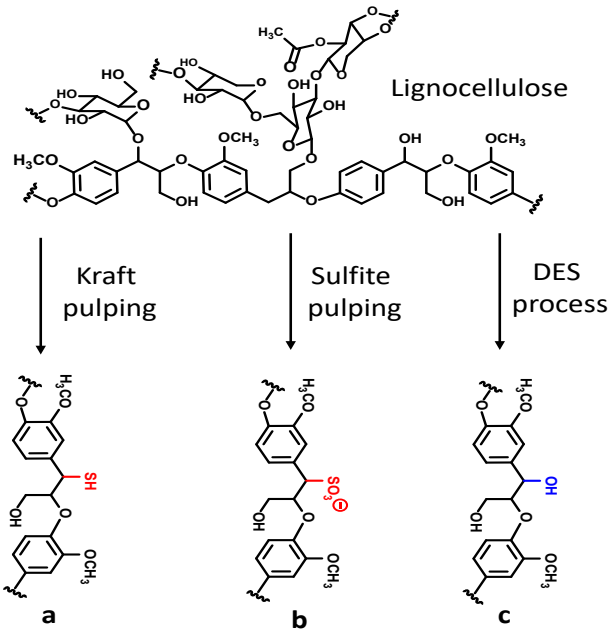

Scheme 5.2. Benzyl thiolation after kraft process (a), Benzyl sulfonylation after sulfite process (b), and Benzyl alcohol after DES process (c)

The above-mentioned advantage of DES-lignin over lignin produced via kraft and sulfite processes underpins our fundamental research to increase the yield of DES-lignin, with a

particular emphasis on the interaction of viscosity, reaction time, and biomass diameter under mild and moderate temperatures.

A first set of experiments was conducted to evaluate the viscosity of the different DES. The diffusivity of a solvent is critical to the process's efficiency in biomass deconstruction, and thus it is desirable to use DES with a low viscosity. Several DES were assessed (Table 1):

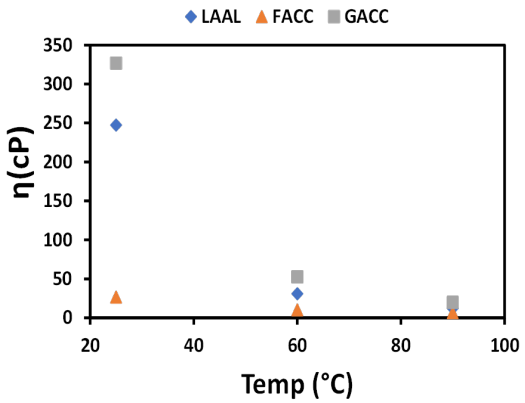

Figure 5. 1. DES profile of viscosity as a function of temperature

GACC (glycolic acid: choline chloride 3:1 molar ratio) exerted the highest viscosity (326 cP), while FACC (formic acid:choline chloride 2:1 molar ratio) had the lowest one (26 cP at 25 °C). Remarkably, at 90 °C, all DESs had viscosities less than 20 cP (Figure 5.1), what confer them potential as delignifying agents, consistent with the literature [28–30]. Subsequently, a screening of WS with different particle size (0.1-0.5 mm) in the three DES was conducted at several processing times (8h, 16h, and 24h) at 60 °C and at 10 wt% WS loadings.(Figure S2). All experiments were conducted with conventional heating. As observed (Figure S2), in all cases delignification occured, regardless the DES and the reaction time. Best results were obtained with WS of 0.1 mm operating under FACC (Formic acid: choline chloride) DES, yielding 13.6 % lignin (ca. 27 % of original lignin content OLC) (Figure S5.2a). Conversely, lower lignin yields were obtained for 0.5 mm WS operated under LAAL system (Figure S5.2c). The higher lignin yield obtained with WS with a diameter of 0.1 mm originates presumably due to the high surface-to-solvent contact ratio compared to the 0.5 mm WS-DES system with the lowest surface-to-solvent contact ratio. Thus, experiments were conducted with WS of 0.1 mm.

Subsequently, WS were subjected to planetary ball milling for 3 hours at a rotational speed of 600 rpm, and were then treated with different DES at varying residence times (8, 16 and 24 h) (Figure 5.2).

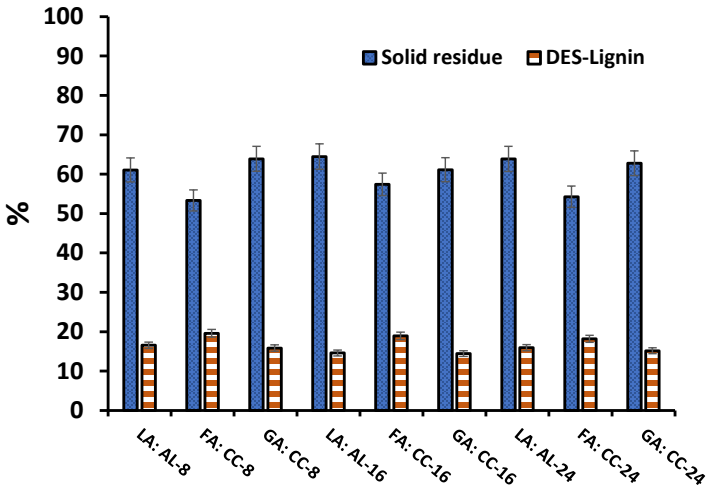

Figure 5. 2. DES-lignin yield and solid residue of ball milled WS at 60 °C for 8 h,16 h and 24 h. Conventional heating was applied in all cases.

When ball-milled WS was treated with FACC DES at 60 °C using conventional heating, a higher lignin yield of 19.8 % (ca. 40 % of OLC) after 8 hours of reaction time was obtained (Figure 5.2). It is worth noting that the surface-to-solvent ratio was not the only factor improving lignin yield, but also the DES and the mechanical disruption of molecular structure in biomass (WS) caused by ball milling[31]. Other authors have reported no significant cleavage of β-O-4 bonds upon 48h of only planetary ball milling of different lignocellulosic biomass [32]. FACC and GACC contain monocarboxylic acids with different alkyl chain length, modulating the acidic strength of the solvent that may result in a more or less efficient agent[33]. Thus, the weak acidity of GACC DES might lead to low lignin yields compared to the lignin yield of FACC-DES (Figure 2), but differences are not significant. LAAL DES led to a lignin yield of ca.17% (ca.34.0% OLC), which is comparable to GACC's yield of 16 % (ca. 32 % OLC) after 8 hours at 60 °C, (Figure 5.2). Interestingly, when the reaction time was increased to 16h and 24h, no significant improvement in lignin yield was observed in any of the DESs. Therefore, the focus of subsequent experiments was put on temperature increment with the shortest reaction time possible. FACC was selected as promising DES for further investigation due to its better performance over LAAL and GACC. At 90 °C, experiments were

carried out under FACC DES system at time interval of 20, 40 and 60 minutes on both un-milled and milled WS. In all processing times the ball milled derivative resulted much more processable than untreated samples, demonstrating the utility of mechanical approaches for delignification. For instance, lignin yield reached 15.8% (ca.32 % OLC) after 60 min of reaction of ball milled WS (CB9060) while un-ball milled WS (C9060) yielded 11.2 % of lignin (ca. 22 % of OLC) (Figure 3).

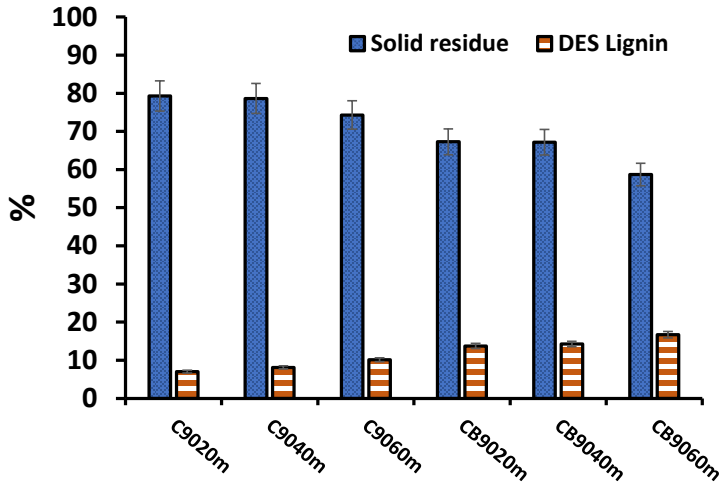

Figure 5. 3. DES-lignin yield and solid residue of ball milled and unmilled WS at 90 °C for 20, 40 and 60 min. Conventional heating was applied in all experiments.

Having successfully tested the use of DES with BM – showing a consistent improved delignification (Figure 5.3) –, subsequent experiments focused on incorporating microwave irradiation instead of conventional heating, and on applying different temperatures. Experiments were carried out at 60 ºC, 90 °C, 120 °C, and 150 °C using FACC DES coupled with microwave heating, and/or incorporating ball milling (Figure 5.3).

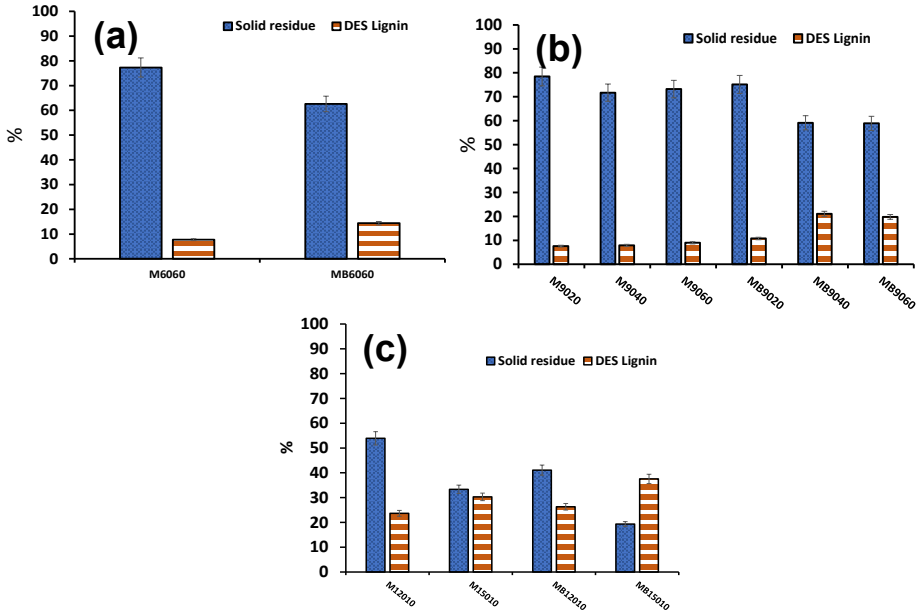

Figure 5. 4. DES-lignin yield and solid residue. (a) MI at 60 °C, 60 min, with or without ball milling (denoted by the "B"); (b) MI at 90 °C, 20-60 min, with or without ball milling (denoted by the "B"); (c) MI at 120 °C and 150 °C for 10 min and loading capacity of 10wt%, with or without ball milling (denoted by the "B").

Preliminary, the influence of the microwave was studied at 60 ºC (Figure 5.4a), clearly showing the synergy created with BM, MI and DES are implemented. Thus, the ball-milled WS and microwave-assisted DES system led to ca. 2-fold higher lignin yield than when conventional heating was applied (ca. 14 % vs. 7 %). Results with microwave at 60 ºC and 1 h were comparable to the obtained with the FACC-16h system (ca. 14 %, Figure S5.2a). Temperature was then increased up to 90 °C, and reaction times of 20, 40 and 60 minutes were set, using both milled and un-milled WS (Figure 5.4b). Results clearly show the largely improved performance (delignification) when BM and MI are applied together with DES. As an example, after only 40 minutes of reaction at 90 °C with microwave heating, MB9040 yielded 24.2% lignin (Figure 5.4b). Stimulated with the promising results, we decided to increase the temperature of the processing, and entries at 120 and 150 ºC were recorded, while reducing residence times to 10 minutes (Figure 4C). Gratifyingly, MB15010 (ball milling + microwave + 150 ºC + 10 minutes) led to 37.7% lignin yield (ca 75.4 % at a conversion rate of 100 % of the original 49.2 % lignin content). DES treatment of ball-milled WS at 120 °C for 10 minutes, on the other hand, yielded 27.9% lignin (ca. 56% OLC). Lignin yields were clearly lower for non-ball milled WS (Figure 5.4c).

Once the delignification took place, the work-up was performed by adding first 0.5 mL of water (to 10 mL of reaction media), to reduce the viscosity and facilitate filtration – recovering the polysaccharide fractions –, and then 20 mL of deionized water were added to the filtered DES liquid (ca. 5.5 - 7.0 mL) to precipate the lignin. When water was added to the DES, high purity lignin was regenerated, as reported by other groups as well [34] . Triggered by the promising concept which enables extensive delignification of materials with high lignin content, we decided to increase the WS loadings up to 20 wt % (200 g L^{-1}), to further explore the potential (or limitations) of the strategy (Figure 5.5).

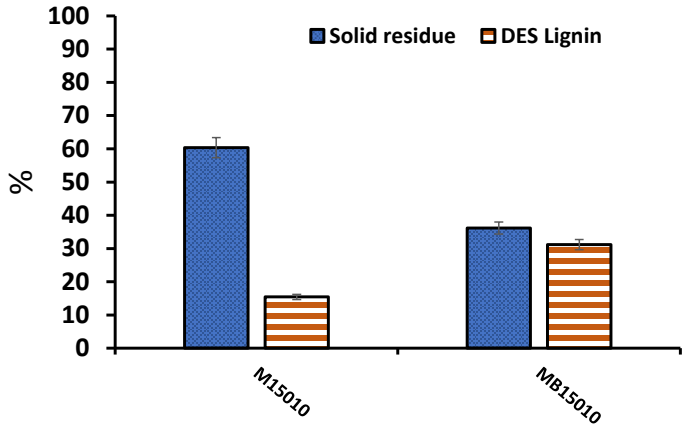

Figure 5. 5. DES-lignin yield and solid residue obtained when using MI at 150 °C for 10 min and loading capacity of 20wt%. Comparison between ball milled and unmilled samples.

As observed (Figure 5.5), after 10 minutes of reaction at 150 °C with ball-milled WS, a DES-lignin yield of 31.7% (ca. 63% OLC) was obtained, what represents a production of 60 g Lignin L^{-1} (under non-optimized conditions). By comparison, WS that had not been ball milled yielded 15.4% of DES lignin (ca.30 % OLC) (Figure 5.5). The observed large delignification at rather high biomass loadings (20 wt%) further reinforces the potential of the synergy for processing recalcitrant biomasses with high lignin content. The low residence time indicates that probably the set-up of continuous delignification processes is feasible, which could significantly improve yields and environmental impact of the pretreatment.

5.3.1. Analysis of solid residue and composition

Once the DES-mediated delignification took place, the solid residue was analyzed to determine the proportion of remaining biopolymers (glucan, xylan, and acid insoluble lignin (AIL)). Both conventional and microwave processes on ball-milled WS resulted in a markedly reduced level of AIL (Figure 6), fully consistent with a (virtually) complete delignification, when the synergy BM+MI+DES was applied for 10 minutes

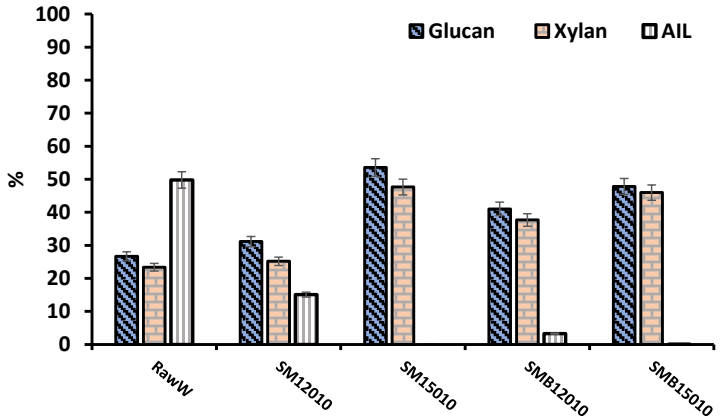

Figure 5. 6. Biopolymer profile solid residue after microwave heating at 120 °C and 150 °C for 10 min and loading capacity of 10 wt%. AIL is reduced depending on the severity of the delignification, while polysaccharide fractions remain constant if no significant degradation of them proceeds.

Apart from the remaining AIL, an interesting profile appears when glucan and xylan fractions are assessed. In the original material, the proportion of both polysaccharides resulted ca. 1:1 (Table S5.1). This profile remained when delignifications at short reaction times (10 minutes) were conducted (Figure 5.6). However, different results were obtained when longer reaction times are set (see Figure S5.4). Thus, at 90 °C, the glucan yields from solid residue of un-ball milled WS with microwave irradiation (SM9020, SM9040, and SM9060) remained at 39-41 %, analogous to the data obtained for un-ball milled WS (SC9020, SC9040, and SC9060) using conventional heating (38-44 % respectively). Likewise, xylan yields of these fractions resulted similar as well, 20-22 % for all samples either with microwave irradiation (SM90 20-60) or with conventional heating (SC90 20-60) (Figure S5.4). Overall, it leads to a glucan/xylan proportion of 2:1, what suggests a partial degradation of the xylan fraction (which is amorphous and more prone to acid-mediated depolymerization at high temperature). Remarkably, that proportion glucan / xylan was further enhanced when ball milling was incorporated to the delignification. Thus, all samples that were ball milled led to glucan amounts of 70 % at lower reaction times (20-40 min), decreasing to 55 % when 60 minutes were applied with conventional heating (this effect was not so significantly observed for MI samples). Likewise,

xylan proportions remained constant at 20-22 %. That means, the glucan / xylan proportion rose up 3:1 (20-40 minutes samples), enhancing 3-fold the glucan proportion compared to the raw material (Figure S5.4). A plausible explanation is the degradation of polysaccharides (hydrolysis, dehydration) at high temperature, long time and acidic media, which will be more severe when ball milling is applied, consistent with mechanocatalysis principles (which may decrease the cellulose crystallinity). To shed light on this, the effect crystallinity indexes of different samples were assessed. As reaction system 90 °C and 60 min were set (Figure S5.8). Untreated WS (RawW), only ball milled WS, labelled as (OB), SM9060, SMB9060, SC9060, and SCB9060 (solid residue from M9060, MB9060,C9060 and CB9060) showed crystallinity indexes of 44.2 %, 19.0 %, 53.0 %, 36.3 %, 49.0 %, and 35.0 %, respectively. After 3 hours of BM WS, the CrI index for RawW decreased by 25.21 %. Pretreated residue from non-ball milled WS, on the other hand, exhibited a higher crystallinity than residue from ball milled WS. This demonstrates that the low crystallinity of ball-milled WS contributes significantly to the increase in lignin yield, which was observed with both microwave and conventional heating at mild temperatures of 60 °C and 90 °C .

Quite importantly, such glycan/xylan proportion remained virtually 1:1 when higher temperatures were set (120 or 150 ºC), but lower reaction times (10 minutes) were applied. Therefore, the synergy of BM+MI+DES not only allows large delignification, but also a diminished degradation of the polysaccharide fractions, due to the low reaction times applied (Figure 5.6). This aspect may have profound implications for future biorefineries, as all raw materials can be obtained with high purity in short reaction times and with high biomass loadings. Surely a compromise could be found, by optimizing aspects like the time for ball milling, microwave irradiation (time and power), residence time (more or less minutes), and temperature (range 120-150 ºC), to obtain high lignin yields with non-degraded polysaccharide fractions.

5.3.2. Fourier transform infrared (FTIR) spectroscopy

To gain a better understanding of the properties associated with the obtained lignin through the DES digestion, milled wood lignin (MWL)[24] and mild acid lignin (MAL)[25] were prepared from WS and used as controls. The effect of BM and temperature on the various DES-lignins was carefully monitored. Major peaks were assigned based on previous research (Table S5.2) [35–39]. As observed (Figure 5.6), MWL, MAL, and DES-lignins all exhibited significant absorption near 3460 cm^{-1} due to the O-H stretching vibrations of phenolic OH and aliphatic

alcohol hydroxyl constituents (not shown). At 1754 cm^{-1}, the absorption band corresponds to the C=O stretching of carbonyl/ester constituents or unconjugated ketones[40]. The distinctive absorption bands at 1600 cm^{-1}, 1500 cm^{-1}, and 1452 cm^{-1} may be related to aromatic vibrations [41] detected in MWL, MAL, and all DES-lignins (Figure 5.6a, and 5.6b). At 1640 cm^{-1}, the absorption band is associated with the unconjugated carbonyl group's stretching vibrations[42]. (Figure 5.6a,5.6b,5.6c).

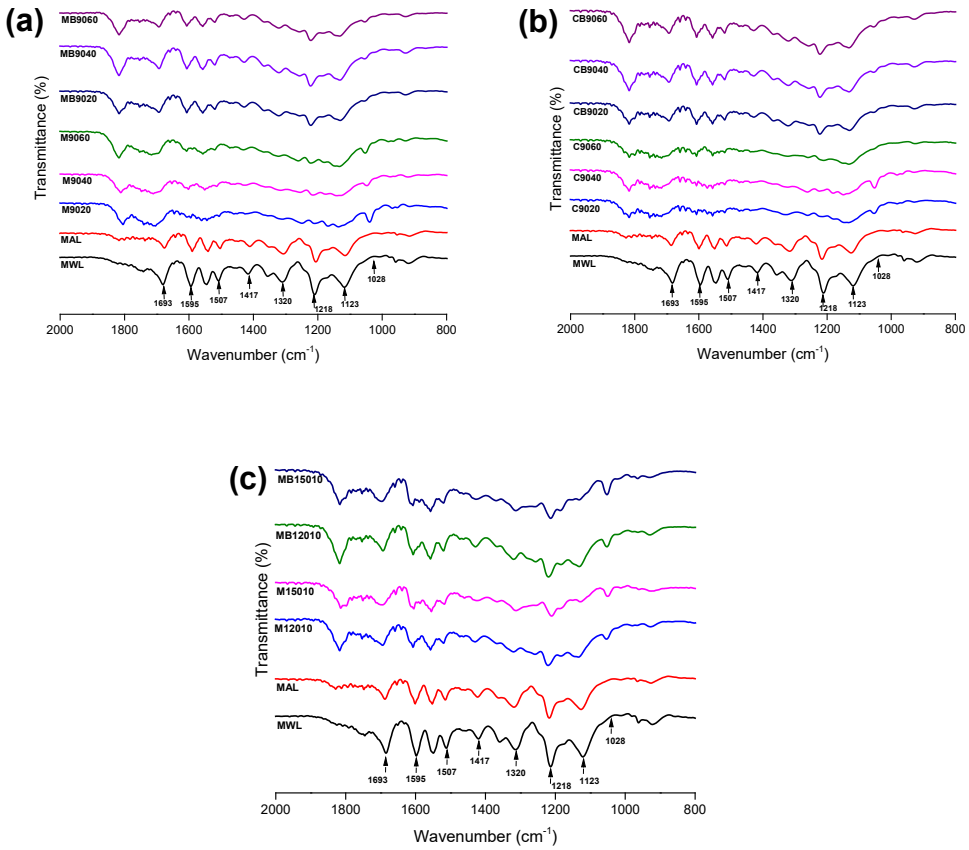

Figure 5.7. FTIR of MWL, MAL and DES lignins. (a) recovered after 90 °C on ball milled and un-milled WS with microwave irradiation; (b) recovered after 90 °C reaction temperature on ball milled and un-milled WS with conventional heating; (c) recovered after 120 °C and 150 °C on ball milled and un-milled WS microwave heating.

MWL, MAL, and DES-lignins exhibited C-O breathing of the guaiacyl ring at 1254 cm^{-1} and in-plane aromatic C-C deformation vibration at 1028 cm^{-1} [38,42] . At 1154 cm^{-1}, ether linkages produced a signal. There are few differences in the absorption bands of some functional groups identified in MWL, MAL, and DES-lignin when compared to published values, which

could be due to variation in the WS composition and DES used[34,42]. A thorough examination of MWL and MAL revealed that MWL had a negligible absorption fingerprint at 1754 cm^{-1}, whereas MAL had a discernible absorption at 1754 cm^{-1} (Figure 5.6a,5.6b,5.6c). The absorption band at 1640 cm^{-1} exhibited a wide range of intensity variations depending on the reaction conditions and system under consideration. 1640 cm^{-1} absorption band was visible in both MWL and MAL, as well as in all ball-milled WS that yielded lignins (MB9060, MB9040, MB9060, CB9060, CB9040, and CB9060), but was absent in lignins (M9020, M9040, M9060, C9020, C9040, and C9060) obtained from non-ball milled WS using both microwave and conventional heating (Figure 5.6a and 5.6b). Interestingly, when the reaction temperature was increased to 120 °C and 150 °C, both milled and unmilled WS DES-lignins exhibited a strong absorption band of the conjugated carbonyl vibrations at 1640 cm^{-1}. In those cases, lignins seemed to retain their conjugated carbonyl vibrations without any adverse effects from DES presumably due to the low processing times applied. Other authors, on the other hand, reported the disappearance of the absorption band 1640 cm^{-1} following DES pretreatment of non-ball milled poplar wood after 6h of processing. [34]. This discrepancy could be explained by either the biomass type or the DES type and composition, as well as the residence time (hours vs. Minutes). All lignins obtained after DES pretreatment exhibited an intense absorption band at 1754 cm^{-1}, originating from conjugated carbonyl (Figure 5.6a,5.6b, and 5.6c), what is found literature [34]. At 1154 cm^{-1}, ether linkages appear to remain defined in lignins obtained from ball-milled WS at 90 °C with the assistance of microwave and conventional heating sources. At 120 and 150 °C, both ball-milled and unball-milled WS DES-lignins exhibited a distinct and pronounced absorption band at 1154 cm^{-1}.This finding indicates the presence of β-O-4 rich and unmodified DES-lignin, which could serve as entry point for downstream processes. At 1254 cm^{-1}, an intense guaiacyl ring absorption was detected in MWL and MAL while the intensity of this absorption band was moderate in DES-lignin (MB9020, MB9040, MB9060, CB9020, CB9040, and CB9060). Moreover, the absence of carbohydrate fingerprints at 1426 cm^{-1} and 1373 cm^{-1} attests to the purity of the lignin obtained in this work, reflecting the selectivity of DES to delignify biomass [43]. Overall, the synergy of mechanical force and microwave irradiation at a mild temperature (90 °C) in the presence of FACC-DES resulted in lignins with identical primary functional constituents to native lignin (MWL). At 120 °C and 150 °C, microwave-assisted FACC-DES delignification of non-ball milled WS also resulted in neat lignin with similar functional constituents to MWL.

After DES delignification, FTIR analysis of soild residue revealed a significant intensity of cellulose and hemicellulose at 1056 cm^{-1} for the C-O stretching vibration[43] (Figure S5.7) (where SMB12010 denotes a solid recovered from pretreated ball-milled WS at 120 °C for 10 minutes with MI, SM15010 denotes a solid recovered from pretreated non-ball milled WS at 150 °C for 10 minutes with MI, SM12010 denotes a solid recovered from pretreated un-ball milled WS at 120 °C for 10 minutes with microwave, OB denotes only ball-milled WS and RawW=Untreated WS). Guaiacyl ring breathing coupled with carbonyl stretching at 1256 cm^{-1}[44] was intense in OB, but decreased significantly in solid residues analyzed following DES pretreatment of both ball-milled and unball-milled WS except OB

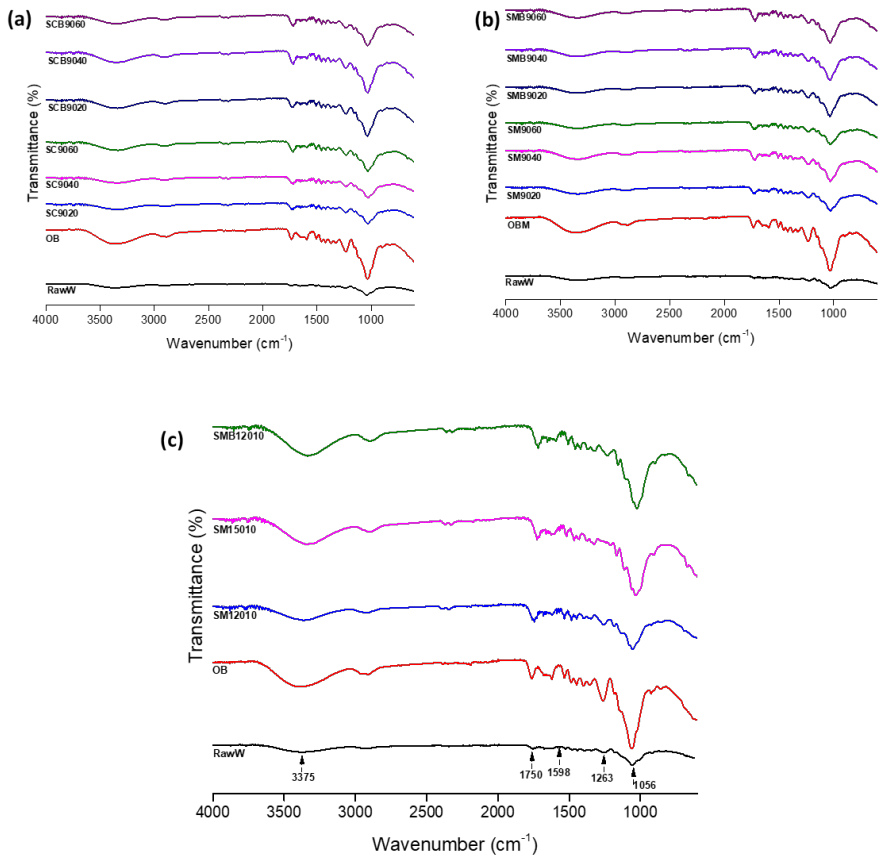

Figure 5. 8. FTIR spectra of raw walnut and solid residue (a) at 90 °C with conventional heating (b) at 90 °C with microwave heating (c) at 120 °C and 150 °C with microwave heating

(Figure 5.8a, 5.8b and 5.8c). Overall, this indicates that lignin was largely removed during the pretreatment process. The aromatic skeletal vibration of lignin and the carbonyl/acetyl constituent of hemicellulose were detected in the solid residue at 1598 cm^{-1} and 1750 cm^{-1},

respectively (Figure 5.8a, 5.8b and 5.8c). However, the absorption intensity at 1750 cm^{-1} was greater in OB, SM12010, SM15010, and SMB12010 than in RawW. Lignin's skeletal vibration at 1598 cm^{-1} was absent from all solid residues except OB and RawW. The observations made above at absorption bands 1056 cm^{-1} and 1750 cm^{-1} confirm the presence of a carbohydrate-rich solid residue. A thorough examination of OB and RawW revealed that mechanical forces have a significant effect on WS. Following ball milling (OB), the intensity of all major functional groups and fingerprint constituents increased.(Figure 5.8a, 5.8b and 5.8c).

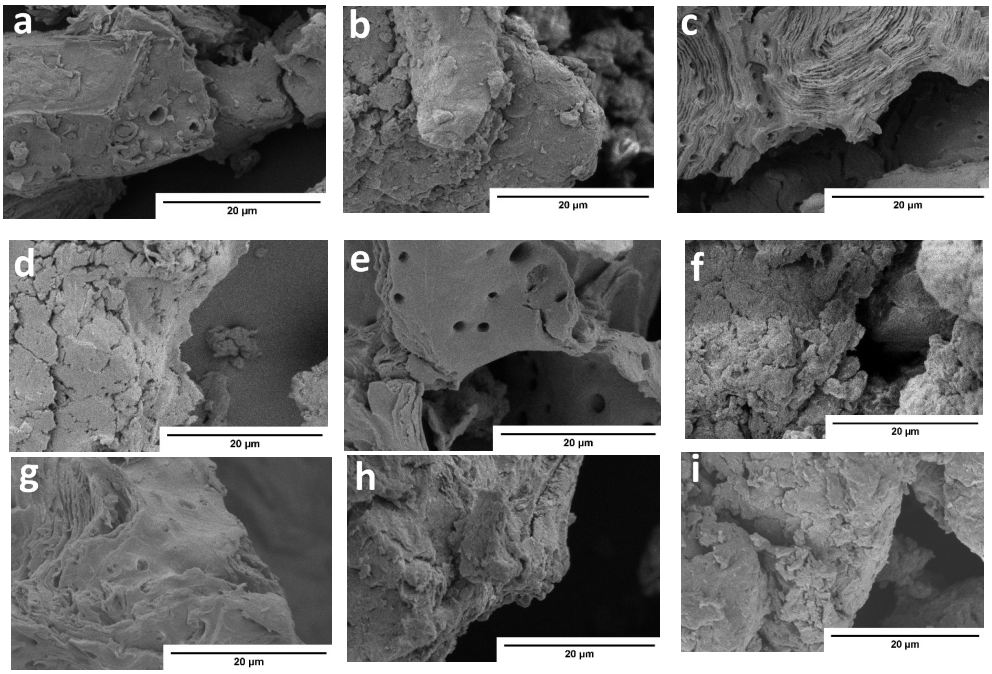

Figure 5. 9. ESEM images of (a) RawW (b) OB (c)SM9060 (d)SMB9060 (e) SC9060 (f) SCB9060 (g) SM12010 (h) SMB12010 (i) SM15010

5.3.3. Morphology of pretreated residue

To complement the anaylsis of the obtained products, the morphology of the residue was assesed. Environmental scanning electron microscopy (ESEM) analysis of the solid residues SM9060, SMB9060, SC9060, SCB9060, SM12010, SMB12010, and SM15010 revealed that DES treatment altered the morphology of the cells compared to Raw WS and OB (only ball milled) (Figures 5.9c, 5.9e and 5.9g). The edges of the solid residues from conventional and microwave heating of WS that were not ball milled demonstrated ridges and holes.

Conversely, pretreated solid residue from ball-milled WS appeared to be as compact as raw WS, RawW. (Figure 5.9b, 5.9d, 5.9f, and S5.9h). Despite the compact morphology of ball-milled pretreated WS, XRD analysis and CrI calculations revealed that SCB9060 and SMB9060 have a lower crystallinity index than SC9060 and SM9060 (Figure 5.10). As a result, it can be predicted that pretreated SCB9060 and SMB9060 residues will be more amenable to further enzymatic hydrolysis than SM9060 and SC9060 residues.

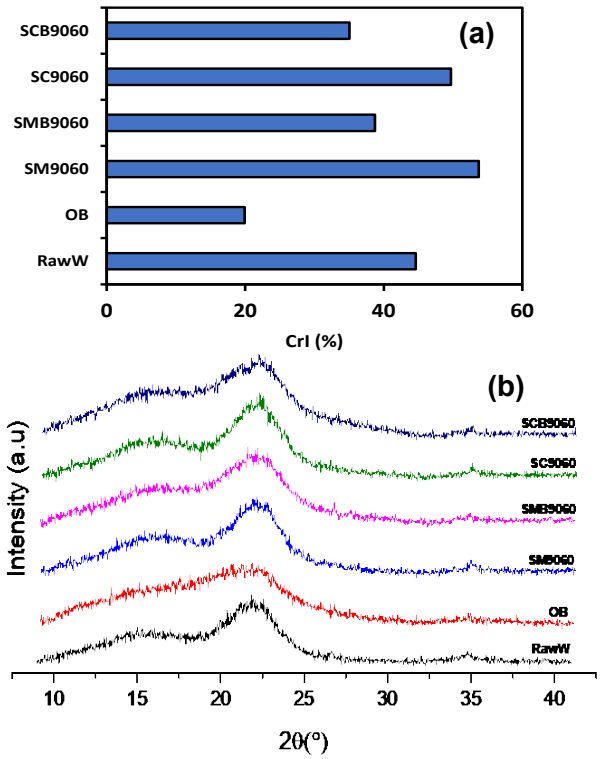

Figure 5.10. Crystallinity index (CrI) (a) and Diffractograms (b) of RawW, (Only ball milled WS=(OB) and pretreated solid residue (SM9060, SMB9060, SC9060 and SCB9060)

5.4. Conclusions

A synergistic concept incorporating ball milling (BM), microwave irradiation (MI) and DES has demonstrated the ability to delignify biomasses with high lignin content (WS) at 10 wt% and 20 wt% in a matter of minutes (after three hours of ball milling). Virtual complete delignification can be achieved, with reduced degradation of both lignin and polysaccharide fractions, due to the rapid processing time. Further fine-tuning of the BM and MI conditions, together with DES versatility, may optimize the herein reported system. The low processing digestion times

suggest that continuous delignification can be implemented. The concept may help valorizing large volumes of recalcitrant biomasses with high lignin contents, which otherwise would have to be subjected to low-value applications.

5.5. Reference

[1] P. Domínguez De María, *INDUSTRIAL BIORENEWABLES: A Practical Viewpoint*, **2016**.

[2] Https://www.atlasbig.com/en-au/countries-by-walnut-production, “Walnut Shell Abrasive,” **n.d.**

[3] R. Ahorsu, G. Cintorrino, F. Medina, M. Constantí, *Journal of Cleaner Production* **2019**, *231*, 1171–1181.

[4] A. Demirbaş, *Energy Sources* **2006**, *27*, 37–41.

[5] A. P. and K. B. Tamás I. Korányi ,* , Bálint Fridrich, *Molecules* **2020**, *25*, 1–22.

[6] A. J. Ragauskas, G. T. Beckham, M. J. Biddy, R. Chandra, F. Chen, M. F. Davis, B. H. Davison, R. A. Dixon, P. Gilna, M. Keller, P. Langan, A. K. Naskar, J. N. Saddler, T. J. Tschaplinski, G. A. Tuskan, C. E. Wyman, *Science* **2014**, *344*, DOI 10.1126/science.1246843.

[7] L. Das, S. Xu, J. Shi, *Frontiers in Energy Research* **2017**, *5*, 1–12.

[8] M. E. Himmel, S. Y. Ding, D. K. Johnson, W. S. Adney, M. R. Nimlos, J. W. Brady, T. D. Foust, *Science* **2007**, *315*, 804–807.

[9] P. M. Grande, J. Viell, N. Theyssen, W. Marquardt, P. Domínguez De María, W. Leitner, *Green Chemistry* **2015**, *17*, 3533–3539.

[10] S. Constant, H. L. J. Wienk, A. E. Frissen, P. De Peinder, R. Boelens, D. S. Van Es, R. J. H. Grisel, B. M. Weckhuysen, W. J. J. Huijgen, R. J. A. Gosselink, P. C. A. Bruijnincx, *Green Chemistry* **2016**, *18*, 2651–2665.

[11] M. Francisco, A. Van Den Bruinhorst, M. C. Kroon, *Green Chemistry* **2012**, *14*, 2153–2157.

[12] C. Alvarez-Vasco, R. Ma, M. Quintero, M. Guo, S. Geleynse, K. K. Ramasamy, M. Wolcott, X. Zhang, *Green Chemistry* **2016**, *18*, 5133–5141.

[13] M. Jablonsky, A. Haz, V. Majova, *Cellulose* **2019**, *26*, 7675–7684.

[14] W. Li, K. Amos, M. Li, Y. Pu, S. DeBolt, A. J. Ragauskas, J. Shi, *Biotechnology for Biofuels* **2018**, *11*, 1–15.

[15] C. W. Zhang, M. F. Li, Z. W. Qi, R. Tao, J. Z. Ye, X. Y. Xue, C. Z. Wang, *Process Biochemistry* **2021**, *100*, 252–259.

[16] Q. Yan, K. Miazek, P. M. Grande, P. Domínguez De María, W. Leitner, M. Modigell, *Energy and Fuels* **2014**, *28*, 6981–6987.

[17] N. Meine, R. Rinaldi, F. Schüth, *ChemSusChem* **2012**, *5*, 1449–1454, S1449/1-S1449/5.

[18] M. D. Kaufman Rechulski, M. Käldström, U. Richter, F. Schüth, R. Rinaldi, *Industrial and Engineering Chemistry Research* **2015**, *54*, 4581–4592.

[19] Y. Liu, W. Chen, Q. Xia, B. Guo, Q. Wang, S. Liu, Y. Liu, J. Li, H. Yu, *ChemSusChem* **2017**, *10*, 1692–1700.

[20] P. D. Muley, J. K. Mobley, X. Tong, B. Novak, J. Stevens, D. Moldovan, J. Shi, D. Boldor, *Energy Conversion and Management* **2019**, *196*, 1080–1088.

[21] X. Zhang, K. Rajagopalan, H. Lei, *Sustainable Energy & Fuels* **2017**, *00*, 1–36.

[22] S. J. Davis, Deep Eutectic Solvents Derived From Inorganic Salts, **2015**.

[23] A. P. Abbott, G. Capper, D. L. Davies, R. K. Rasheed, V. Tambyrajah, *Chemical Communications* **2003**, 70–71.

[24] M. Jablonsky, V. Majova, K. Ondrigova, J. Sima, *Cellulose* **2019**, *26*, 3031–3045.

[25] A. Barakat, C. Mayer-Laigle, A. Solhy, R. A. D. Arancon, H. De Vries, R. Luque, *RSC Advances* **2014**, *4*, 48109–48127.

[26] Z. Wang, X. Zhu, P. J. Deuss, *Industrial Crops and Products* **2021**, *167*, 113493.

[27] A. R. R. Teles, E. V. Capela, R. S. Carmo, J. A. P. Coutinho, A. J. D. Silvestre, M. G. Freire, *Fluid Phase Equilibria* **2017**, *448*, 15–21.

[28] Y. Chen, L. Zhang, J. Yu, Y. Lu, B. Jiang, Y. Fan, Z. Wang, *Royal Society Open Science* **2019**, *6*, 181757.

[29] A. Björkman, *Nature* **1954**, *174*, 1057–1058.

[30] T. Q. Yuan, S. N. Sun, F. Xu, R. C. Sun, *Journal*

Chapter 6: Towards zero-waste biorefineries: Hypercrosslinked benzene polymer as a task-specific reusable adsorbent for detoxification of lignocellulosic hydrolysates for downstream fermentation

….to be submitted to Green Chemistry

6.1. Introduction

As one of the most plentiful renewable feedstocks on the planet, lignocellulosic biomass has the potential to pave the way to a sustainable, carbon-neutral future [1,2]. In this context, the hemi-cellulosic and cellulosic fractions of lignocellulose can yield C5 and C6 sugars that can be further processed to produce valuable platform chemicals such as furans, H_2, gluconic acid, and sorbitol [3,4] or can be used as a feedstock for fermentation to produce biofuels and chemicals [5]. While using lignocellulosic biomass in place of corn starch and sucrose from sugar cane[6] has the potential to alleviate competition between bioeconomy products and food/feed supply[7] , it requires sophisticated pretreatment processes that efficiently separate and depolymerize the various biomass components [2,8]. Additionally, for fermentation purposes, it is critical to maintain low quantities of by-products that impair the microorganism's potency in the final sugar stream. In industrial usage, lignocellulosic biomass is used to create ethanol by first solubilizing the lignin or hemicellulose using thermochemical treatments and then hydrolyzing the cellulose and hemicellulose using a cocktail of fungal enzymes[9–12]. Additional ethanol production processes utilizing lignocellulosic feedstocks include simultaneous saccharification and fermentation [13].

While the pretreatment methodologies used in these techniques result in high yields of monosaccharides, the addition of exogenous enzymes to both processes increases the overall cost of production at industrial scales [14]. On the other hand, thermochemical pretreatment procedures such as steam explosion or dilute-acid treatments are sometimes hampered by the development of inhibiting microbiological byproducts [15–17]. Pretreatment conditions that are too harsh, such as high temperatures, breakdown hexoses and pentoses extensively into 5-hydroxymethylfurfural (HMF) and furfural, respectively.

Even at low concentrations, these breakdown products are known to have a considerable inhibitory effect on microbial activity [18]. Furfural concentrations as low as 4 g/L can completely suppress S. cerevisiae development [19]. Additionally, it was observed that an HMF concentration of 4 g/L greatly inhibited yeast growth during ethanol fermentation [20]. Boyer et al. argued that the inhibitory action of furfural and HMF was concentration-dependent [21]. Another class of microbial inhibitors created during biomass pretreatment operations are low molecular weight phenolics obtained from lignin (such as vanillin, syringaldehyde, and conferyl aldehyde), which exhibit a significant level of toxicity for yeast fermentation [16,17,22]. Vanillin and vanillic acid, for example, displayed a 50% inhibition at 1.3 g/L and 3.7 g/L, respectively[23] Cinnamic acid and cinnamaldehyde were found to have a significant

inhibitory effect on yeast during the fermentation of glucose from poplar wood hydrolysate[24]. Detoxification techniques such as evaporation[25], ion-exchange resins[26], overliming [27], and neutralization [25] have been researched to reduce these chemicals' detrimental effects on microbial activity. However, these detoxication procedures have drawbacks, including an increase in non-volatile hazardous chemicals, large cost increases, sugar degradation, and the development of toxic precipitates [27–29].To address the aforementioned issues, we describe a straightforward and fast approach for converting raw biomass into a purified, high-quality sugar stream suitable for fermentation.

Thus, a mechanocatalytic depolymerization technique was paired with a simple purification step to remove inhibitory by-products to generate high yields of C5 and C6 sugars under mild circumstances. The applied mechanocatalytic depolymerization strategy – a combination of mechanical force and chemical catalysis – entails dry milling of an acid-impregnated (ligno)cellulosic substrate, which results in the conversion of the substrate to depolymerized, water-soluble products (WSP)[30,31]. Research on the mechanocatalytic process has established a positive relationship between mechanical energy transfer and product yields [32-38] and established the technique's economic viability [31–33]. Further saccharification of the WSP under low-severity conditions precipitates lignin and produces sugars in high yields with negligible monosaccharide breakdown into HMF and furfural [34]. To efficiently purify sugar streams generated from mechanocatalytic depolymerization of cellulose, we have proposed hypercrosslinked polymer (HCP) sorbents. Thus, through – interactions, it was possible to obtain a selective and full elimination of furfural compounds as well as the acid catalyst p-toluene sulfonic acid (p-TSA) [35]. The purpose of this work is to determine the adsorbent's suitability for removing furfurals and phenolic lignin residues from a wood hydrolysate solution. The depolymerization of poplar wood by mechanocatalysis, subsequent saccharification of the WSP, and purification of the hydrolysates via adsorption of inhibitory by-products on hyperbranched benzene as a source of fermentable sugars is investigated. The hydrolysate solutions were then fermented with Saccharomyces Cerevisiae to produce ethanol. Figure 1 illustrates the described procedure schematically, including the attempt to recover the lost inhibitors via polymer desorption. To determine the deleterious effect of residual furfurals and phenolic chemicals on microbial metabolism and ethanol production, fermentation procedures were conducted using unpurified (crude) and purified hydrolysate solutions. Thus, the process was ramped up to yield a glucose concentration of 80–100 g/L in the fermentation medium while maintaining a working capacity of up to 200 mL.

6.2. Materials and Methods

Poplar wood (2 mm chips, J. Rettenmaier & Söhne); diethyl ether (VWR Chemicals); sulfuric acid (VWR Chemicals, 95%); Mg(OH)2 (Acros Organics, 95 %); Benzene (Sigma-Aldrich, anhydrous); dimethoxymethane (Sigma-Aldrich, 99 %); 1,2-dichloroethane (Sigma-Aldrich, 99.8 %); iron(III)chloride (Fisher Scientific, anhydrous); Yeast from Saccharomyces cerevisiae Type 1 (Sigma-Aldrich); D-glucose (Fisher Scientific, anhydrous); methanol (VWR Chemicals); agar (Sigma-Aldrich); peptone from casein (Sigma-Aldrich); peptone from meat (Sigma-Aldrich); $KH2PO_4$ (Sigma-Aldrich); $MgSO_4$ (VWR Chemicals); NaOH (VWR Chemicals); malt extract (Sigma-Aldrich); yeast extract (Sigma-Aldrich)

6.2.1. Acid Impregnation

The required amount of poplar wood was added to an acidic solution containing diethyl ether (80 mL per 10 g wood) and sulfuric acid (0.9 mmol per g wood). The impregnation was carried out for 2 h using a magnetic stirrer at room temperature. Then, all diethyl ether was removed under reduced pressure using a rotary evaporator. If not used immediately, the acid-impregnated wood was stored overnight in an air-tight vial at -10 °C.

2.1.2. Mechanically assisted depolymerisation

A Fritsch Pulverisette 7 ball mill and a Retsch MM500 mixer ball mill with stainless-steel vials (80 mL and 125 mL filling capacity, respectively) were used for substrate depolymerisation. The acid-impregnated substrate (7 g when using the Pulverisette 7 mill; 10 g when using the MM500 mill) together with stainless-steel milling balls (4 balls with a diameter of 20 mm when using the Pulverisette 7; 6 balls with a diameter of 20 mm when using the MM500 mill) were added to each vial. The substrate was milled in the Pulverisette 7 and MM500 for 3 hours at 600 rpm and for 8 hours at 35 Hz, respectively. During the milling process, the vial temperature was controlled manually and held between 35 and 45 °C by applying cooling cycles. The milled substrate was removed from the vials in a fume cupboard and used immediately to determine the water-soluble product yield. The remaining powder was stored in an air-tight vial at -10 °C.

6.2.3. Water Solubility Test

The exact mass of an empty centrifugal tube was measured. 0.5 g of the milled sample was added to the tube and suspended in 5 mL distilled water. The soluble parts of the sample were dissolved in the water by sonicating in an ultrasonic bath and manually shaking (20 min

in total) at room temperature. The resulting solution was centrifuged for 10 min at 9000 rpm. The liquid was then decanted off. After drying the centrifugal tube with the remaining, non-soluble content overnight at 40 °C under vacuum, the mass of the dried tube and, hence, the mass of the solid residue ($m_{solid\ residue}$) were determined. Finally, the water-soluble product (WSP)-yield was calculated through equation (1).

$$\boldsymbol{WSP}\ [\%] = \left(\mathbf{1} - \frac{\boldsymbol{m_{solid\ residue}}}{\boldsymbol{m_{sample} * f}}\right) * \mathbf{100}\ \% \qquad (1)$$

$\boldsymbol{m_{sample}}$ represents the mass of the milled sample added to the centrifugal tube and $\boldsymbol{f}$ is the substrate-to-impregnated-substrate weight ratio.

6.2.4. Saccharification of water-soluble products

The milled substrate (WSP-yield ≥ 95 %) was dissolved in water to form a 22 % solution (pH = 0.9). The solution was heated in closed glass vials (10 mL each) at 140 °C for 1 h. The solid residue formed upon heating was separated from the sugar solution by centrifugation. The sugar solutions were combined, and the pH value adjusted to 5.5 using $Mg(OH)_2$. If not immediately used, the solution was stored overnight at 4 °C.

6.2.5. Saccharification of water-soluble products (alpha cellulose)

Milled alpha cellulose with WSP yield >96 % was dissolved in water to obtain 22.8 wt % solution with respect to cellulosic component. Saccharification reaction was performed at 140 ^{O}C for 1 h in closed capped glass vial. A working volume of 10 ml was used.

6.2.6. Synthesis of hypercrosslinked benzene-polymer

A two-necked round bottom flask attached to a reflux condenser was charged with benzene (40 mmol), dimethoxymethane (120 mmol) and anhydrous 1,2-dichloroethane (100 mL). The flask was then purged with N_2 for a minimum of 30 min. Thereafter, the iron (III)chloride catalyst (120 mmol) was added under continuous N_2 flow. The flask was then sealed and heated under reflux at 80 °C overnight. The resulting benzene polymer was quickly washed with methanol in a Büchner funnel before further washing via Soxhlet extraction in methanol for 24 h. Finally, residual solvent was removed from the polymer by drying in a vacuum oven under reduced pressure at 40 °C, overnight.

6.2.7. Purification of the sugar solution with hypercrosslinked benzene polymer

In a typical purification step, the neutralised sugar solution obtained from the saccharification of the water-soluble products was exposed to a certain amount of hypercrosslinked benzene-polymer (2.5 g polymer per 50 mL solution) and shaken for 30 min. The polymer was then separated from the solution by filtration. The filtrate was collected and again purified with the same procedure using fresh polymer. If not used immediately, the purified sugar solution was stored overnight at 4 °C. The used polymer was washed with water and dried in a vacuum oven under reduced pressure at 40 °C, overnight. Through the weight difference of the dry polymer before and after the exposure to the solution, the amount of adsorbed material could be determined.

2.1.8. Yeast Fermentations

Yeasts (Saccharomyces cerevisiae type I (sigma Aldrich)) were grown on an agar plate with a medium containing 30 g/L of glucose, 3 g/L yeast extract, 2.5 g/L of peptone from casein, 2.5 g/L of peptone from meat extract, 3 g/L of malt extract and 15 g/L agar at 30 °C for 24 h. A loopful of single colony was then selected for preculture growth in an orbital shaker at 30 °C for 18 h. The preculture medium contained the nutrient composition as described above without agar.

Ethanol fermentations were carried out using the purified and non-purified sugar solutions produced via mechanocatalytic depolymerisation and further saccharification. As a control experiment, a sugar solution was produced using D-glucose. Nutrients were added to the required amount of the sugar solutions to produce final fermentation mediums containing 77-88 g/L of Glucose, 40 g/L of peptone from casein, 40 g/L of peptone from meat extract and 0.6 g/L of KH_2PO_4. $MgSO_4$ was formed during the neutralisation of the sugar solution produced by the mechanocatalytic pathway. In the control fermentation $MgSO_4$ (12 g/L) was added to the medium. The bioreactor was autoclaved at 121 °C for 20 min and all mediums were sterile filtered prior to inoculation with the preculture (10 % of the working volume). Fermentations (working volume of 100 to 200 mL) were carried out in an applikon MiniBio 500 bioreactor (maximum filling capacity of 500 mL) with a my-control system at 30 °C with 250 rpm for 26 h. During the process, the pH was controlled to a value of 5.5 with a 3 M NaOH solution and the DO_2 value was kept below 0.5 with intermittent N_2 purging. Samples (2mL) were taken every 2h.

6.2.9. Characterisation

To determine the biomass concentration during the fermentations, 1 mL of each sample was added to an Eppendorf tube and centrifuged for 5 minutes at speed of 6000 rpm. The supernatant was decanted off and kept for further analysis. The pellet was washed twice with 0.9 % NaCl and dried in a vacuum oven under reduced pressure at 40 °C, overnight. The mass of the dried solid residue (biomass) was determined.

The supernatant was diluted and analysed using a Perkin Elmer Series 200 HPLC at 40°C with a Bio-Rad Aminex HPX-87H Column (300 x 7.8 mm) column. A 5 mM H_2SO_4 solution with a flowrate of 0.6 mL/min was used as mobile phase. Cellobiose, glucose, xylose and ethanol were detected by an RI detector. For HMF and furfural determination, a UV/Vis detector at 270 nm was used.

6.3. Results and discussion

The requisite to high glucose yield is dependent on high water-soluble products (WSP). To achieve high WSP, various milling parameters were investigated. Based previous work reported in literature, 0.88 mmol/g of H_2SO_4, 0.5-3 h and 800 rpm were sufficient to give 80-100 % WSP from either cellulose or α-cellulose [30]. Due to the heterogeneity of biomass, we tested various milling parameter on poplar wood. We found the WSP was dependent on the speed of ball mill when all other parameters were kept constant. The optimum condition to achieve WPS >95% was to set ball speed at 600 rpm,3h of actual milling, 0.90mmol/g of H_2SO_4 impregnation and 4 balls with a diameter of 20mm. Other parameters were also tested, see Table 1. Apparently, 0.88 mmol/g H_2SO_4 as applied to α-cellulose did not yield the same quantitative WSP when poplar wood was subjected to similar condition. Probably, it could be due to the presence of lignin present in poplar wood.

Table 6. 1. Impact of milling parameters on water soluble products (WSP), 7g of substrate

Entry	H_2SO_4 (mmol/g)	No.balls	Ball size (mm)	Time (h)	Speed (rpm)	WSP %
1	0.88	15	10	2.5	300	30.3
2	0.88	15	10	2.5	400	34.4
3	0.88	10	15	2.5	400	36.8
4	0.88	10	15	2.5	500	41.3
5	0.88	3	20	2.5	500	58.3
6	0.90	3	20	2.5	500	87.3
7	1.00	3	20	2.5	500	84.1
8	0.90	3	20	4	500	94.2
9	0.90	4	20	4	500	92.4
10	0.90	3	20	3	600	93.9
11	0.90	4	20	3	600	96.2
12	0.90	4	20	2.5	600	92.1
13	0.90	4	20	2.0	700	90.1
14	0.90	4	20	2.5	700	94.2
15	0.90	4	20	3	700	98.2

The depolymerization of H_2SO_4-impregnated poplar wood was carried out mechanocatalytically to produce a lignocellulose powder with a WSP content of 97.3 %. The saccharification stage was carried out in aqueous solution at a pH of 0.9 and a temperature of 140 °C for 1 hour. This procedure resulted in glucose yields of 80.3 % and xylose yields of 98.2 %. Figure 6.1b

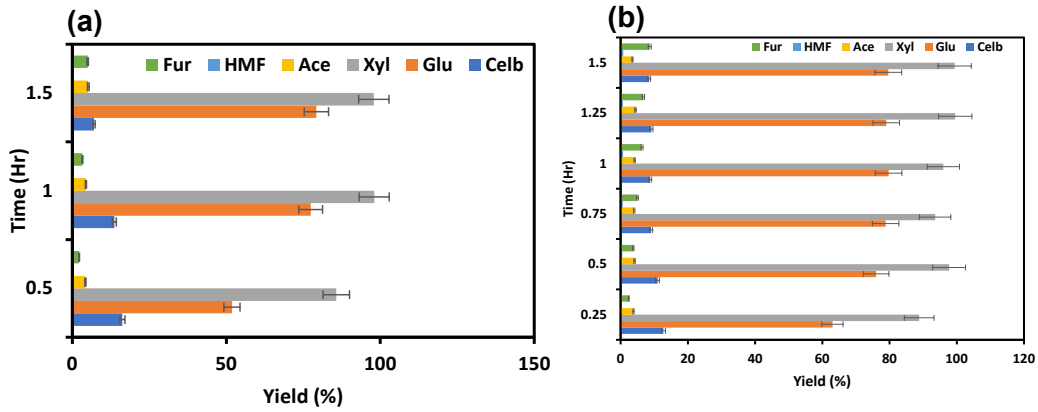

Figure 6.1. Effects of temperature on solubilized compounds at various residence time 130°C (a) and 140 °C.

Following the synthesis of glucose and xylose, HMF and furfural were produced with yields of 0.8% and 6.4 %, respectively. These results are comparable to those obtained in our previous study[34] using a variety of lignocellulosic substrates, demonstrating the highly efficient nature of the mechanocatalytic process for the production of water-soluble oligosaccharides capable of being hydrolyzed at temperatures as low as 140 °C with minimal degradation to furfurals. Saccharification of the WSP resulted in the precipitation of lignin, which could then be filtered away from the sugar solution. Nonetheless, a small amount of lignin remained dissolved (i.e., acid-soluble lignin). The filtrate (crude hydrolysate) was red/brown in color (Figure 6.2(a)). $Mg(OH)_2$ was utilized as a neutralizer, reacting with H_2SO_4 to form $MgSO_4$. Magnesium ions aid in the division and growth of yeast and accelerate the synthesis of ethanol in an anaerobic environment. Additionally, they have been shown to mitigate the detrimental effects of ethanol poisoning[36]. Notably, the current neutralization technique generates no salt precipitate, hence avoiding additional costly separation operations and greatly reducing waste streams, which are a major concern in industrial bioethanol production[37].

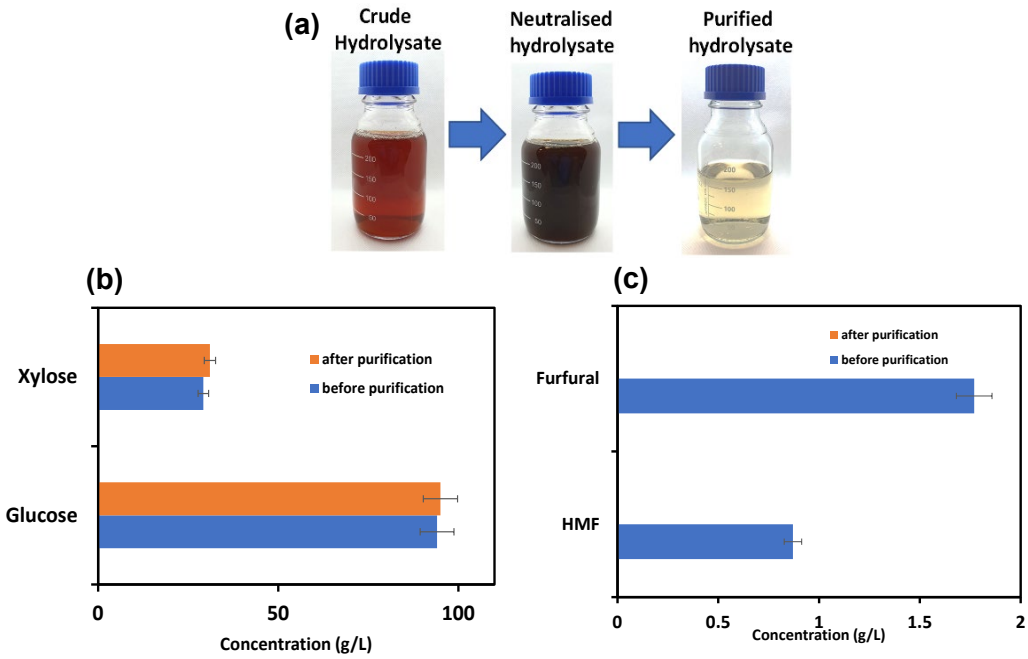

Figure 6. 2. Color difference of hydrolysate solutions (a), glucose and xylose concentrations in crude and purified hydrolysate (b) and HMF and furfural concentrations in crude and purified hydrolysate (c)

S. cerevisiae was used a biocatalyst in anaerobic fermentations of hydrolysate as well as a model D-glucose solution as a control experiment without the addition of any inhibiting substances. Before using the yeast as an inoculum (10% v/v of the total working volume), it was activated and pre-cultured for 18 hours. The neutralized crude hydrolysate was fermented to determine the adverse effect of sugar degradation products (HMF and furfural) as well as lignin-derived phenolics. After 24 hours of inoculation, no ethanol was produced and no cell growth was detected (figure 6.3(a)), showing that the crude hydrolysate has a significant level of toxicity. As previously stated, the present HMF and furfural concentrations (in the fermentation broth) of 0.51 – 0.56 g/L and 0.86 – 1.24 g/L, respectively, should not totally prevent yeast from converting glucose and restrict fermentation in relation to the volume of initial inoculum [19,20]. Although both compounds impede cell growth and ethanol production at very low concentrations, cell growth and good ethanol production have been recorded with HMF and furfural concentrations of up to 2.0 and 1.3 g/L, respectively, after 24 hours of fermentation[17,38].

To determine the effect of the predominant HMF and furfural concentrations, α-cellulose was pretreated using mechanocatalytic procedure followed by hydrolysis and subsequent

fermentation of hydrolysate using *S.cerevisiae*. As a result, the HMF and furfural concentrations in the α-cellulose hydrolysate were comparable to/even greater than those in the poplar wood hydrolysates (4.49 g/L and 7.76 g/L, respectively). Fermentation of the α-cellulose hydrolysate resulted in complete glucose consumption after 14 hours, as well as good cell growth and ethanol production S6.1 at annex indicating that the yeast cells were not affected by the concentrations of HMF and furfural present.

These findings support the hypothesis that, during fermentation of crude poplar wood hydrolysates, phenolic residues originating from lignin contribute significantly to the complete suppression of microbial activity. Purification of the wood hydrolysate stream via adsorption with the hypercrosslinked benzene polymer was used to test this theory. Thus, the neutralized hydrolysate was agitated for 30 minutes before being subjected to the purification process by using hypercrosslinked benzene polymer (2.5 g polymer per 50mL hydrolysate solution) as an adsorbent. After filtering, the filtrate was exposed to fresh polymer (2.5 g polymer per 50 mL filtrate) and filtered again. As illustrated in Figure 6.3(a), the purification process gave a clear hydrolysate and had no effect on the glucose or xylose concentrations (Figure 6.3 (b)).

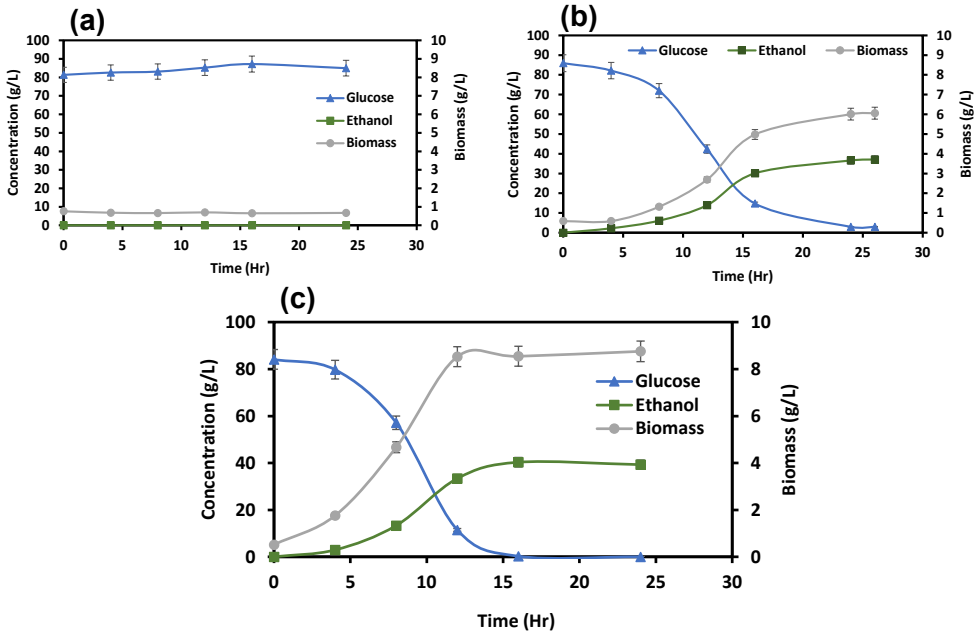

Figure 6. 3. Glucose, ethanol and biomass profile during fermentations of crude hydrolysate **(a)** purified hydrolysate **(b)** and model D-glucose solution **(c)**

The concentrations of glucose and xylose remain fairly the same. Notably, the final filtrate contained neither HMF nor furfural (Figure 6.3 (c), indicating that the benzene polymer adsorbed and eliminated putative fermentation inhibitors selectively.

As illustrated in Figure 6.4(b), 89.8% of glucose was consumed during the 16-hour fermentation of purified hydrolysates. This resulted in a 0.44 g/g ethanol yield (88.6% of the theoretical maximum yield) and a 2.2 g/L/h productivity. Extending the fermentation for an additional 8 hours boosted the ethanol yield to 0.45 g/g (90% of the theoretical maximum yield) and resulted in a 97% total glucose consumption.

These findings are quite consistent with those obtained in the control experiment using D-glucose (Figure 6.3(c)). The yield of ethanol from glucose was 0.46 g/g in this case, which corresponds to 94% of the theoretical maximum. After 14 hours of fermentation, 96 % of the D-glucose was utilized, yielding a 2.8 g/L/h ethanol yield. The highest growth of biomass was observed around 12h into fermentation and then halted. From 4 to 14 h, the ethanol content gradually increased. The rapid growth of the yeast at the commencement of the procedure (as early as two hours after inoculation), as well as the rapid start of ethanol production after only four hours, were both owing to the non-complex fermentation matrix (peptone, magnesium sulfate, potassium hydroxide, and D-glucose).

In comparison to the control experiment, the purified hydrolysate-based biomass development was modest throughout the initial six hours of the fermentation process, Figure 6.4b. This indicates that it took longer for the yeast to adapt to the slightly different fermentation matrix, which included low concentrations of other degradation products formed during the saccharification process, such as acetic acid (5.5 to 6.8 g/L), formic acid (concentration n.a.), and levulinic acid (concentration n.a.). However, this lag phase at the start of fermentation had no effect on the total amount of glucose consumed or the eventual ethanol yield. It well known that smaller molecular weight lignin is also lethal to microbial activity. The principal inhibitors in the hydrolysate solution were successfully removed via adsorption on the hypercrosslinked benzene polymer. As a result, dissolved phenolic compounds are anticipated to play a significant role in the complete inhibition in the current investigation that we reported.

6.4. Conclusion and future perspective

In summary, we offer a simple and effective mechanocatalytic technique for the efficient deconstruction of poplar wood to give fermentable sugars streams. It is demonstrated how to neutralize an acid catalyst that produces in situ $MgSO_4$ salts which contribute to enrich medium for yeast growth and ethanol generation without generating additional waste streams or cost. Additionally, sugar degradation products such as HMF and furfural, as well as phenolic inhibitors formed from lignin, can be completely eliminated by adsorption on a hypercosslinked benzene polymer. Thus, 97 % of glucose was consumed during fermentation of purified hydrolysates, yielding 0.45 g/g ethanol (90 % of the theoretical maximum yield). It is important to state that HMF and Furfural adsorbed on polymer could easily br recovered by ethanol wash. HMF and furfural are good candidates platform chemicals for biojet fuels precursors generation. As a result, the strategy given here demonstrates an environmentally friendly method for producing ethanol and also consolidating the overall strategy of achieving circular bioeconomy.

Notably, the presented work serves as a proof-of-concept for batch adsorption. However, continuous flow-through production techniques, in which a stream enters and exits an adsorption column constantly, are favoured in industrial practice (e.g., in the petroleum and bulk chemicals industries). In comparison to batch processing, flow-through procedures provide various advantages, including the elimination of the requirement for intermediate storage or transit and the ease with which laboratory processes can be scaled up.

6.5. Reference

[1] Cerveró JM, Skovgaard PA, Felby C, Sørensen HR, Jørgensen H. Enzymatic hydrolysis and fermentation of palm kernel press cake for production of bioethanol. Enzyme and Microbial Technology 2010;46:177–84. doi:10.1016/j.enzmictec.2009.10.012.

[2] Sheldon RA. The Road to Biorenewables: Carbohydrates to Commodity Chemicals. ACS Sustainable Chemistry and Engineering 2018;6:4464–80. doi:10.1021/acssuschemeng.8b00376.

[3] Wettstein SG, Alonso DM, Gurbuz EI, Dumesic JA. A roadmap for conversion of lignocellulosic biomass to chemicals and fuels. Current Opinion in Chemical Engineering 2012;1:218–24. doi:10.1016/j.coche.2012.04.002.

[4] Corma A, Iborra S, Velty A. Chemical Routes for the Transformation of Biomass into Chemicals. Chem Rev 2007;107:2411–502.

[5] Binder JB, Raines RT. Fermentable sugars by chemical hydrolysis of biomass. Proc Natl Acad Sci U S A 2010;107:4516–21. doi:10.1073/pnas.0912073107.

[6] Öhgren K, Bura R, Lesnicki G, Saddler J, Zacchi G. A comparison between simultaneous saccharification and fermentation and separate hydrolysis and fermentation using steam-pretreated corn stover. Process Biochemistry 2007;42:834–9. doi:10.1016/j.procbio.2007.02.003.

[7] Mussatto SI, Dragone G, Guimarães PMR, Silva JPA, Carneiro LM, Roberto IC, et al. Technological trends, global market, and challenges of bio-ethanol production. Biotechnology Advances 2010;28:817–30. doi:10.1016/j.biotechadv.2010.07.001.

[8] Sheldon RA. Green chemistry, catalysis and valorization of waste biomass. Journal of Molecular Catalysis A: Chemical 2016;422:3–12. doi:10.1016/j.molcata.2016.01.013.

[9] Hendriks ATWM, Zeeman G. Pretreatments to enhance the digestibility of lignocellulosic biomass. Bioresource Technology 2009;100:10–8. doi:10.1016/j.biortech.2008.05.027.

[10] Silveira MHL, Morais ARC, Da Costa Lopes AM, Olekszyszen DN, Bogel-Łukasik R, Andreaus J, et al. Current Pretreatment Technologies for the Development of Cellulosic Ethanol and Biorefineries. ChemSusChem 2015;8:3366–90. doi:10.1002/cssc.201500282.

[11] Narron RH, Kim H, Chang HM, Jameel H, Park S. Biomass pretreatments capable of enabling lignin valorization in a biorefinery process. Current Opinion in Biotechnology 2016;38:39–46. doi:10.1016/j.copbio.2015.12.018.

[12] Jansen MLA, Bracher JM, Papapetridis I, Verhoeven MD, de Bruijn H, de Waal PP, et al. Saccharomyces cerevisiae strains for second-generation ethanol production: from academic exploration to industrial implementation. FEMS Yeast Research 2017;17:1–20. doi:10.1093/femsyr/fox044.

[13] Van Zyl WH, Lynd LR, Den Haan R, McBride JE. Consolidated bioprocessing for bioethanol production using saccharomyces cerevisiae. Advances in Biochemical Engineering/Biotechnology 2007;108:205–35. doi:10.1007/10_2007_061.

[14] Klein-Marcuschamer D, Oleskowicz-Popiel P, Simmons BA, Blanch HW. The challenge of enzyme cost in the production of lignocellulosic biofuels. Biotechnology and Bioengineering 2012;109:1083–7. doi:10.1002/bit.24370.

[15] Palmqvist E, Hahn-Hägerdal B. Fermentation of lignocellulosic hydrolysates. I: Inhibition and detoxification. Bioresource Technology 2000;74:17–24. doi:10.1016/S0960-8524(99)00160-1.

[16] Palmqvist E, Hahn-Hägerdal B. Fermentation of lignocellulosic hydrolysates. II: Inhibitors and mechanisms of inhibition. Bioresource Technology 2000;74:25–33. doi:10.1016/S0960-8524(99)00161-3.

[17] Klinke HB, Thomsen AB, Ahring BK. Inhibition of ethanol-producing yeast and bacteria by degradation products produced during pre-treatment of biomass. Applied Microbiology and Biotechnology 2004;66:10–26. doi:10.1007/s00253-004-1642-2.

[18] Klinke HB, Olsson L, Thomsen AB, Ahring BK. Potential inhibitors from wet oxidation of wheat straw and their effect on ethanol production of Saccharomyces cerevisiae: Wet oxidation and fermentation by yeast. Biotechnology and Bioengineering 2003;81:738–47. doi:10.1002/bit.10523.

[19] N. Banerjee and L. Viswanathan. refere. Effects of furfural and 5-hydroxymethylfurfural on the growth and alcohol production by yeast Proceedings of the 40th Annual Convention of Sugar Technologists' Association of India, n.d., p. Section GI-4.

[20] Taherzadeh MJ, Gustafsson L, Niklasson C, Lidén G. Physiological effects of 5-hydroxymethylfurfural on Saccharomyces cerevisiae. Applied Microbiology and Biotechnology 2000;53:701–8. doi:10.1007/s002530000328.

[21] Boyer LJ, Vega JL, Klasson KT, Clausen EC, Gaddy JL. The effects of furfural on ethanol production by saccharomyces cereyisiae in batch culture. Biomass and Bioenergy 1992;3:41–8. doi:10.1016/0961-9534(92)90018-L.

[22] Mussatto SI, Roberto IC. Alternatives for detoxification of diluted-acid lignocellulosic hydrolyzates for use in fermentative processes: A review. Bioresource Technology 2004;93:1–10. doi:10.1016/j.biortech.2003.10.005.

[23] Clark TA, Mackie KL. Fermentation Inhibitors in Wood Hydrolysates Derived From the Softwood Pinus Radiata. Journal of Chemical Technology and Biotechnology Biotechnology 1984;34 B:101–10. doi:10.1002/jctb.280340206.

[24] Ando S, Arai I, Kiyoto K, Hanai S. Identification of aromatic monomers in steam-exploded poplar and their influences on ethanol fermentation by Saccharomyces cerevisiae. Journal of Fermentation Technology 1986;64:567–70. doi:10.1016/0385-6380(86)90084-1.

[25] Dominguez H, Domhguez JM. Improved xylitol production with. Enzyme 1997;0229:18–24.

[26] Gong CS, Chen CS, Chen LF. Pretreatment of sugar cane bagasse hemicellulose hydrolyzate for ethanol production by yeast. Applied Biochemistry and Biotechnology 1993;39–40:83–8. doi:10.1007/BF02918979.

[27] Martinez A, Rodriguez ME, Wells ML, York SW, Preston JF, Ingram LO. Detoxification of dilute acid hydrolysates of lignocellulose with lime. Biotechnology Progress 2001;17:287–93. doi:10.1021/bp0001720.

[28] Lanka S, Adivikatla VR, Shaik N, Kothagauni SY, Panda SH, Yenumula GP, et al. Studies on Different Detoxification Methods for the Acid Hydrolysate of Lignocellulosic Substrate Saccharum spontaneum. Dynamic Biochemistry, Process Biotechnology and Molecular Biology 2011;5:2–6.

[29] Canilha L, Cássia R De, Brambilla L, Almeida G, Silvério S. World ' s largest Science , Technology & Medicine Open Access book publisher Bioconversion of Hemicellulose from Sugarcane Biomass Into Sustainable Products n.d.

[30] Meine N, Rinaldi R, Schüth F. Solvent-Free Catalytic Depolymerization of Cellulose to Water-Soluble Oligosaccharides. ChemSusChem 2012;5:1449–54, S1449/1-S1449/5. doi:10.1002/cssc.201100770.

[31] Schüth F, Rinaldi R, Meine N, Käldström M, Hilgert J, Rechulski MDK. Mechanocatalytic depolymerization of cellulose and raw biomass and downstream processing of the products. Catalysis Today 2014;234:24–30. doi:10.1016/j.cattod.2014.02.019.

[32] Kaufman Rechulski MD, Käldström M, Richter U, Schüth F, Rinaldi R. Mechanocatalytic Depolymerization of Lignocellulose Performed on Hectogram and Kilogram Scales. Ind Eng Chem Res 2015;54:4581–92. doi:10.1021/acs.iecr.5b00224.

[33] Amirjalayer S, Fuchs H, Marx D. Understanding the Mechanocatalytic Conversion of Biomass: A Low-Energy One-Step Reaction Mechanism by Applying Mechanical Force. Angewandte Chemie - International Edition 2019;58:5232–5. doi:10.1002/anie.201811091.

[34] Käldström M, Meine N, Farès C, Rinaldi R, Schüth F. Fractionation of "water-soluble lignocellulose" into C5/C 6 sugars and sulfur-free lignins. Green Chemistry 2014;16:2454–62. doi:10.1039/c4gc00168k.

[35] Woodward RT, Kessler M, Lima S, Rinaldi R. Hypercrosslinked microporous polymer sorbents for the efficient recycling of a soluble acid catalyst in cellulose hydrolysis. Green Chemistry 2018;20:2374–81. doi:10.1039/c8gc00573g.

[36] Dombek KM, Ingram LO. Magnesium limitation and its role in apparent toxicity of ethanol during yeast fermentation. Applied and Environmental Microbiology 1986;52:975–81. doi:10.1128/aem.52.5.975-981.1986.

[37] Rinaldi R, Schüth F. Design of solid catalysts for the conversion of biomass. Energy Environ Sci 2009;2:610–26. doi:10.1039/b902668a.

[38] Banerjee N, Bhatnagar R, Viswanathan L. Inhibition of glycolysis by furfural in Saccharomyces cerevisiae. European Journal of Applied Microbiology and Biotechnology 1981;11:226–8. doi:10.1007/BF00505872.

Chapter 7: Catalytic cross-aldol condensation of furanics to produce C10 and C15 bio-jet fuel precursors with microwave-assisted process

…to be submitted to ChemSuSchem

7.1 Introduction

Biomass-sourced chemicals include cyclic C–C rings, they make excellent starting materials for the manufacture of aviation fuel. These biofuels for aviation have a stronger impact on global warming mitigation and on reducing reliance on fossil fuels [1]. The general strategy to synthesis biofuel involves (1) dehydration of carbohydrates into furfural (FF) and 5-hydroxymethylfurfural (HMF); (2) aldol condensation reaction of furfural and HMF with a ketone to create C–C bonds between biomass-sourced intermediates; (3) hydrodeoxygenation. To obtain structurally tailored fuel precursors, the second phase of aldehyde and ketone cross aldol condensation is essential. Various base-catalysed aldol condensation has been extensively used to generate an enolate intermediate, which is then converted into a C–C condensation fuel precursor [2].

A simple hydrolysis and dehydration process of hemicellulose can be used to produce furfural on an industrial scale, which is both simple and cost effective [3] . Valuable chemicals such as, cyclopentanone (CPO) tetrahydrofurfuryl alcohol (THFA), 2-methylfuran (2-MeF), furfuryl alcohol (FA) tetrahydrofuran (THF), pentylene, pentadiol [4,5]. In the presence of a metal catalyst, FF and FA can also undergo selective hydrogenation and rearrangement, resulting in the formation of cyclopentanone, a ketone [6]. The reaction mechanism proposed for FF to CPO was that, the carbocation of the carbon of aldehyde group first bonded to the metal surface, which then interacted with the co-absorbed water and rearranged to a possible intermediate before further hydrogenation to CPO [7].

FF-Acetone (AC) or HMF-AC aldol condensation has been extensively studied with both homogenous and heterogenous catalyst [8–14]. The CPO instead of AC offers added advantage such as (1) possesses two α-hydrogen positions that can alternatively be labile for aldol reaction (2) FF and CPO route to produce condensation adduct is completely renewable (3) FF and CPO condensation adducts offers longer and branched carbon chain precursors, hence better fuel quality is obtained [15–18].

Aldol condensation of CPO and FF has yielded two prominent fuel precursors 2,5-bis(2-furylmethylidene) cyclopentanone (F_2Cp) and 2-(2-furylmethylidene) cyclopentanone (FCp) in the presence both heterogenous and homogenous catalysts at varying temperature. Wang et al obtained 37.48 % and 23.77 % yields of F_2Cp and FCp respectively, at 60 °C for 6h under solvent free conditions [19]. Mg-Zr heterogeneously catalyzed FA–CC cross-aldol condensation yielded up to 60% desired F_2Cp within 4 hours at 30 °C in aqueous medium

[17]. J. Cueto et al employed Mg-Zr mixed oxide in another experiment where they employed a novel binary mixture of water and ethanol as solvent for cross-aldol condensation of FA-CPO. At optimum reaction condition of 30 °C, 24h and Mg-Zr catalyst weight of 0.1g, a combined F2Cp and FCp yield was 36 % [16]. From previous works on condensation of FF-CPO using NaOH as catalyst yielded 95% of F_2Cp aqueous medium at 40 °C [20]. However, the major drawback of using homogenous catalyst is it's corrosivity and recyclability [21]. From the studies done by the above authors and others, the type and amount of catalyst, temperature, solvent, total working volume with respect to FF:CPO, reaction time played a major role in the final determination of the global yield of F_2C_P and FC_P.

Microwave process have been employed in many organic reactions with excellent yield at faster reaction rate making it economically competitive. Loupy et al., observed an increase in yield from 2% to 95% under microwave conditions, in the Leuckart reductive amination [22]. Microwave assisted α,α'-bis (substituted benzylidene) cycloalkanones were synthesized by reacting benzaldehyde and other cyclic ketones in a solvent free conditions in the presence of both basic and acidic heterogenous catalyst with yield of 10 to 98% .

The goal of our study is to reduce the reaction time and improve the global yield of F_2C_P and FC_P with microwave process in the presence of Mg-Zr catalyst. The reaction will be carried out in both solvent free condition and in water/ethanol mixtures. The dielectric effect FF, CC, water and ethanol aldol reaction was also investigated.

7.2 Materials and Methods

Furfural, cyclopentanone, magnesium nitrate hexahydrate, sodium hydroxide, Zirconyl (IV) oxynitrate (hydrated) and 2-(2-furylmethylidene) cyclopentanone (FCp) were all purchased from Sigma Aldrich. 2,5-bis(2-furylmethylidene) cyclopentanone (F_2Cp) was synthesized in the laboratory according to the procedure published elsewhere [23].

Magnesia-Zirconia (MgZr) catalyst was obtained by sol-gel technique as was reported in literature [24]. Mg $(NO3)_2$ $6H_2O$ and $ZrO(NO_3)_2$ xH_2O in a quantity of 50.9 and 4.04 g respectively, was dissolved in 1L of deionized water. Under constant agitation, 1M NaOH was added into the mixture dropwise until pH of 10 was reached. The mixture was aged for 24 h and was subsequently washed until a pH of 7 was recorded for the filtrate. The recovered precipitate was dried at 50 °C for 24h. It was crushed into a powder and calcined at 600 °C

(10 °C/min) under both air and helium and designated as MgZr-A and MgZr-H respectively. Pure MgO was synthesized with same procedure and calcined in air designated as MgO-A.

7.3 Catalyst characterization

FTIR (Fourier transform infrared spectroscopy) was used to analyze the freshly prepared and used catalyst. The FTIR spectra were recorded with a Jasco FT/IR-600 Plus equipped with ATR Specac Golden Gate, which directly measures the sample. The sample spectra were recorded with 100 scans using 2cm^{-1} resolution. Thermogravimetric analysis. The thermal degradation of the samples was studied by a Sen Sysevo TG-DSC analyzer. Samples of ~10mg were heated from 25 to 800 °C at a rate of10 °C min^{-1}, using a constant N_2 flow at 40 ml min^{-1} to generate an inert environment.

SEM-EDX and TEM were used to both morphological study and elemental distribution. Specific surface area and pore volume were estimated by physisorption in Quantachrome apparatus at temperature of 77 K. The data acquired was processed using Brunauer–Emmett–Teller method (BET) and Barret-Joyner-Halena (BJH) for specific surface area and pore size distribution respectively.

The catalyst's basic and acidic site distribution were determined by temperature programmed desorption (TPD) of predesorped CO_2 or N_2 in Chemometrics coupled with mass spectrometry (MS). ~10mg of catalyst was outgassed in helium for 2.5 h at 500 °C and further exposed to CO_2 at 50 °C to reach a saturation. Weakly adsorbed CO_2 was eliminated by flushing the catalyst with helium at 50 °C for ~1 h. The temperature was elevated to 500 °C at a linear rate of 5 °C min^{-1}. The same procedure was repeated for NH_3 TPD.

7.3.1 Reaction set-up.

0.1 g of catalyst was applied in all reactions with 5% reactants in 1:1 mol ratio at total working volume 0.5L. Ethanol and water was used as solvent in 2:1 (v/v) ratio. Microwave power was set 1000 watts and different temperature and residence time were investigated. And a stirring of 60 % was set. After every reaction, sample was withdrawn and extracted with ethyl acetate and analyzed in GC-FID and GC-MS for quantitative and qualitative analysis respectively.

7.4 Results and Discussion

7.4.1 Catalyst characterisation

Morphological images with SEM did not reveal the usual hexagonal shape of MgO and its mixed oxides as shown in figure 7.1 (a), (e) and (j). However, elemental constituent was revealed in the SEM-EDX mapping shown in figure 7.1 (a-c) and combined map (d) for pure

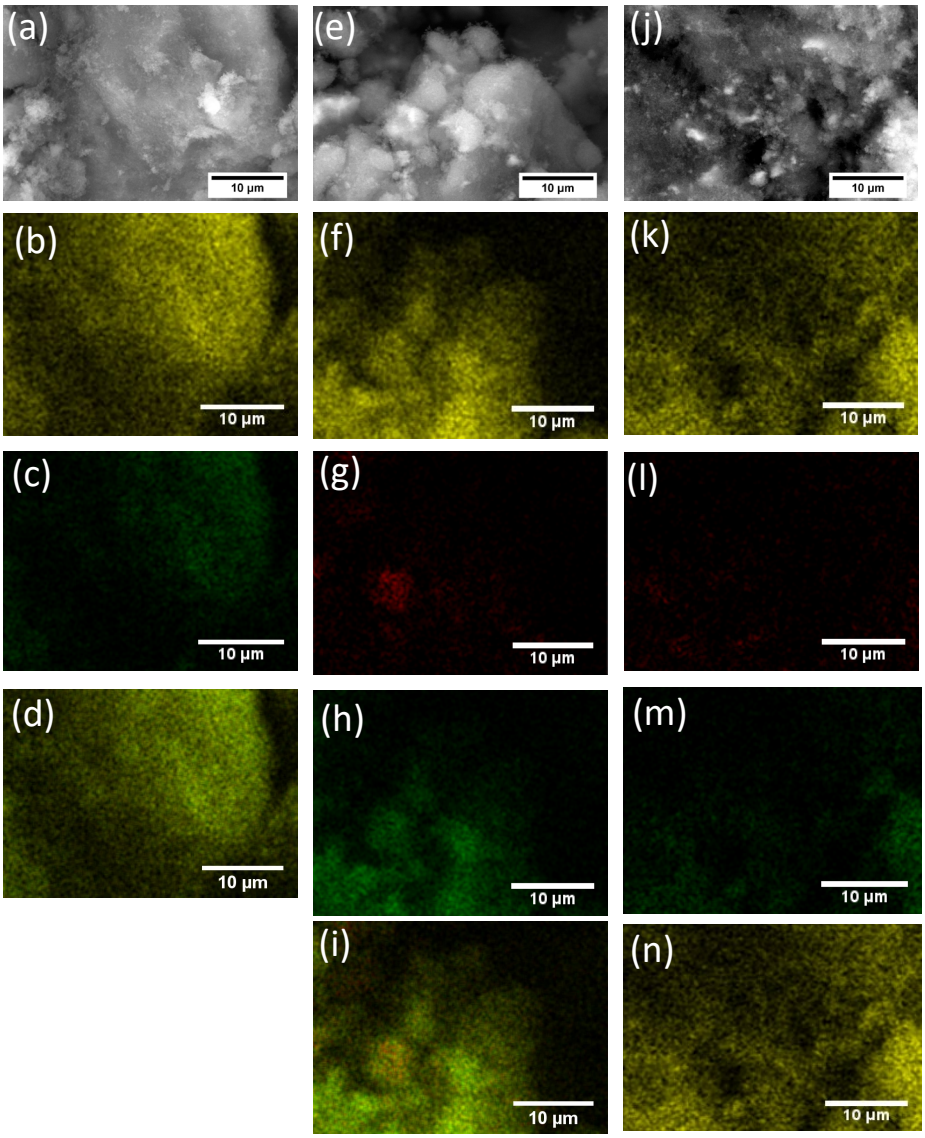

Figure 7. 1. SEM image of (a) MgO-A with its elemental maps shown in (b) Mg (c) O (d) MgO; (e) MgZr-H with its elemental maps shown in (f) Mg, (g) Zr, (h) O, (i) Mg,Zr,O and (j) MgZr-A with its elemental maps shown (K) Mg, (l) Zr, (m) O, and (n) Mg, Zr, O.

MgO. Clearly Mg was dominant with 62.2 wt % and O at 37.8 wt% in freshly prepared catalysts. The elemental representation in MgZr-H catalyst shown in figure 1 (e) also revealed the presence of Mg, Zr and O. Mg and O was mapping was more intense compared to Zr which is plausible due to lower precursor ratio of Zr employed during the synthesis of MgZr-H catalyst. MgZr-A also showed similar elemental representation as MgZr-H.

The EDX spectra and Wt% are shown in Figure S1 The colour elemental mapping shows moderate distribution of Mg and O while Zr was not evenly distributed when a six-point sample analysis was done on MgZr-A catalyst see Figure S2. EDX analysis of re-use catalyst revealed some minimal amount of carbon on surface of all catalysts. TEM images of MgO, MgZr-H and MgZr-A also show the hexagonal shape usually observed for MgO and MgO mixed oxides. However, calcination environment had effect on the final morphological characteristics. MgO-A and MgZr-A catalysts which were calcined in air showed raptured or holes on the surface while MgZr-H catalyst has intact hexagonal shape, see Figure 7.2 (a, b, and c). MgZr-H appears to be larger than MgZr-A in terms of particles size. Also, TEM images of reused catalysts shows no major change after microwave reaction at ETOH:H_2O solvent phase for 60 min at 140 °C. Although SEM-EDX and TEM shows the presence elemental constituents and morphological shapes of fresh and used-catalysts, we could differentiate any observable concentration of zirconia particle either on the surface of MgO or embedded within the layers of MgO.

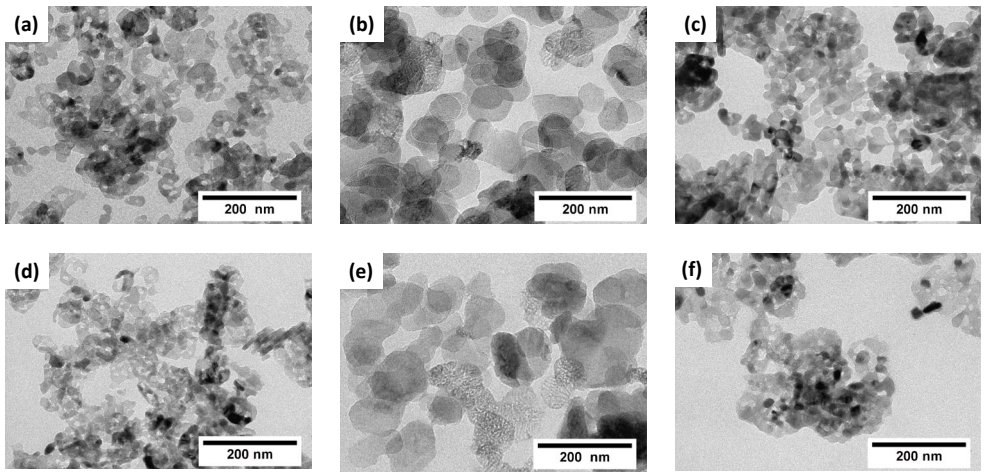

Figure 7.2. TEM image of (a) pure MgO (b) MgZr-H (c) MgZr-A (d) re-use MgO (e) re-use MgZr-H and (f) re-use MgZr-A

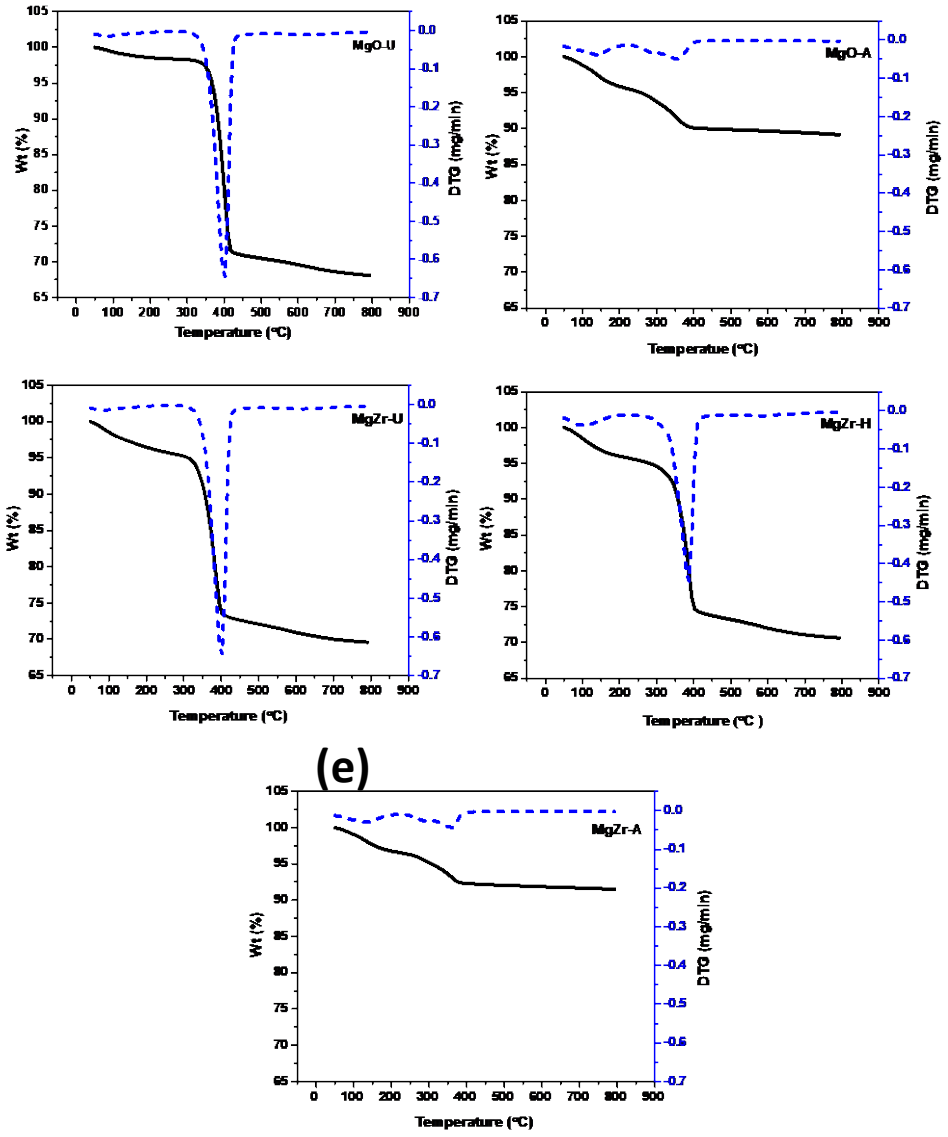

Figure 7. 3. TGA and DTG profile of freshly prepared catalysts

However, reaction tested from solvent free experiment with only reactants and catalyst shows precipitation of products, see Figure S3.

Generation of mixed oxides from precipitated precursors involves calcination and most reactions associated with temperature, hence thermal analysis of catalysis is needed to understand thermal decomposition of the catalyst. When non-calcined MgO-U $Mg(OH)_2$ was treated under N_2 in an increasing temperature rate of 10 °C min^{-1} from 50 to 600 °C, there

was thermal decomposition. At early temperature of 54 °C to 200 °C, 1.5 wt% weight loss was recorded and between 200 °C to 650 °C, 29.3 wt% weight loss was observed. However, a different thermal profile was observed for MgO-A. A first step weight loss of 4.4 wt% was realized between 50-220 °C due to loss of physically adsorbed interlayer water molecules [25,26]. A second stage weight loss of 6 wt% which is usually associated with loss of OH^- groups and degradation of interlayer carbonates adsorbed on MgO-U surfaces [26]. The thermal profile recorded for MgO-A was identical to MgZr-A with two stages of weight loss occurring between 50-200 °C and 200-620 °C. 3.3 wt% reduction in weight was recorded in the first stage while similar weight of 4.8 wt% was observed at the second stage of decomposition.

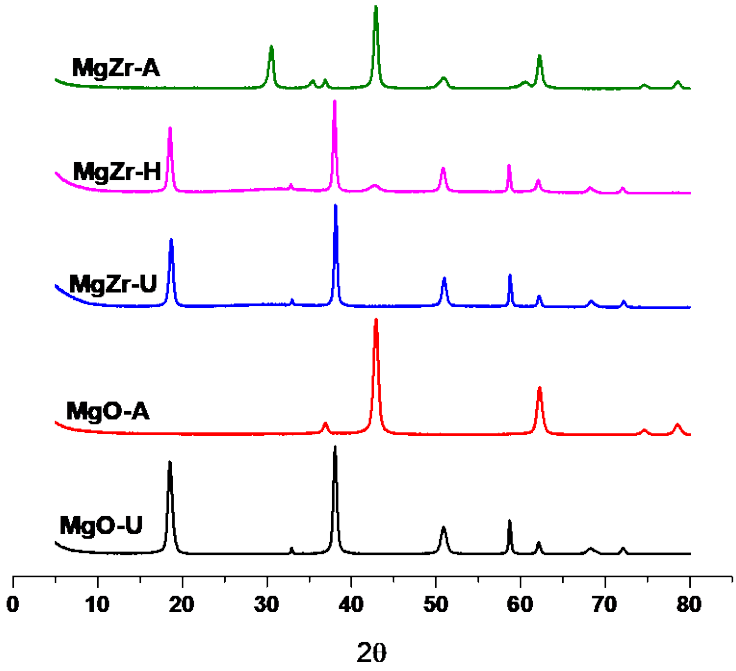

Figure 7. 4. XRD diffractograms of catalysts of non-calcined (MgO-U and MgZr-U) and calcined (MgO-A, MgZr-H and MgZr-A).

Meanwhile, MgZr-U and MgZr-H exhibited thermal profile similar to MgO-U. XRD analysis of MgO-U [$Mg(OH)_2$], MgO-A, MgZr-U, and MgZr-A exhibited diffractograms usually reported in the literature. MgO-U revealed intense peak at (2θ=38°) JCPDS00-002-1092 associated with brucite in $Mg(OH)_2$ [9]. MgZr-A mixed oxide consisting of periclase MgO at (2θ=43°, 62°,) and tetragonal zirconia at (2θ=30° 32° and 39°) [27,28], see Figure 7.4. MgZr-U and MgZr-H revealed similar diffractogram patterns with some minimum intensity of periclase MgO at 2θ= 43° shown in MgZr-H. The brucite peak at 2θ=38°was apparent in both MgZr-U and MgZr-H

suggesting an incomplete calcination of MgZr-H under helium environment. This observation corroborates the identical thermal profile of MgZr-U and MgZr-H during thermogravimetric analysis.

Table 7. 1. Morphological and chemical characteristics of MgZr-A

Catalyst	Total acidity (mmol/g)	Total Basicity (mmol/g)	surface area (m^2/g)	pore volume (cm^3/g)	pore diameter (nm)
MgZr-A	0.17	0.19	86	0.93	8

The acidity and basicity of MgZr-A (table 7.1) prepared by co-precipitation followed by calcination in air were determined by NH_3- and CO_2-TPD respectively. Deconvolution of peaks revealed temperature regions of 200 °C-350°C as (weak), 350°C-450°C (medium) and >450°C (strong), see Figure 7.5(a) and 7.5 (b). A moderate size peak was observed in the region of 375°C often associated NH_3 physiosorbed [29] and a big proportion of peak was located at 475°C (medium strength) of NH_3-TPD analysis. In addition, another broad peak at 540 °C signal strong strength acid distribution. From CO_2-TPD analysis as shown Figure 7.5(a), no weak basic strength was observed but rather a broad moderate basic strength was recorded at 450°C. Both acid and basic properties of catalysts are presented in Table 7.1.

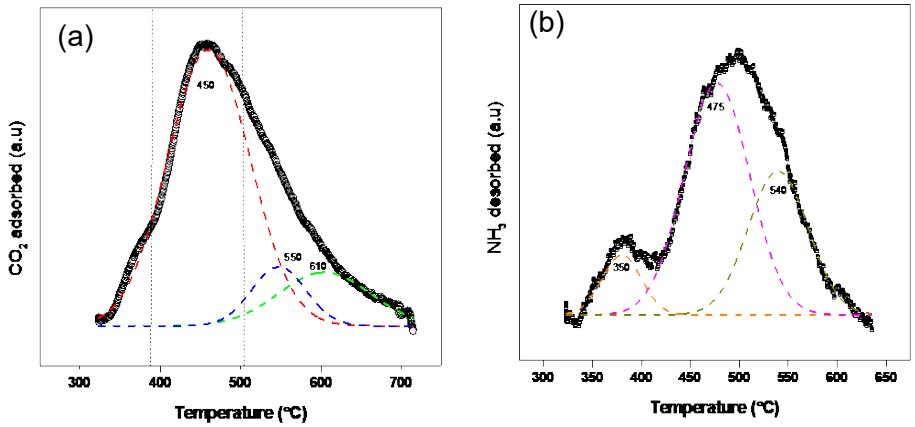

Figure 7. 5. Deconvolution analysis of CO_2-TPD (a) and NH_3-TPD (b) of MgZr-A

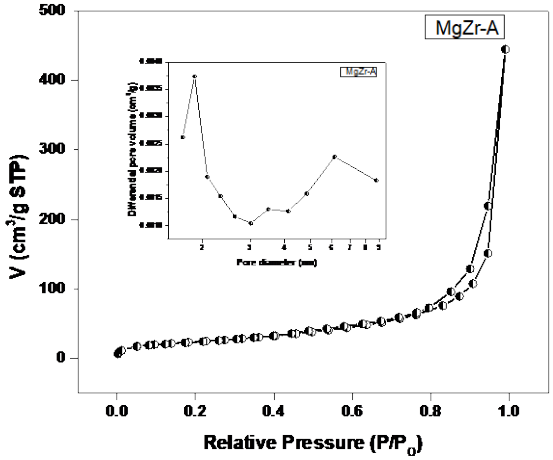

Figure 7. 6. N_2 adsorption-desorption isotherms of MgZr-A at 77K, insert (pore diameter distribution).

The BET surface area and pore size distribution of MgZr-A catalyst are recorded in table 1, and profile of pore diameter distribution is shown in Figure 6. (insert). The hysteresis loop obtained after N_2 adsorption revealed isotherm indicative of type IV material, see Figure 6. This is in agreement of the pore diameter distribution and placed the MgZr-H mixed oxides as mesoporous material.

7.4.2. Catalytic activity

Several experiments have been carried out to investigate the catalytic effect on aldol condensation reaction between ketones and aldehydes under different reaction conditions. Recently, most studies have focused on utilization of furan derivatives such furfural and HMF as an aldehyde component and acetone, cyclopentanone and other cyclic ketones to form adduct that can be further hydro-deoxygenated into biofuels [14,19,30–34]. Three catalysts (MgO-A, MgZr-H, and

MgZr-A) were screened at 120 °C and the best performing catalyst MgZr-A was selected for further investigation (not shown). Most aldol condensation reactions are carried out under mild conditions. However, longer reaction time and product precipitation are observed. In this study, both reaction time and effect of temperature on product evolution was done.

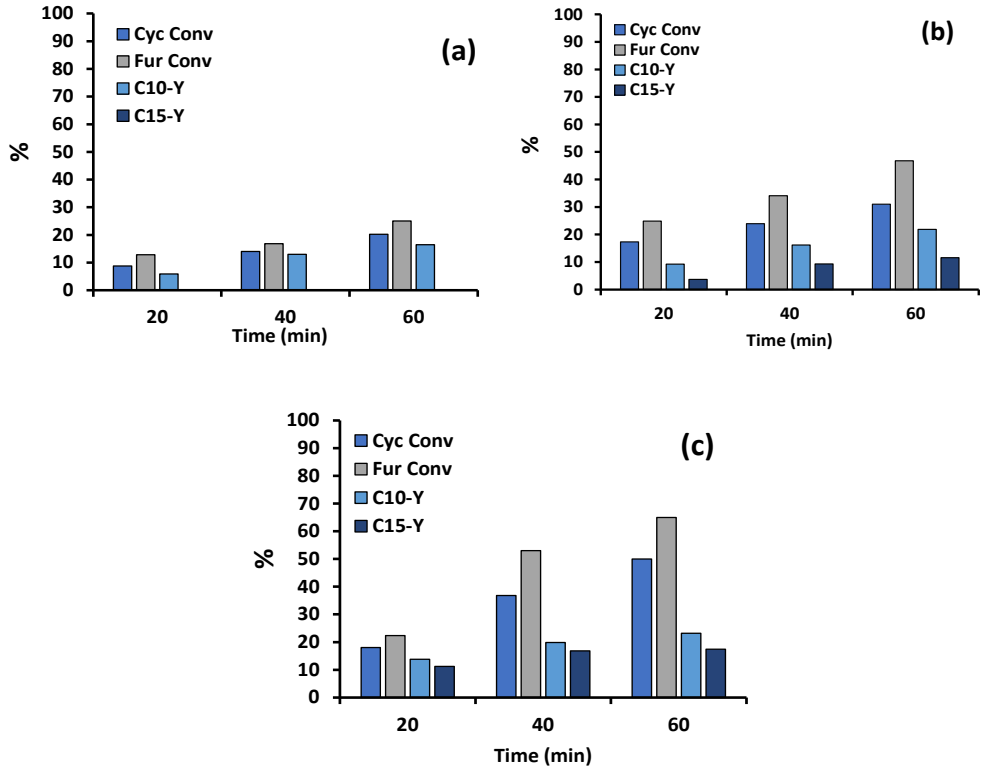

Figure 7.7. Cyclopentanone conversion (Cyc conv), furfural conversion (Fur conv), C10 yield (C10-Y) and C15 yield (C15-Y) at 120 °C (a), 140 °C (b) and 160 °C (c)

7.4.3 Effect of reaction time and temperature

Between 120 °C and 160 °C, the influence of temperature on reaction rate and product generation was investigated. Temperature up to 160 °C increased the rate of C10 and C15 production, indicating that the reaction is kinetically regulated. With an increase in temperature, the conversion of furfural and the rate of creation of C10 both increased. After 60 minutes at 160 °C, the final conversion was not significantly different from that at 140 °C, hence 140 °C was chosen as the best temperature. The reaction time played a major role on product yield. At all temperatures investigated, C10-Y and C15-Y increased with increased reaction time except 120 °C. At 120 °C, no C15-Y was observed at 20, 40 and 60 min. At 120 °, 60 min Fur convention reached 28 % and 14 % at 20 min. This signals that 40 °C increment, doubles furfural conversion. The increase of 20 °C between time 40 and 60 min improved C10 yield to 4% making 120 °C less favorable reaction temperature. Upon raising the temperature to moderate 140 °C, there was 13 %, 19% and 23% improvement in Furfural conversion at 20, 40 and 60 min in comparison to furfural conversion observed at 120 °C. Higher furfural conversion was obtained at 160 °C but did not necessarily translate into higher

C15 and C10 yield. However, some side products began to appear at reaction at 160 °C 60 min. It can be observed that selectivity of products at 120 °C was only directed towards C10 product. Apparently, increasing the reaction did not also favor C15 selectivity, see Figure 8a. At 140 °C there was an appreciable increase in selectivity to C15 product, indicative that the aldol condensation product was temperature dependent, see figure 7.8 (b). While there was improvement in C15 selectivity at 140 °C, 60 min showed some decrease in C10 selectivity. This suggests 1 mol FF was reacting with C10 to yield C15, hence, the decrease in C10 selectivity. Since long chain- alkanes biofuels are preferred over short chains, high C15 yield is desired compared to C10.

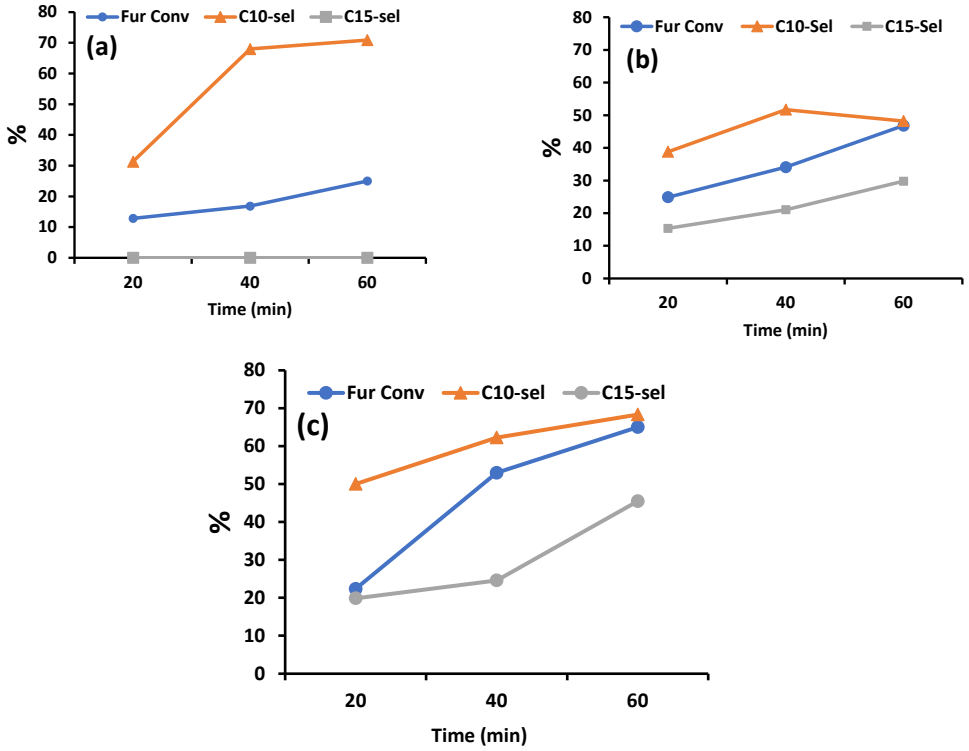

Figure 7. 8. Fur Conv, C10 selectivity (C10-sel) and C15 selectivity (C15-sel) profile of reaction at (a) 120 °C, (b) 140 °C, and 160 °C (c)

Contrarily, at 160 °C, 60min there was increase in both C10 and C15. This is not desirable, since it could lead to product mixture and rendering product purification difficult and probably affect quality of biofuel.

7.4.4. Solvent free reaction

A solvent free phase reaction was carried out under the optimum reaction condition of 140 °C, 60 min. I was revealed that, solvent-free reaction occurs faster than solvent phase reaction because the reactant concentration is higher. The conversion of cyclopentanone and furfural is essentially equivalent, with the converted cyclopentanone yielding 78% and furfural reaching 83% after 60 min, see Figure 7.9 (a). C15 selectivity of the solvent-free reaction reached 21 % while that of solvent (ETOH: H_2O) reached 25% indicative that the reaction equilibrium can be attained faster in the solvent-free reaction. This observation was consistent with the literature [35]. C15 is non-polar and will not dissolve in either the reactant or the water created in situ, hence making it be separable. However, catalyst recovery is challenging and can also increase product mixture.

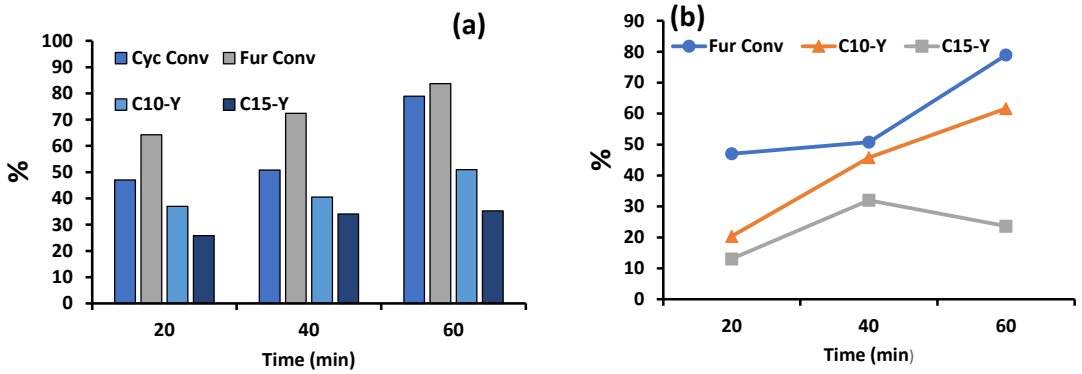

Figure 7. 9. Cyclopentanone conversion (Cyc conv), furfural conversion (Fur conv), C10 yield (C10-Y) and C15 yield (C15-Y) at 140 °C

7.5. Conclusions

Many studies employed mixed oxides for furanic and ketone aldol condensation over several basic or acid heterogenous catalysts to achieve good product yield. However, most of the reaction took longer reaction time to yield those results. In this study, we achieved global C10 and C15 yield of 37.5 % after 60 min of reaction. This reduction in reaction could be attributed to the better solvent polarity that enhanced the heating rate of the microwave process. At optimum reaction condition, 51% of furfural was converted. Considering, 0.1 g of catalyst with 5wt% of organics (reactants; furfural: cyclopentanone) in 0.25 L solvent working volume, a global yield of 37.5 % was promising. This catalyst was easily recovered.

7.6 References

[1] Alonso DM, Bond JQ, Dumesic JA. Catalytic conversion of biomass to biofuels. Green Chemistry 2010;12:1493–513. doi:10.1039/c004654j.

[2] Van De Vyver S, Odermatt C, Romero K, Prasomsri T, Román-Leshkov Y. Solid Lewis acids catalyze the carbon-carbon coupling between carbohydrates and formaldehyde. ACS Catalysis 2015;5:972–7. doi:10.1021/cs5015964.

[3] Azadi P, Carrasquillo-Flores R, Pagán-Torres YJ, Gürbüz EI, Farnood R, Dumesic JA. Catalytic conversion of biomass using solvents derived from lignin. Green Chemistry 2012;14:1573–6. doi:10.1039/c2gc35203f.

[4] Guo J, Xu G, Han Z, Zhang Y, Fu Y, Guo Q. Selective conversion of furfural to cyclopentanone with Cuznal catalysts. ACS Sustainable Chemistry and Engineering 2014;2:2259–66. doi:10.1021/sc5003566.

[5] Yang Y, Du Z, Huang Y, Lu F, Wang F, Gao J, et al. Conversion of furfural into cyclopentanone over Ni-Cu bimetallic catalysts. Green Chemistry 2013;15:1932–40. doi:10.1039/c3gc37133f.

[6] Hronec M, Fulajtarová K. Selective transformation of furfural to cyclopentanone. Catalysis Communications 2012;24:100–4. doi:10.1016/j.catcom.2012.03.020.

[7] Hronec M, Fulajtarová K, Liptaj T. Effect of catalyst and solvent on the furan ring rearrangement to cyclopentanone. Applied Catalysis A: General 2012;437–438:104–11. doi:10.1016/j.apcata.2012.06.018.

[8] West RM, Liu ZY, Peter M, Dumesic JA. Liquid alkanes with targeted molecular weights from biomass-derived carbohydrates. ChemSusChem 2008;1:417–24. doi:10.1002/cssc.200800001.

[9] Faba L, Díaz E, Ordóñez S. Aqueous-phase furfural-acetone aldol condensation over basic mixed oxides. Applied Catalysis B: Environmental 2012;113–114:201–11. doi:10.1016/j.apcatb.2011.11.039.

[10] Liu Q, Zhang C, Shi N, Zhang X, Wang C, Ma L. Production of renewable long-chained cycloalkanes from biomass-derived furfurals and cyclic ketones. RSC Advances 2018;8:13686–96. doi:10.1039/c8ra01723a.

[11] Huber GW, Chheda JN, Barrett CJ, Dumesic JA. Chemistry: Production of liquid alkanes by aqueous-phase processing of biomass-derived carbohydrates. Science 2005;308:1446–50. doi:10.1126/science.1111166.

[12] Huang XM, Zhang Q, Wang TJ, Liu QY, Ma LL, Zhang Q. Production of jet fuel intermediates from furfural and acetone by aldol condensation over MgO/NaY. Ranliao Huaxue Xuebao/Journal of Fuel Chemistry and Technology 2012;40:973–8. doi:10.1016/S1872-5813(12)60035-8.

[13] Hora L, Kikhtyanin O, Čapek L, Bortnovskiy O, Kubička D. Comparative study of physico-chemical properties of laboratory and industrially prepared layered double hydroxides and their behavior in aldol condensation of furfural and acetone. Catalysis Today 2015;241:221–30. doi:10.1016/j.cattod.2014.03.010.

[14] Jennifer Cueto, Laura Faba, Eva Díaz SO. Performance of basic mixed oxides for aqueous-phase 5-hydroxymethylfurfural-acetone aldol condensation. Applied Catalysis B: Environmental 2017;201:221–31. doi:10.1016/j.apcatb.2016.08.013.

[15] Wang Y, Sang S, Zhu W, Gao L, Xiao G. CuNi@C catalysts with high activity derived from metal-organic frameworks precursor for conversion of furfural to cyclopentanone. Chemical Engineering Journal 2016;299:104–11. doi:10.1016/j.cej.2016.04.068.

[16] Cueto J, Faba L, Díaz E, Ordóñez S. Enhancement of furfural–cyclopentanone aldol condensation using binary water–ethanol mixtures as solvent. Journal of Chemical Technology and Biotechnology 2018;93:1563–71. doi:10.1002/jctb.5522.

[17] Cueto J, Faba L, Díaz E, Ordóñez S. Cyclopentanone as an Alternative Linking Reactant for Heterogeneously Catalyzed Furfural Aldol Condensation. ChemCatChem 2017;9:1765–70. doi:10.1002/cctc.201601655.

[18] Li H, Riisager A, Saravanamurugan S, Pandey A, Sangwan RS, Yang S, et al. Carbon-Increasing Catalytic Strategies for Upgrading Biomass into Energy-Intensive Fuels and Chemicals. ACS Catalysis 2018;8:148–87. doi:10.1021/acscatal.7b02577.

[19] Wang W, Ji X, Ge H, Li Z, Tian G, Shao X, et al. Synthesis of C15and C10fuel precursors with cyclopentanone and furfural derived from hemicellulose. RSC Advances 2017;7:16901–7. doi:10.1039/c7ra02396k.

[20] Hronec M, Fulajtárova K, Liptaj T, Prónayová N, Soták T. Bio-derived fuel additives from furfural and cyclopentanone. Fuel Processing Technology 2015;138:564–9. doi:10.1016/j.fuproc.2015.06.036.

[21] Kelly GJ, King F, Kett M. Waste elimination in condensation reactions of industrial importance. Green Chemistry 2002;4:392–9. doi:10.1039/b201982p.

[22] Loupy A, Petit A, Hamelin J, Texier-Boullet F, Jacquault P, Mathé D. New solvent-free organic synthesis using focused microwaves. Synthesis 1998;5:1213–34.

[23] Ma S-Y, Zheng Z-B. (2 *E* ,5 *E*)-2,5-Difurfurylidenecyclopentanone. Acta Crystallographica Section E Structure Reports Online 2009;65:o3084–o3084. doi:10.1107/S1600536809047278.

[24] Aramendía MA, Boráu V, Jiménez C, Marinas A, Marinas JM, Navío JA, et al. Synthesis and textural-structural characterization of magnesia, magnesia-titania and magnesia-zirconia catalysts. Colloids and Surfaces A: Physicochemical and Engineering Aspects 2004;234:17–25. doi:10.1016/j.colsurfa.2003.11.026.

[25] Xiao PW, Jun JY, Cheng J, Zheng PH, Zhi PX. High-temperature adsorption of carbon dioxide on mixed oxides derived from hydrotalcite-like compounds. Environmental Science and Technology 2008;42:614–8. doi:10.1021/es072085a.

[26] Abelló S, Medina F, Tichit D, Pérez-Ramírez J, Groen JC, Sueiras JE, et al. Aldol condensations over reconstructed Mg-Al hydrotalcites: Structure-activity relationships related to the rehydration method. Chemistry - A European Journal 2005;11:728–39. doi:10.1002/chem.200400409.

[27] Grover V, Shukla R, Tyagi AK. Facile synthesis of ZrO2 powders: Control of morphology. Scripta Materialia 2007;57:699–702. doi:10.1016/j.scriptamat.2007.06.053.

[28] Gulková D, Šolcová O, Zdražil M. Preparation of MgO catalytic support in shaped mesoporous high surface area form. Microporous and Mesoporous Materials 2004;76:137–49. doi:10.1016/j.micromeso.2004.07.039.

[29] Kuśtrowski P, Sułkowska D, Chmielarz L, Rafalska-Łasocha A, Dudek B, Dziembaj R. Influence of thermal treatment conditions on the activity of hydrotalcite-derived Mg-Al oxides in the aldol condensation of acetone. Microporous and Mesoporous Materials 2005;78:11–22. doi:10.1016/j.micromeso.2004.09.011.

[30] Hora L, Kelbichová V, Kikhtyanin O, Bortnovskiy O, Kubička D. Aldol condensation of furfural and acetone over MgAl layered double hydroxides and mixed oxides. Catalysis Today 2014;223:138–47. doi:10.1016/j.cattod.2013.09.022.

[31] Desai DS, Yadav GD. Green Synthesis of Furfural Acetone by Solvent-Free Aldol Condensation of Furfural with Acetone over La2O3-MgO Mixed Oxide Catalyst. Industrial and Engineering Chemistry Research 2019;58:16096–105. doi:10.1021/acs.iecr.9b01138.

[32] Sádaba I, Ojeda M, Mariscal R, Fierro JLG, Granados ML. Catalytic and structural properties of co-precipitated Mg-Zr mixed oxides for furfural valorization via aqueous aldol condensation with acetone. Applied Catalysis B: Environmental 2011;101:638–48. doi:10.1016/j.apcatb.2010.11.005.

[33] Cueto J, Faba L, Díaz E, Ordóñez S. Optimization of the process conditions for minimizing the deactivation in the furfural-cyclopentanone aldol condensation in a continuous reactor. Applied Catalysis B: Environmental 2020;263:118341. doi:10.1016/j.apcatb.2019.118341.

[34] Faba L, Díaz E, Ordõñez S. One-pot aldol condensation and hydrodeoxygenation of biomass-derived carbonyl compounds for biodiesel synthesis. ChemSusChem 2015;7:2816–20. doi:10.1002/cssc.201402236.

[35] Deng Q, Xu J, Han P, Pan L, Wang L, Zhang X, et al. Efficient synthesis of high-density aviation biofuel via solvent-free aldol condensation of cyclic ketones and furanic aldehydes. Fuel Processing Technology 2016;148:361–6. doi:10.1016/j.fuproc.2016.03.016.

Chapter 8:
Conclusions

This thesis' principal objective was to validate the circular bioeconomy paradigm in both upstream and downstream processes. The next section contains general conclusions based on the data collected during the course of this thesis.

- Hemicellulose, the most pretreatment-sensitive heteropolymer, was easily separated from the walnut shell at a moderate temperature without the need of a catalyst. The entire process is described as green, utilizing a microwave as a heat source and water as a solvent. In batch operations, the xylose was converted successfully to L-lactic acid.

- To minimize wastage and maximize the usage of *Bacillus coagulans DSM 2314,* lignin was employed as a substrate for immobilization from the residue left after hydrolysis. This procedure was used to incorporate the circular bioeconomy's closed-loop concept into a single integrated biorefinery.

- To begin, a novel strategy was taken in which lignin was isolated first. The walnut shell was deconstructed using deep eutectic solvents, exposing the abundant holocellulose for subsequent valorization. After 3 hours of ball milling and 10 minutes of microwave irradiation, a good yield of unaltered lignin was achieved. This procedure proved critical in overcoming the recalcitrance of lignin. This paves the door for easy access to cellulose substrates for enzymes. The lignin recovered is of excellent quality and can be used as a feedstock for the synthesis of biofuels and biochemicals. Thus, both the lignin and holocellulose recovered are beneficial in the closed-loop process.

- We demonstrate in Chapter 6 that mechanocatalytic processes can provide a high yield of glucose, which can then be transformed to bioethanol. The acid hydrolysate presented no significant difficulties due to its neutralization with $Mg(OH)_2$. $MgSO_4$ in-situ was created at no additional expense. $MgSO_4$ is a necessary mineral for yeast fermentation to occur during the synthesis of bioethanol. To purify and recover furans and phenolics, an effective purification procedure was used. These furans serve as useful building blocks for the synthesis of biojet precursors. All chemicals and residues retrieved have the potential to be valuable in sustaining a closed-loop system.

- In the cross-aldol condensation procedure, the commercial furfural and cyclopentanone were successfully assessed. Microwave technologies were used to generate heat for the first time. This reaction was completed in a short amount of time and produced a high yield of product. The effect of the solvent on the catalytic reaction was then demonstrated. The binary solvent system used enabled the catalyst to be easily recovered. Historically, the majority of solvent systems or solventless systems resulted in product precipitation. This significantly complicated the catalyst's recuperation.

By and large, this thesis met its objective of confirming the close-loop notion by demonstrating the entire valuing of inexpensive agricultural waste (circular bioeconomy). All residues were consumed completely.

8.1. Observations and future work

- This thesis revealed the complete usage of agricultural waste; hence, future study should focus on the full-scale implementation of an integrated multiple upstream and downstream processes, complete with life cycle analysis and economic evaluation.

- Prior to any further valorization of the feedstock, lignin should be removed in upstream processes.

- The direct usage of furfural and 5-HMF recovered from hydrolysate as a platform chemicals for aldol condensation should be encouraged.

8.2. List of Publications

- Ahorsu R, Medina F, Constantí M. Significance and Challenges of Biomass as a Suitable Feedstock for Bioenergy and Biochemical Production: A Review. Energies 2018;11:3366. doi:10.3390/en11123366.

- Ahorsu R, Cintorrino G, Medina F, Constantí M. Microwave processes: A viable technology for obtaining xylose from walnut shell to produce lactic acid by Bacillus coagulans. Journal of Cleaner Production 2019;231:1171–81. doi:10.1016/J.JCLEPRO.2019.05.289.

- Ahorsu R, Constanti M, Medina F. Recent Impacts of Heterogenous Catalysts in Biorefineries. Industrial & Engineering Chemistry Research 2021; Under review.

- Ahorsu R, Constanti M, Dominguez de Maria P, Medina F. Synergy of ball milling, microwave irradiation and Deep Eutectic Solvents for a rapid and selective delignification: Walnut shells as model for lignin-enriched recalcitrant biomass. Chemical Engineering Journal 2021; Submitted

Papers in preparation

- Martin K, Ahorsu R, Medina F, Constanti M, Rinaldi R; Towards zero-waste biorefineries: Hypercrosslinked benzene polymer as a task-specific reusable adsorbent for detoxification of lignocellulosic hydrolysates for downstream fermentation. To be submitted to Green Chemistry

- Catalytic cross-aldol condensation of furanics to produce C10 and C15 bio-jet fuel precursors with microwave-assisted process; To be submitted to ChemSusChem

8.3. Conferences and posters

- Ahorsu R, Constanti M, Medina F. L-Lactic acid production from cellulose and hemicellulose extract of Walnut Shell through microwave-assisted autohydrolysis followed by microbial fermentation. Biomass and Bioenergy Conference, Young Research Fellow Speaker, September 2018, Zurich,
- Martin K, Ahorsu R, Medina F, Constanti M, Rinaldi R. An integrated cellulase-free approach to produce sugars from lignocellulose at high quality for fermentation processes [Poster] August 2020. Chemie Ingenieur Technik 92(9):1263-1263. https://doi.org/10.1002/cite.202055127
- Andhalkara V, Ahorsu R, Rohit R, Medina F, Constantí M, Effect of mechano-catalytic pretreatment on poly(3-hydroxybutyrate) production using sulfuric acid impregnated rice-husk September 2021, [14th Mediterranean Congress of Chemical Engineering (MeCCE14)]
- Ahorsu R, Constanti M, Medina F. Production of liquid fuel from furan derivatives through microwave-aided process in bi-mixtures with monophasic configuration. October 2021 [Catalysis conference]

UNIVERSITAT ROVIRA I VIRGILI
INTEGRATING PRETREATMENT TECHNIQUES IN A "BENIGN-BY-DESIGN STRATEGY"
IN THE CONTEXT OF BIOMASS VALORIZATION
Richard Ahorsu

Annex A.

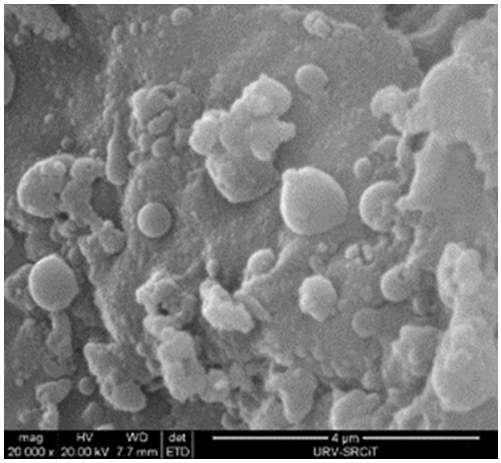

Figure A3.1: ESEM image for walnut shell autohydrolyzed at 170 °C for 25 minutes

Annex B

Table S5.1 Biochemical composition of walnut shell.

Biopolymer	Dry matter (% w/w)
Cellulose	26.7
Hemicellulose	23.4
Klason Lignin	49.8
Extractives	4.1
Ash	0.9

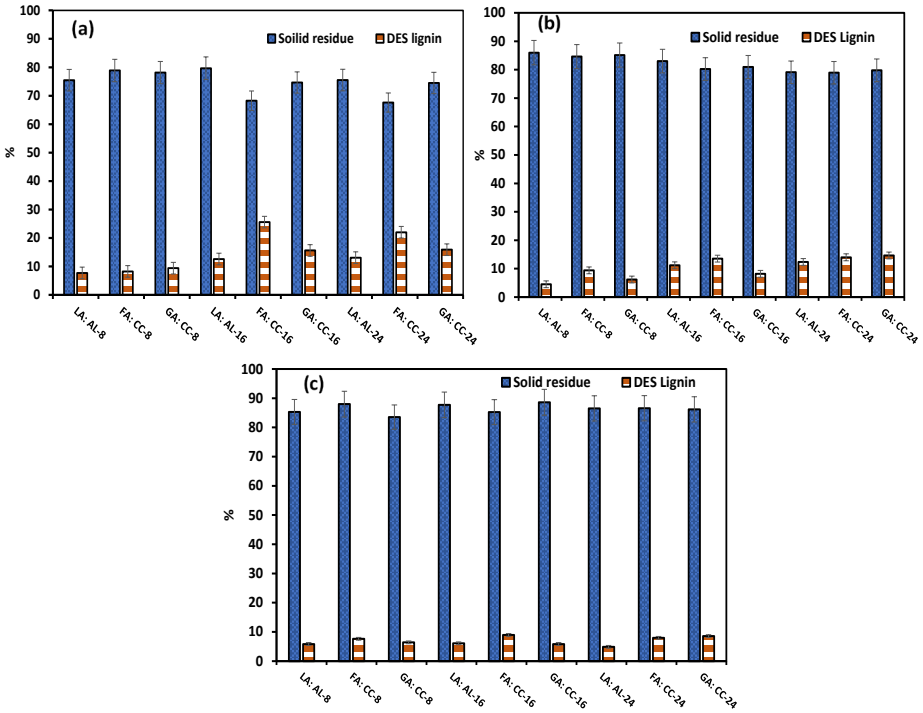

Figure S5.2: Profile of Des lignin and solid residue at 60°C for 8h, 16h and 24h °C (a) 0.1mm (b) 0.3 mm (c) 0.5mm

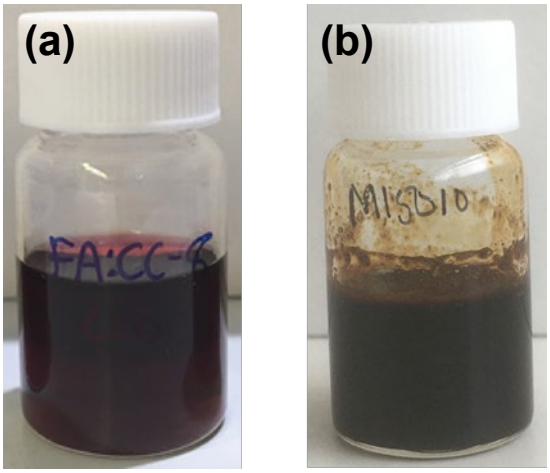

Figure S5.3. Solubilized lignin in DES after pretreatment (a) 8h at 60 °C (b) 10 min at 150 °C

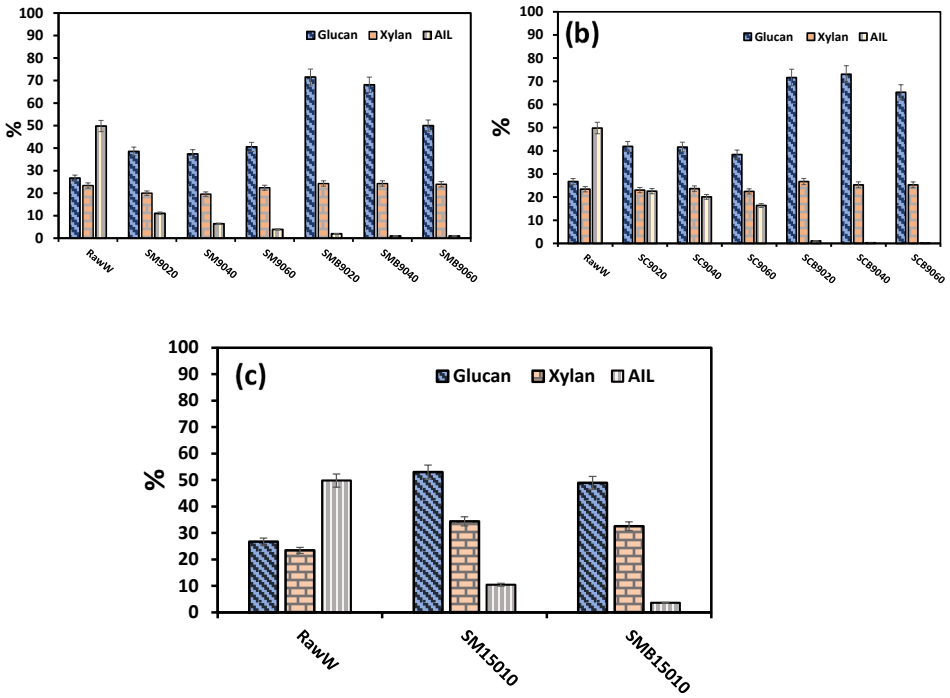

Figure S3.4: Biopolymer profile of pretreated solid residue (a) microwave heating at 90 °C (b) conventional heating at 90 °C (c) microwave heating of 20wt % WS loading at 150 °C

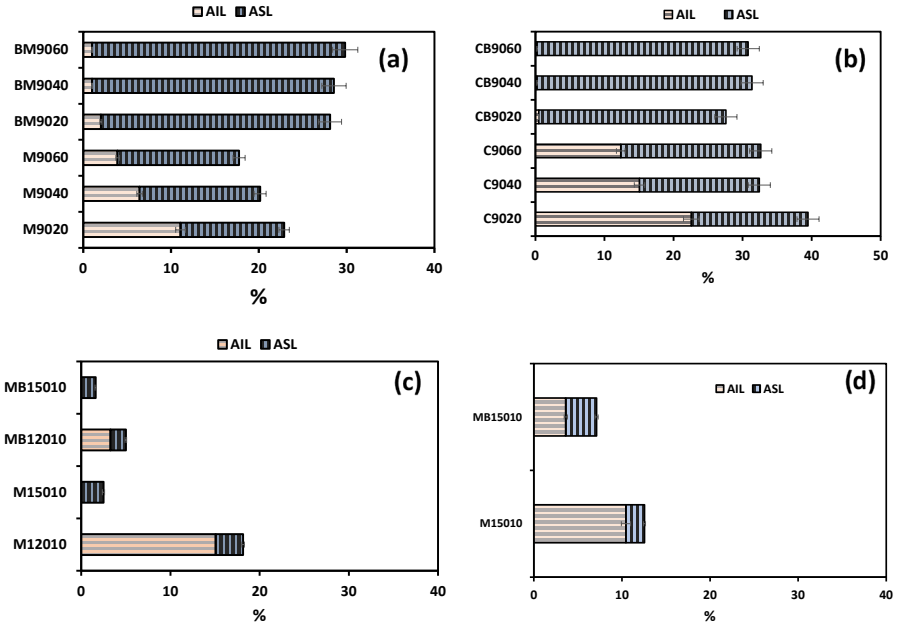

Figure S5: Acid insoluble lignin (AIL) and Acid Soluble lignin (ASL) profile of pretreated solid residue (a) at 90 °C microwave heating (b) at 90 °C conventional heating (c) at 120 °C and 150 °C microwave heating (d) at 150 °C microwave heating of 20wt % WS loading

Table S2: FTIR spectra band assignment

Wavenumber (cm^{-1})	Bond characteristics	Constituent group
3400	O-H Stretching	Alcohols/ Phenols
2940	C-H stretching	Aliphatic methyl
2500	O-H stretching	Carboxylic acids
1720	C=O stretching	Aromatic carbonyl/carboxyl
1710	C=O stretching	Unconjugated aryl ketones
1645	C=O stretching	Conjugated aryl ketones
1590	Aromatic skeletal vibrations	Aromatic
1460	C-H deformations (asymmetric CH_3 and CH_2).	Aromatic
1420	Aromatic skeletal vibration associated C-H in plane deformations	Aromatic
1360	Aliphatic CH_3 deformation	Aliphatic chain
1330	C-H bending	Syringyl and condensed Guaiacycl
1270	G ring and C=O stretching	Aromatic, aliphatic carbonyl Group
1220	C-C, and C=O stretching	Alkyl aryl ether, carbonyl Groups
1160	C-O stretching	Tertiary alcohol and esters
1120	Aromatic C-H in-plane deformation And C-O stretching	Typical of Syringyl monomer
1030	Aromatic C-H in plane deformation And C-O deformations	Aromatic H, and aromatic O Groups, G ring primary alcohols
985	HC=CH out of plane deformation(trans)	Vinylic groups
915	C-H out of plane	Aromatic
830	C-H out of plane in positions 2,5 and 6	G unit

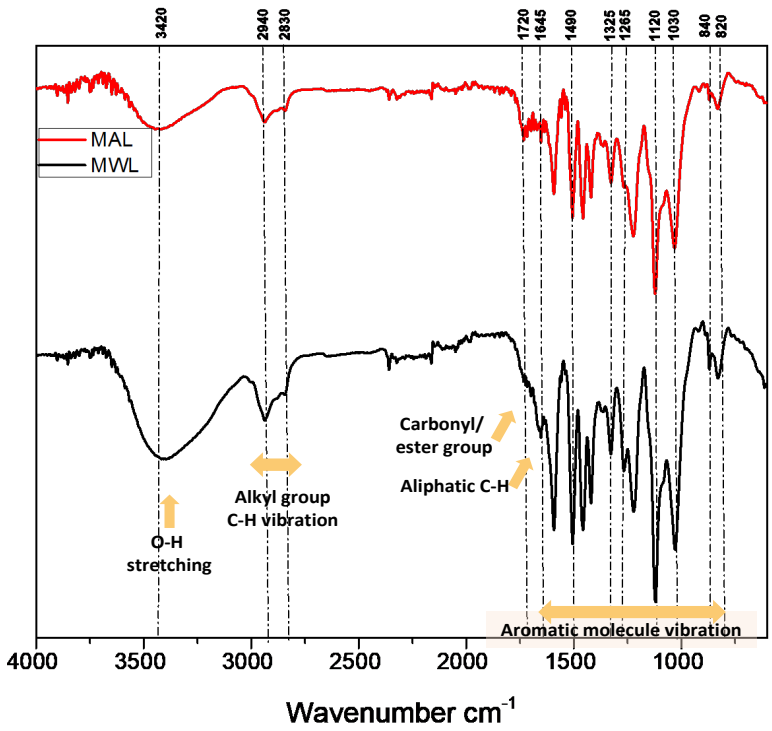

Figure S5.6: FTIR spectra of milled wood lignin (MWL) and mild acid lignin (MAL)

Annex C

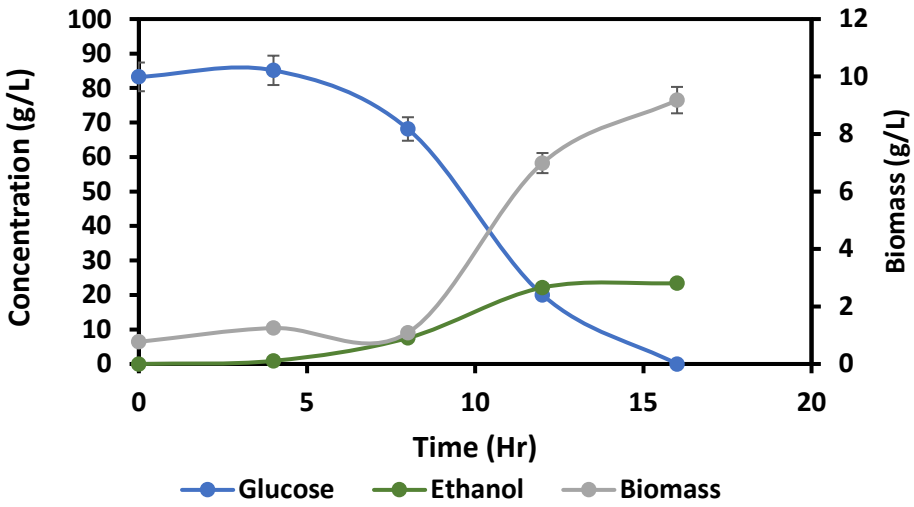

Figure S 6.1: Ethanol evolution of glucose from α-cellulose hydrolysate

Annex C

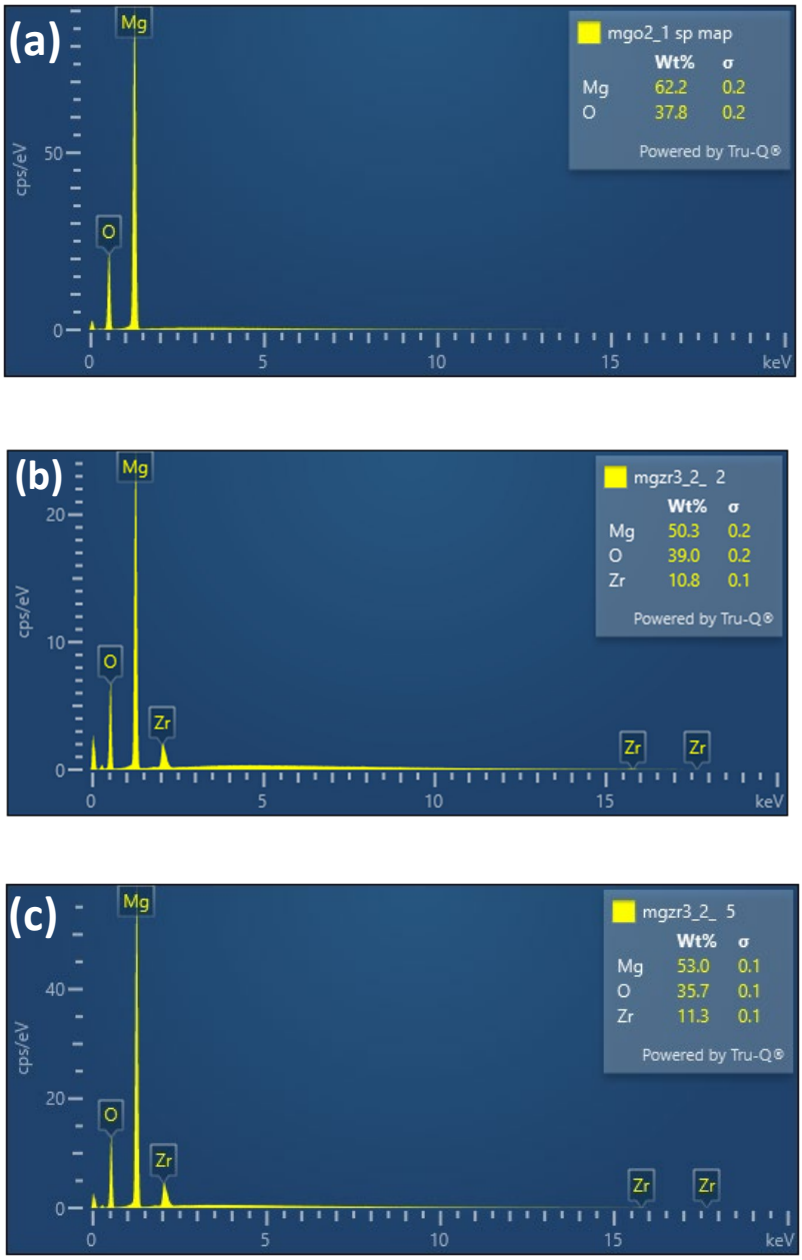

S7.1 EDX of MgO-A (a), MgZr-H (b) MgZr-A (c)

UNIVERSITAT ROVIRA I VIRGILI
INTEGRATING PRETREATMENT TECHNIQUES IN A "BENIGN-BY-DESIGN STRATEGY"
IN THE CONTEXT OF BIOMASS VALORIZATION
Richard Ahorsu